RESEARCH ON OCULAR EFFECTS PRODUCED BY THERMAL RADIATION

THOMAS A. ALEXANDER, M. S.,

RALPH G. ALLEN, Ph. D.,

ROGER L. BESSEY, M. S.,

WILLIAM R. BRUCE,

EARL R. LAWLER, JR., B. S.,

CHARLES A. POLASKI, M. E.

JULY 1966

USAF School of Aerospace Medicine
Aerospace Medical Division (AFSC)
Brooks Air Force Base, Texas

RESEARCH ON OCULAR EFFECTS PRODUCED BY THERMAL RADIATION*

Alexander, T. A., R. G. Allen, Jr.,
R. L. Bessey, W. R. Bruce,
E. R. Lawler, Jr., and C. A. Polaski

*This work was supported by the Department of Ophthalmology, Air Force School of Aerospace Medicine, Brooks Air Force Base, Texas and the Medical Division, Defense Atomic Support Agency, Washington, D. C.

BLANK PAGE

RESEARCH ON OCULAR EFFECTS PRODUCED BY THERMAL RADIATION

This report was prepared by the Life Sciences Division of Technology Incorporated for the USAF School of Aerospace Medicine under Contract AF 41(609)-2906 and covers the period 15 June 1965 to 15 June 1966. Project Leader for Technology Incorporated was Dr. Ralph G. Allen, Jr.

The program was initiated by the Ophthalmology Branch of the School of Aerospace Medicine, Brooks Air Force Base, Texas with additional support from the Defense Atomic Support Agency, Washington, D. C. Mr. E. O. Richey, SAM, was Contract Monitor during the contractual period. Grateful acknowledgement is hereby made of the assistance provided by Mr. E. O. Richey, Lt. Col. J. F. Culver, Major A. V. Alder, and Major D. J. Pitts--all from the Ophthalmology Branch of the School of Aerospace Medicine.

This report covers the study of chorioretinal burns carried out by Technology Incorporated and it follows earlier work (1) in which (a) a Meyer-Schwickerath photo coagulator, manufactured by the Carl Zeiss Company, was modified for the production of retinal burns under closely controlled conditions and (b) preliminary techniques were developed for the production and detection of minimal retinal burns in rabbits.

The primary efforts and results obtained in this study are documented in detail in the series of reports attached hereto. These reports cover:

(a) Calibration of the energy output of the photo coagulator in physical units (for various modes of operation) and interpretation of this output in terms of energy deposited on the rabbit retina (2).

(b) Complete operating and maintenance instructions for the modified Zeiss coagualtor and associated pulse control unit (3).

(c) Results obtained from a thorough study of the production of 5-minute minimal retinal burns in rabbits for exposure durations ranging from 165 μseconds to 250 mseconds and image sizes ranging from 0.11 mm to 1.0 mm (4).

(d) Results of a study aimed at correlating calculated temperature distributions in the rabbit retina with the production of minimal observable lesions (5).

(e) Measurement of the light emitted in the pulses from several Strobonar flash units used by personnel of the Oculo-Thermal Branch in flash blindness simulation studies (6).

A major effort not yet described in a report is the modification of a ruby laser system acquired from Maser Optics.

This laser system, capable of approximately 100 joules output, has been installed and operated in the normal mode, and is now being modified for the experimental production of retinal burns. A water treatment system for the laser has been designed and constructed and consists of mixed bed water demineralizer and a water cooling system for the ruby rod and flash lamps.

Studies have also been made on various methods of Q-switching and a tentative decision has been to use a Kerr cell shutter since it appears that the system will give the most reliable and most flexible control of the beam.

Other support systems for the laser are also in the study or design state. These include a temperature controlled laser dump circuit, a beam intensity control system, several calibration systems, and animal irradiation equipment. The temperature controlled dump circuit will prevent firing of the laser unless the cooling water temperature is within specified temperature limits. This is necessary since the power output of the laser is temperature sensitive. The beam intensity control is necessary in order that the beam intensity can be

varied for a given exposure time or laser pulse width. Several calibration techniques are under study and it is anticipated that two methods will be adopted in order to verify calibration results. The animal irradiation equipment will be similar to that used with the Zeiss light coagulator and consist of a movable ophthalmoscope and mirror with which the operator can locate the area to be exposed, irradiate the area, and then observe the area post exposure. The movable mirror will simultaneously direct the laser beam into the rabbit eye and protect the operator's eye.

In addition to the efforts described in the attached reports and the work with the laser described above,

(a) The conventional battery power system for the Zeiss coagulator was replaced with a 24 volt Nickle-Cadmium system in order to achieve a more constant light output for long duration exposures,

(b) initial experiments were conducted for the development of techniques for making long exposures ($>$ 10 seconds) with rabbits, and

(c) equipment was assembled for sterioscopic fundus photography.

It is anticipated that these developments and improvements will contribute materially to the study of retinal injury resulting from exposure to high intensity light sources.

REFERENCES

1. Alexander, T. A., R. L. Bessey, and E. R. Lawler, Jr. Ocular Effects of Thermal Radiation. Final Report of Air Force Contract AF 41(609)-2464, Task No. 630103, 1965.

2. Bessey, R. L. and R. G. Allen, Jr. Calibration of Zeiss Coagulator. Contract AF 41(609)-2906, 1966.

3. Lawler, E. R., Jr. and W. R. Bruce. Operating Instructions for Modified Zeiss Photo Coagulator. Contract AF 41(609)-2906, 1966.

4. Alexander, T. A., R. L. Bessey, E. R. Lawler, Jr., W. R. Bruce, and R. G. Allen, Jr. A Study of the Production of Chorioretinal Lesions by Thermal Radiation. Contract AF 41(609)-2906, 1966.

5. Allen, R. G., Jr., A. F. Muller, E. R. Lawler, Jr., and W. R. Bruce. An Examination of the Production of Chorioretinal Burns in Terms of Temperature Distributions. In Publication, Aerospace Medical Journal, 1966.

6. Polaski, C. A. and R. G. Allen, Jr. Measurements of the Total Luminous Energy Output of Two Honeywell Strobonar Flash Units. Contract AF 41(609)-2906, 1966.

BLANK PAGE

CALIBRATION OF ZEISS PHOTO COAGULATOR*

Bessey, R. L. and R. G. Allen, Jr.

*This work was supported by the Department of Ophthalmology, Air Force School of Aerospace Medicine, Brooks Air Force Base, Texas and the Medical Division, Defense Atomic Support Agency, Washington, D. C.

FOREWORD

This report was prepared by personnel of the Life Sciences Division of Technology Incorporated--

Roger L. Bessey, M.S.

Ralph G. Allen, Jr., Ph. D.

The effort was sponsored jointly by the Ophthalmology Branch of the United States Air Force School of Aerospace Medicine, and the Medical Division, Defense Atomic Support Agency, Washington, D. C. Grateful acknowledgement is made of the assistance provided by Lt. Col. J. F. Culver and Major D. G. Pitts of the Ophthalmology Branch.

Other major contributors to the effort were Messrs. E. R. Lawler, Jr., and W. R. Bruce of Technology Incorporated.

ABSTRACT

A modified Meyer-Schwickerath photo coagulator was developed to study the production of thermal lesions in rabbits and primates. In order to obtain quantitative data on the thermal exposures administered to animals being investigated, it was necessary to measure the spectral irradiance as well as the total irradiance for the conditions under which the source was to be operated.

The method of calibration, calibration results, and a comparison between directly measured total irradiance and spectral irradiance integrated over wavelength are presented in this paper.

BLANK PAGE

CALIBRATION OF ZEISS PHOTO COAGULATOR

1. INTRODUCTION

Past work in this laboratory (1), and others (2), (3) has led to the development of a xenon light source for the production of chorioretinal burns under very carefully controlled conditions. This source, a modified Meyer-Schwickerath photo coagulator, was developed to study the production of thermal lesions in rabbits and primates for exposure times ranging from several seconds to approximately 150 useconds--and for image sizes (in rabbits) which vary from approximately 0.1 to 1.0 mm in diameter. In order to obtain quantitative data on the thermal exposures administered to subjects, it was necessary to measure the spectral irradiance as well as the total irradiance for the conditions under which the source was to be operated. Such measurements were made with and without a Fish-Sherman KG-3 filter using a calibrated Jarrell-Ash Ebert monochromator, an Eppley 14-junction silver bismuth thermopile, and a Bureau of Standards calibrated DXL-59 tungsten lamp.

The method of calibration, calibration results, and a comparison between directly measured total irradiance and spectral irradiance integrated over wavelength are presented in this paper.

2. LIGHT SOURCE

The basic light source was a Meyer-Schwickerath Light Coagulator manufactured by the Carl Zeiss Company. For the purpose of studying chorioretinal burns, this machine was modified as follows: (a) a Keeler ophthalmoscope with a pop-up mirror replaced the standard pinhole-mirror, (b) a KG-3 phosphate glass filter was added to the optical system to reduce the infrared energy in the beam, (c) one of the beam-size apertures was changed from 0.8 mm (4.5° light cone) to 0.2 mm (1° light cone), (d) the maximum opening of the iris was increased in order to obtain a 200-to-1 intensity control of the beam in 72 graded steps, (e) the lamp holder was modified to permit use of an Osram 2500W xenon lamp, and (f) an auxiliary light control unit was added for accurate and automatic control of the length of the light pulse (4). Figure 1 shows the modified machine with its auxiliary equipment and figure 2 shows the optical system in schematic.

Light pulses of specified durations were obtained by controlling the power applied to the lamp. To accomplish this, a solid state switch was used to connect the xenon lamp to a source of power--either a set of aircraft batteries or a capacitor bank. With the batteries, pulses could be obtained with durations of about 1 msecond to 10 seconds. For

shorter pulses, 150 μseconds to 1 mseconds, the capacitor bank was used in place of the batteries. Current through the lamp was approximately 200 amps for battery operation (50 volts) and 2000 amps for capacitor operation (130 volts).

3. PROCEDURES

For the measurement of spectral irradiance, a Jarrell-Ash 0.25 meter Ebert monochromator equipped with an RCA 7102 photomultiplier was used. The circuit diagram used with the photomultiplier is shown in figure 3. First, this combination was set up 50 cm from a DXL-59 tungsten filament iodine containing lamp for which the spectral irradiance, $H_s(\lambda)$, had been determined by the National Bureau of Standards. The response of the photomultiplier, $V_s(\lambda)$, was determined in 10 mu bandwidth from 400 to 800 mu and in 200 mu bandwidths from 800 to 1100 mu. For the interval 800 to 1100 mu a Corning Glass filter number 2550 was used to eliminate the second order spectrum. The resolution of the apparatus was checked by noting the wavelength interval corresponding to the width at half maximum of the photomultiplier voltage when one of the lines in the mercury spectrum was swept across the monochromator exit slit. The bandwidth, measured in this manner, was 10 mu for $400 < \lambda < 800$ mu and approximately 20 mu for $800 < \lambda < 1100$ mu.

After calibration with the standard source, the monochromator was placed in the beam from the Zeiss coagualtor (300 cm from the focal point of the system) and measurements made from 400 to 1100 mu. For the measurements between 400 and 800 mu a 6000 Å blaze grating was used. In the range 800 to 1100 mu a 12,000 Å blaze grating was used. Spectral irradiance, $H(\lambda)$, was then calculated using the expression

$$H(\lambda) = H_s(\lambda) \quad \frac{V(\lambda)}{V_s(\lambda)} \tag{1}$$

where it is assumed that the voltage output of the detector is directly proportional to the irradiance at the detector for all values of irradiance of concern in this investigation.

Since the cross-sectional area of the light beam varied as the square of the distance from the source (the beam being a circular cone of rays), the spectral irradiance varied as the inverse square of this distance. Thus, $H_D(\lambda)$, the irradiance at a distance D other than the distance at which it was originally measured, is given by

$$H_D(\lambda) = \frac{A}{A_D} \quad H(\lambda) \tag{2}$$

where: A = cross sectional area of the beam at the distance at which $H_c(\lambda)$ was measured

A_D = cross sectional area of the beam at distance D.

Since the Zeiss was to be pulsed at two voltage values, 50V and 130V corresponding to the two current values 200A and 2000A, spectral irradiance measurements were taken for both of these conditions. Spectral irradiances were also measured for two different xenon lamps--1000 and 2500 watt lamps--with and without a KG-3 filter.

Two methods were used to obtain the total irradiance (a) integration of the measured spectral irradiance over the wavelength interval and (b) direct total irradiance measurements using the Eppley thermopile.

In the first method, the total irradiance, H_D is given by

$$H_D = \int_{\lambda} H_D(\lambda)\, d\lambda \qquad (3)$$

Written as a discrete sum to correspond to the actual measurement, equation 3 becomes:

$$H_D = \sum_{\lambda = 400}^{1100} H_D(\lambda)\, \Delta\lambda \qquad (4)$$

where $\Delta\lambda = 10$ for $400 \leq \lambda \leq 800$ mu

$\Delta\lambda = 20$ for $800 \leq \lambda \leq 1100$ mu

For the direct measurement of the total irradiance:

$$H_D = I \cdot C \cdot V'_E, \tag{5}$$

where: $I = \frac{V_E}{V'_E}$ (corresponds to the setting of an iris diaphragm used to vary irradiance)

V_E = voltage response of Eppley (at equilibrium) with the iris setting actually used for the measurement

V'_E = voltage response of Eppley (at equilibrium) with the iris fully open--other conditions being the same

C = calibration constant of the Eppley thermopile #6909 furnished by the manufacturer (1.150×10^{-3} cal/cm^2-sec-mv)

Figure 4 shows the value of I as a function of iris setting.

Determination of the retinal irradiance at time t, $H_r(t)$, has been considered for two cases (a) the subject sufficiently close to the eye piece so that the entire light beam enters the pupil, and (b) the case in which the pupil is smaller than the beam at the eye and consequently intercepts only a portion of the beam.

CASE A. LIGHT BEAM SMALLER THAN PUPIL.

In this case, $H_r(t)$, the time dependent retinal irradiance is given by:

$$H_r(t) = \int_\lambda H_B(\lambda, t) \frac{A_B}{A_i} T_e(\lambda) \, d\lambda \tag{6}$$

Here: $H_B(\lambda, t)$ = spectral irradiance at distance B--the distance from the focal plane to the eye

A_B = area of the beam at distance B

A_i = area of the image on the retina

$T_e(\lambda)$ = spectral transmission of the clear media of the eye.

λ = wavelength

t = time

$H_r(t)$ is treated as a time dependent variable since in some cases the time dependence may be significant. Noting that

$$H_B(\lambda, t) A_B = H_D(\lambda, t) A_D, \tag{7}$$

$$A_D = (D\Theta)^2, \tag{8}$$

and

$$A_i = (F\Theta)^2, \tag{9}$$

where, A_D is the area of the beam at distance D, F is the effective focal length of the eye, and Θ is the beam cone angle, equation 6 can be written as

$$H_r(t) = \left(\frac{D}{F}\right)^2 \int_\lambda H_D(\lambda, t) \, T_e(\lambda) \, d\lambda \tag{10}$$

Assuming that the spectrum does not vary with time

$$H_D(\lambda, t)\, d\lambda = \frac{R(\lambda)\, d\lambda}{\int_\lambda R(\lambda)\, d\lambda} \quad H_D(t) \tag{11}$$

where: $H_D(t) = \int_\lambda H_D(\lambda, t)\, d\lambda$

and $R(\lambda) = \dfrac{H_D(\lambda)\, d\lambda}{H_D(\lambda \text{ max})}$ (Relative Spectrum)

Using (11) in (10)

$$H_r(t) = \left(\frac{D}{F}\right)^2 \left[\frac{\int_\lambda R(\lambda)\, T_e(\lambda)\, d\lambda}{\int_\lambda R(\lambda)\, d\lambda}\right] H_D(t) = GK\, H_D(t) \tag{12}$$

Letting

$$\overline{T}_e = \frac{\int_\lambda R(\lambda)\, T_e(\lambda)\, d\lambda}{\int_\lambda R(\lambda)\, d\lambda}$$

$$G = \left(\frac{D}{F}\right)^2$$

Using (5), equation (12) becomes:

$$H_r(t) = I\, C\, G\, \overline{T}_e\, V'_E\, (t) \tag{13}$$

However, in this expression, $V'_E(t)$ corresponds to the equilibrium value of the Eppley thermopile--a quantity which changes relatively slowly. To account for rapid changes in irradiance, an EG&G SD-100 photodiode was incorporated into the system. Its response is related to the response

of the Eppley thermopile through the expression

$$S = \frac{V'_E}{V'_{pd}} \tag{14}$$

V'_E = Voltage response of the Eppley thermopile with iris in m volts (at equilibrium and with the iris fully open)

V'_{pd} = Corresponding voltage response of photodiode in volts.

Then:

$$H_r(t) = B\, V'_{pd}(t) \tag{15}$$

where: $B = I\, C\, S\, G\, \overline{T}_e$

The voltage response of the photodiode was measured with a Tektronix cathode ray scope with polaroid camera attachment so that the light pulse could be described in terms of irradiance as a function of time and/or average irradiance. (figures 5, 6, 7 and 8).

CASE B. LIGHT BEAM AT EYE LARGER THAN PUPIL

In this case, the retinal irradiance may be described as follows:

$$H_r(t) = \int_\lambda H_c(\lambda, t)\, \frac{A_p}{A_i}\, T_e(\lambda)\, d\lambda = GG'K\, H_D(t) \tag{16}$$

where: G, K, and $H_D(t)$ have same significance as before and,

$$G' = \frac{A_p}{A_c}$$

A_p = area of pupil

A_c = area of beam at distance C (exposure distance measured from the focal plane).

Using (5) and (14), equation (16) may be written as

$$H_r(t) = B' V'_{pd}(t) \; ; \; B' = G'B \tag{17}$$

If the light pulse is nearly square, as in the case for relatively long pulses using batteries as the power source, the average retinal irradiance is given by:

$$\overline{H}_r = B \overline{V}'_{pd} \quad \text{(for beam smaller than pupil)} \tag{18a}$$

$$\overline{H}_r = B' \overline{V}'_{pd} \quad \text{(for beam larger than pupil)} \tag{18b}$$

For non-square symmetrical or semi-symmetrical pulses, the case for relatively short pulses using a condensor discharge, the average retinal irradiance is given by:

$$\overline{H}_r = B V'_{pd}(Eff) \tag{19a}$$

where: $V'_{pd}(Eff) \quad \dfrac{\int_o^T V'_{pd}(t)\, dt}{T_{1/2}}$; $T_{1/2}$ = light pulse width at half-maximum

Experimentally it was found that for any iris setting

$$\int_0^T V'_{pd}(t)\ dt = T_m\, V'_{pd}(Max) = T_{1/2}\, V'_{pd}(Eff)$$

where T_m = light pulse width, which, if the energy were delivered at the maximum pulse intensity, $V_{pd}(Max)$, would give the same total energy.

Thus, as a practical convenience for short pulses:

$$\overline{H}_r = B\left(\frac{T_m}{T_{1/2}}\right) V'_{pd}(Max) \qquad \text{(for beam smaller than pupil)} \qquad (19b)$$

and,

$$\overline{H}_r = B'\left(\frac{T_m}{T_{1/2}}\right) V'_{pd}(Max) \qquad \text{(for beam larger than pupil)} \qquad (19c)$$

4. RESULTS

Results of the spectral measurements between 400 and 1100 mu are shown in figures 9, 10, 11 and 12. The solar spectrum, a 5800°K black body spectrum, and the 5800°K black body spectrum modified by a KG-3 filter are shown for comparison in figure 13. In these figures, the spectra are shown normalized to the total irradiance of a 5800°K black body spectrum for this same wavelength region.

Table 1 shows the comparison between the integrated spectral irradiance and the directly measured total irradiance.

Calibration constants appropriate to rabbits, as determined by these measurements, are given below:

$$G_r = \left(\frac{D}{F_r}\right)^2 = \left(\frac{300}{1.0}\right)^2 = 9 \times 10^4$$

D = distance at which calibration measurements were made (cm)

F_r = effective focal length of the rabbit's eye (cm)

$$(T_e)_r = \frac{\int_\lambda R(\lambda)\ T_e(\lambda)\ d\lambda}{\int_\lambda R(\lambda)\ d\lambda} = 0.89$$

where the spectrum is that obtained using a KG-3 filter and the spectral transmission of the clear media of the rabbit eye, $\left[T_e(\lambda)\right]_r$, is taken from Geeraets, et al. (5).

$C = 1.150 \times 10^{-3}$ (calories/cm^2-sec-mv) for Eppley thermopile #6909.

$T_m/T_{1/2}$, as a function of effective pulse length, is shown in figure 14.

From this figure

$T_m/T_{1/2}$ = 0.99 for 1 msec pulse
0.96 for 400 usec pulse
0.90 for 145 usec pulse

S is a constant that is determined prior to each experiment.

5. SUMMARY

Spectral irradiance and total irradiance were measured for the light beam from a modified Zeiss photocoagulator. These measurements were made over the wavelength region 400 - 1100 mu for two high pressure xenon lamps--one a 1600 watt lamp and the other a 2500 watt lamp--for two operating conditions. Spectral measurements show an energy shift towards the blue end of the spectrum with increased current through the lamps.

Total irradiance measured by integrating the spectral irradiance measurements compared favorably with direct measurements of the total irradiance using a black body receiver.

The influence of pulse shape on the total energy determined during the very short pulse was examined and practical procedures for considering this factor was established.

REFERENCES

1. Alexander, T. A., R. L. Bessey, and E. R. Lawler, Jr. Research for Ocular Effects of Thermal Radiation. Final Report of Contract AF 41(609)-2464, Task No. 630103. December 1965.

2. Jacobson, J. H., B. Cooper, and H. W. Najac. Effects of Thermal Energy on Retinal Function. Technical Documentary Report, No. AMRL-TDR-62-96, August 1962.

3. Ham, W. T., et al. Electronically Pulsed Light Source for the Production of Retinal Burns. Am. J. of M. E., Vol. 2, No. 4, pp. 308-315, Oct - Dec 1963.

4. Alexander, T. A., E. R. Lawler, Jr., P. W. Wilson, Jr., and R. I. McDonald. High D. C. Power, Solid-State Switch for Pulsing an Arc Lamp. Review of Sci. Inst., 36, pp. 1707-1709, December 1965.

5. Geeraets, W. J., et al. The Loss of Light Energy in Retina and Choroid. Archives of Ophthalmology, Vol. 64, pp. 606-615, October 1960.

TABLE I

	H (total) using Eppley Thermopile (m cal/cm^2-sec)	H (total) by Spectral Integration (m cal/cm^2-sec)	Percent Difference
2500W Lamp (50V)	7.38	7.03	4.7
2500W Lamp (130V)	23.0	24.3	5.6
2500 Lamp (50V--KG-3)	1.14	1.11	2.7
2500W Lamp (130V--KG-3)	8.13	8.46	4.1
1600W Lamp (50V--KG-3)	2.18	1.88	14.7
1600W Lamp (130V--KG-3)	10.40	9.86	5.2

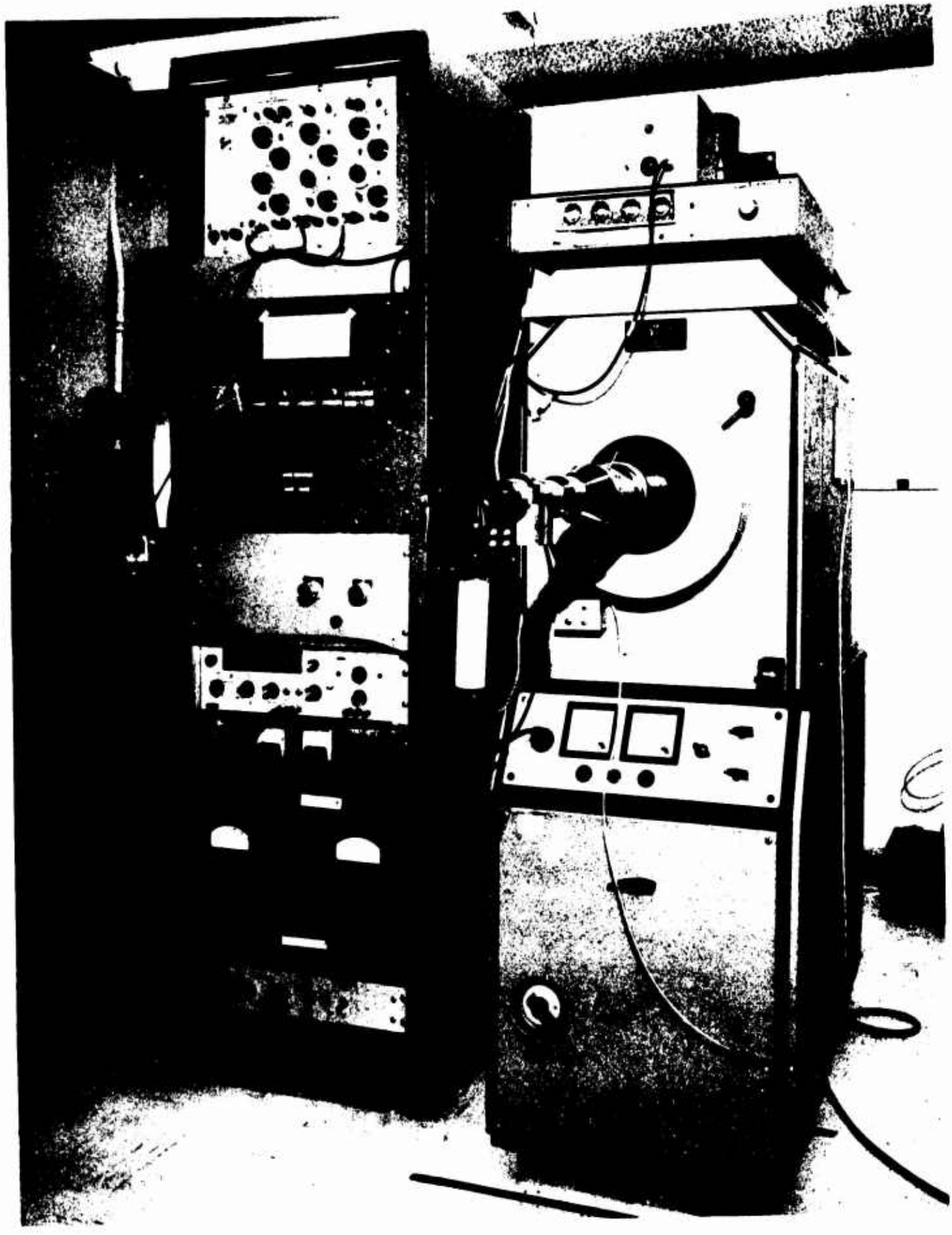

FIGURE 1. Modified light coagulator with auxiliary equipment.

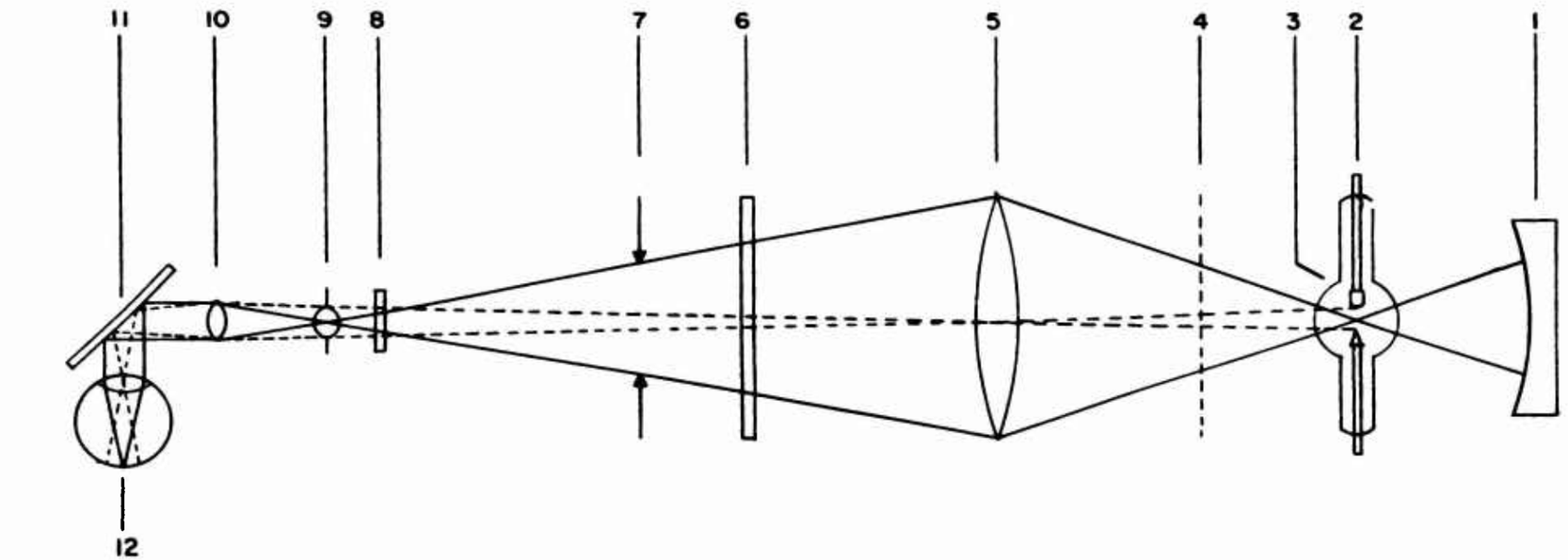

FIGURE 2. Optical beam director.

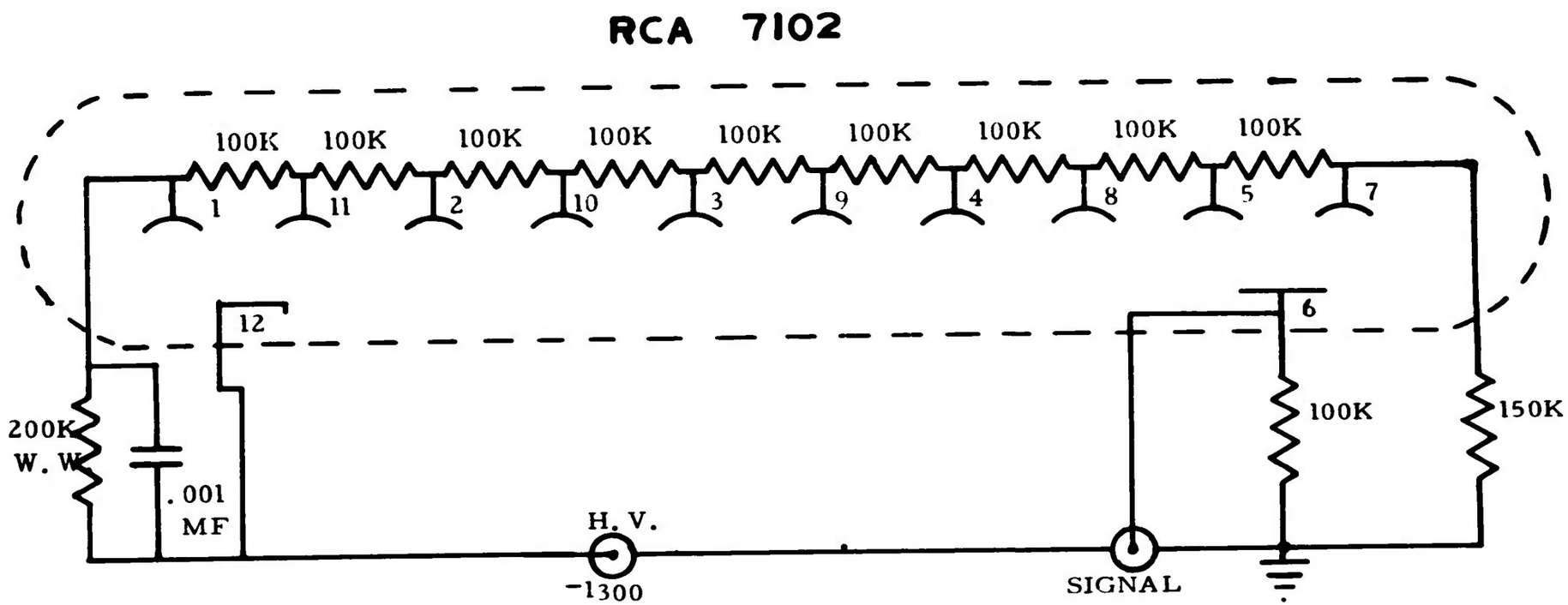

FIGURE 3. Photomultiplier circuit diagram.

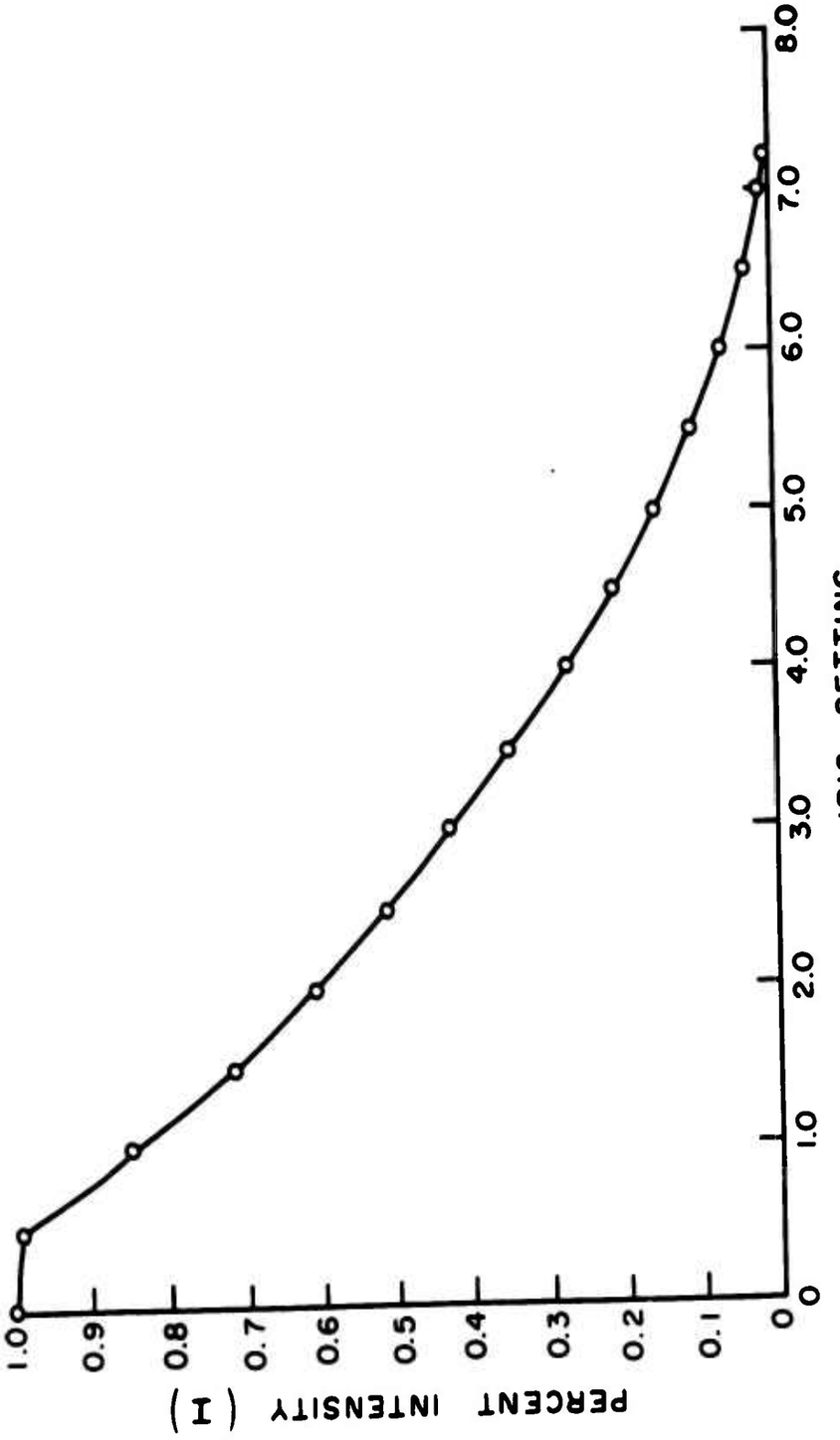

FIGURE 4. Value of intensity I as a function of iris settings.

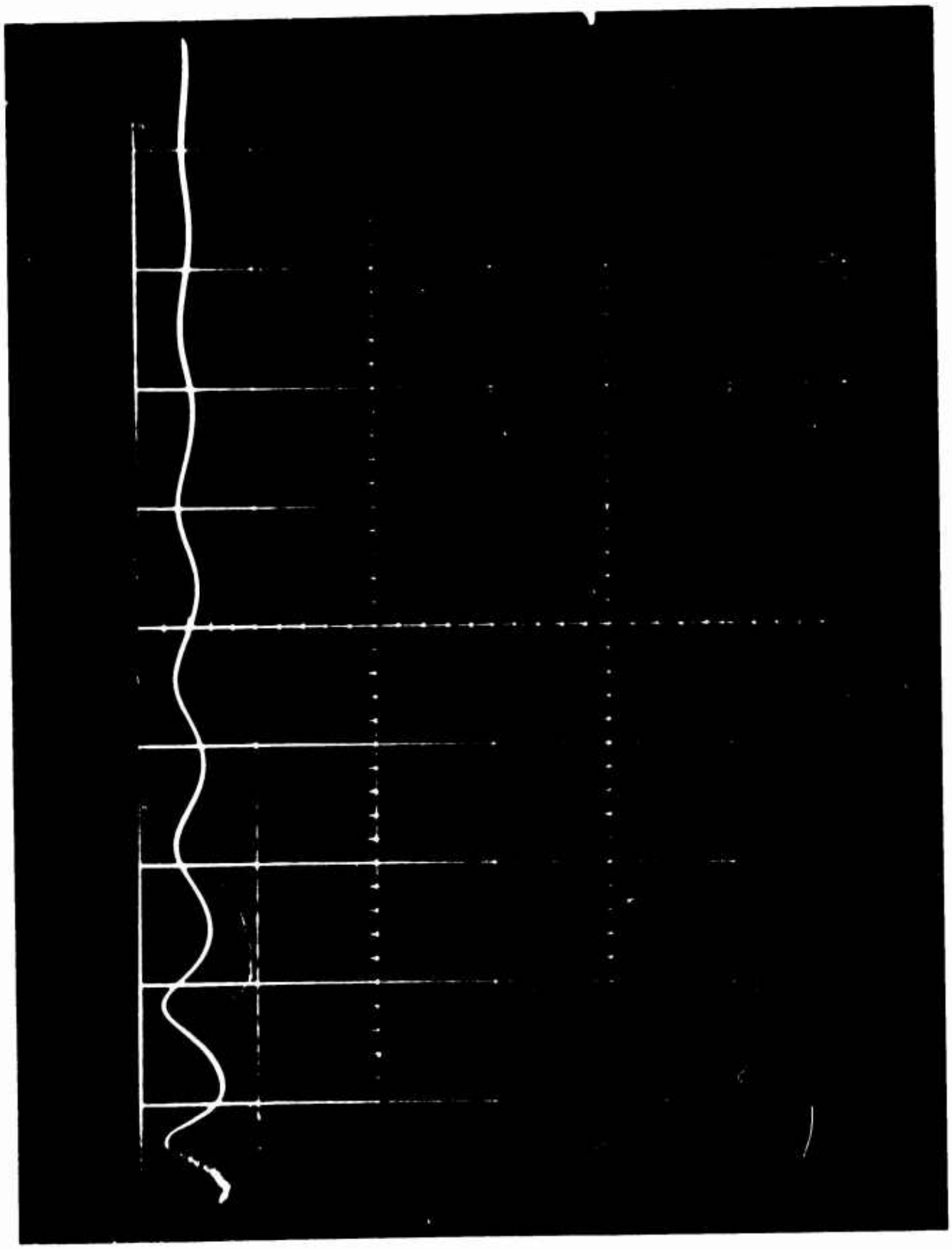

FIGURE 5. Irradiance as a function of time for 100 msecond pulse.

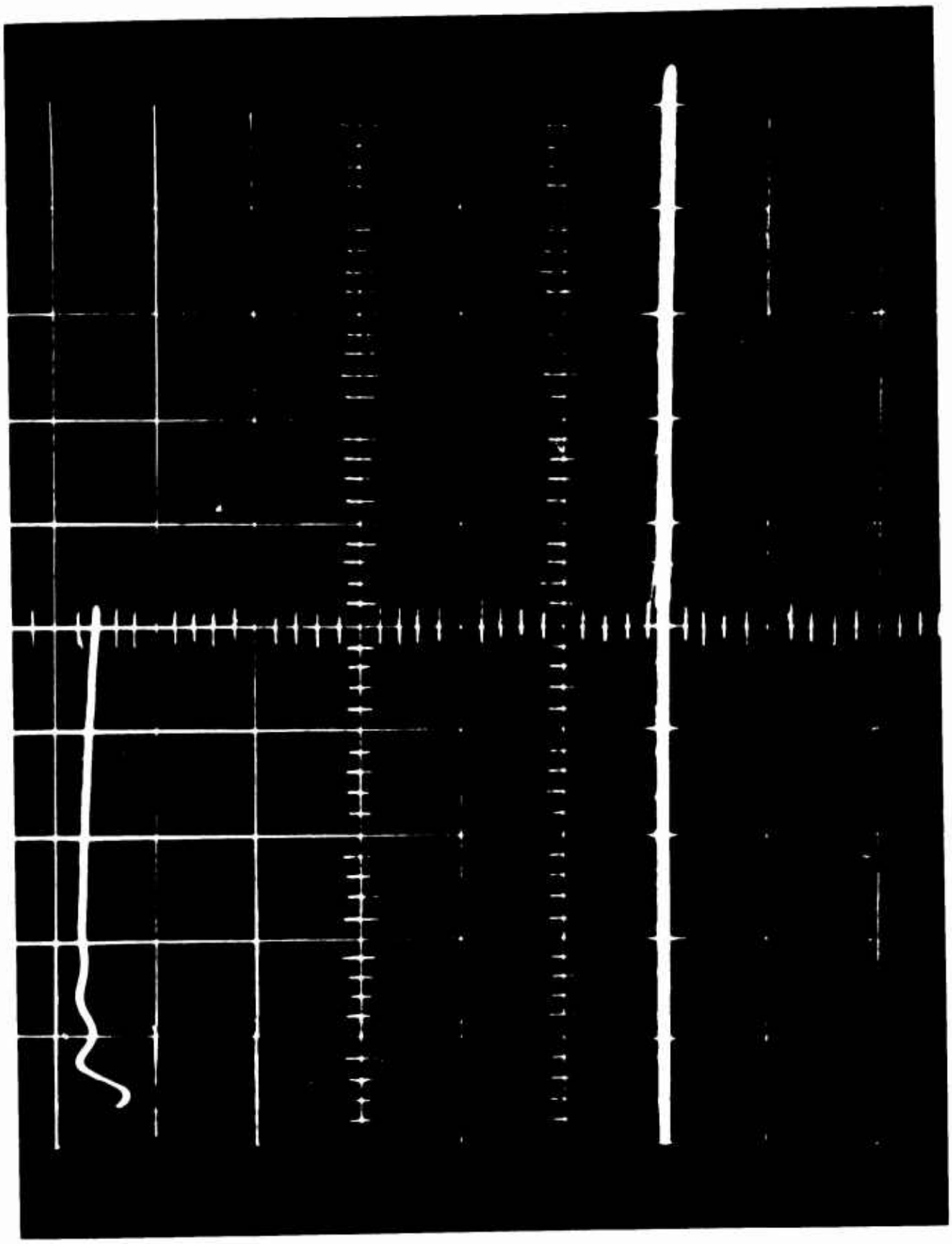

FIGURE 6. Current through lamp as a function of time for 100 msecond pulse.

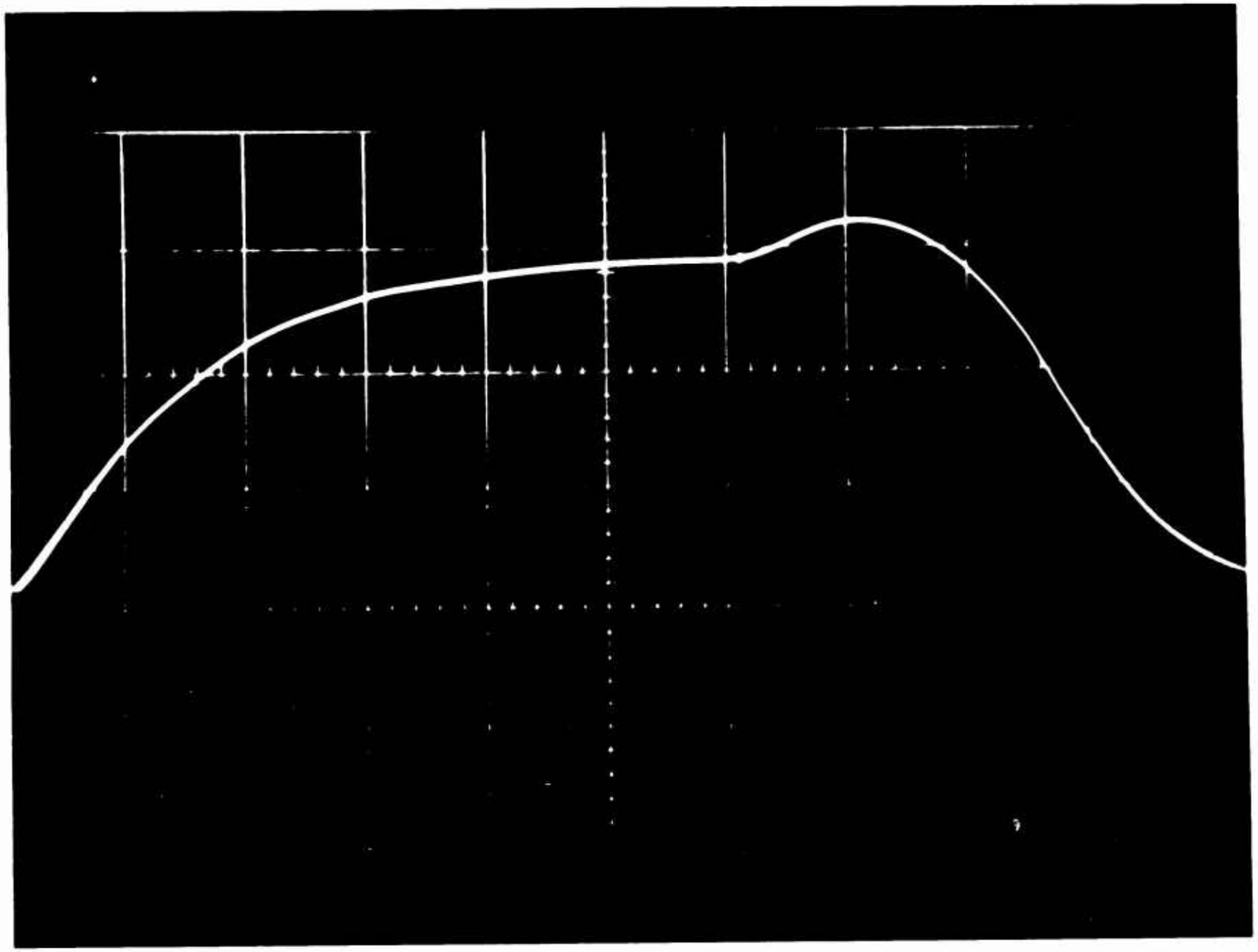

FIGURE 7. Irradiance as a function of time for 1 msecond pulse.

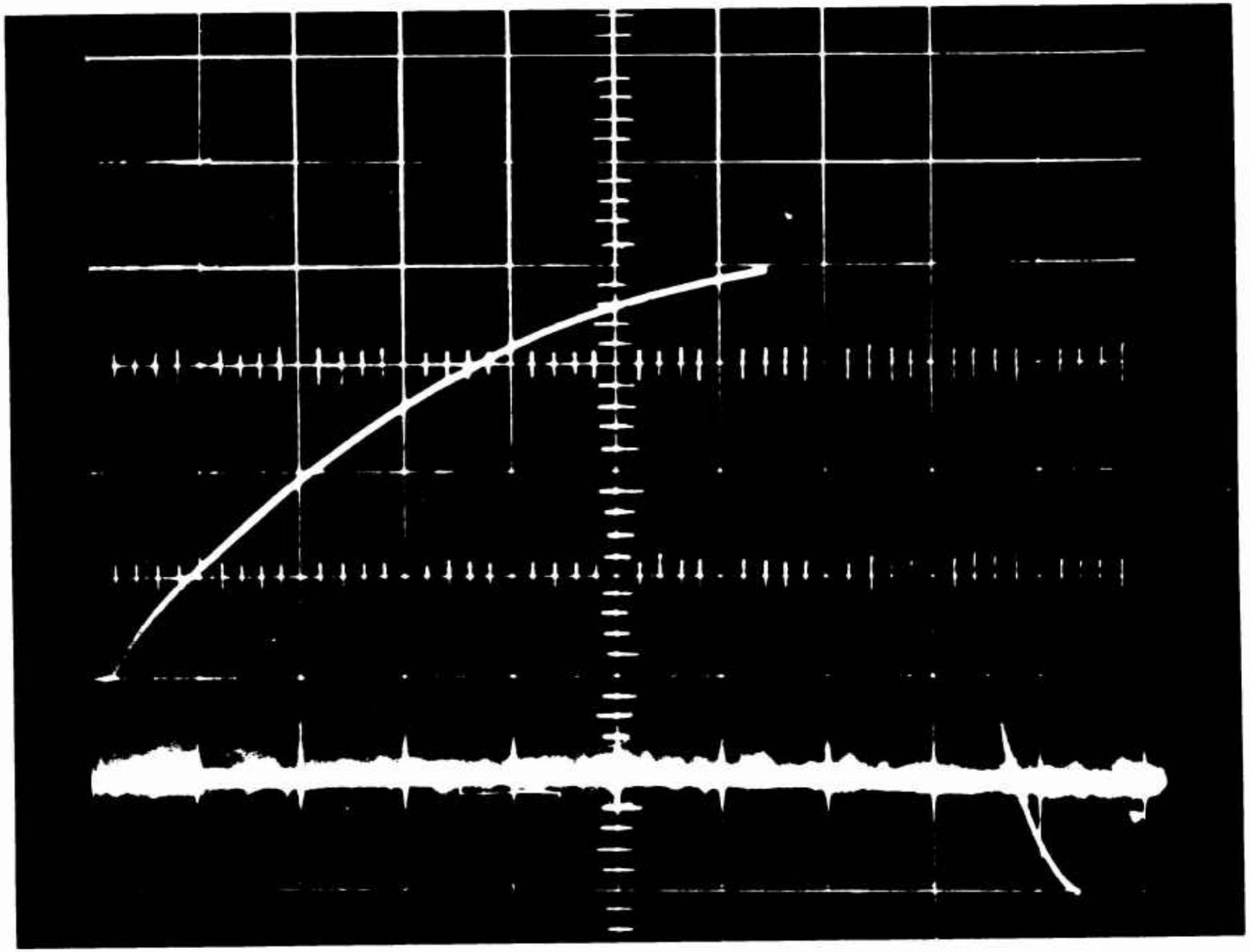

FIGURE 8. Current through lamp as a function of time for 1 msecond pulse.

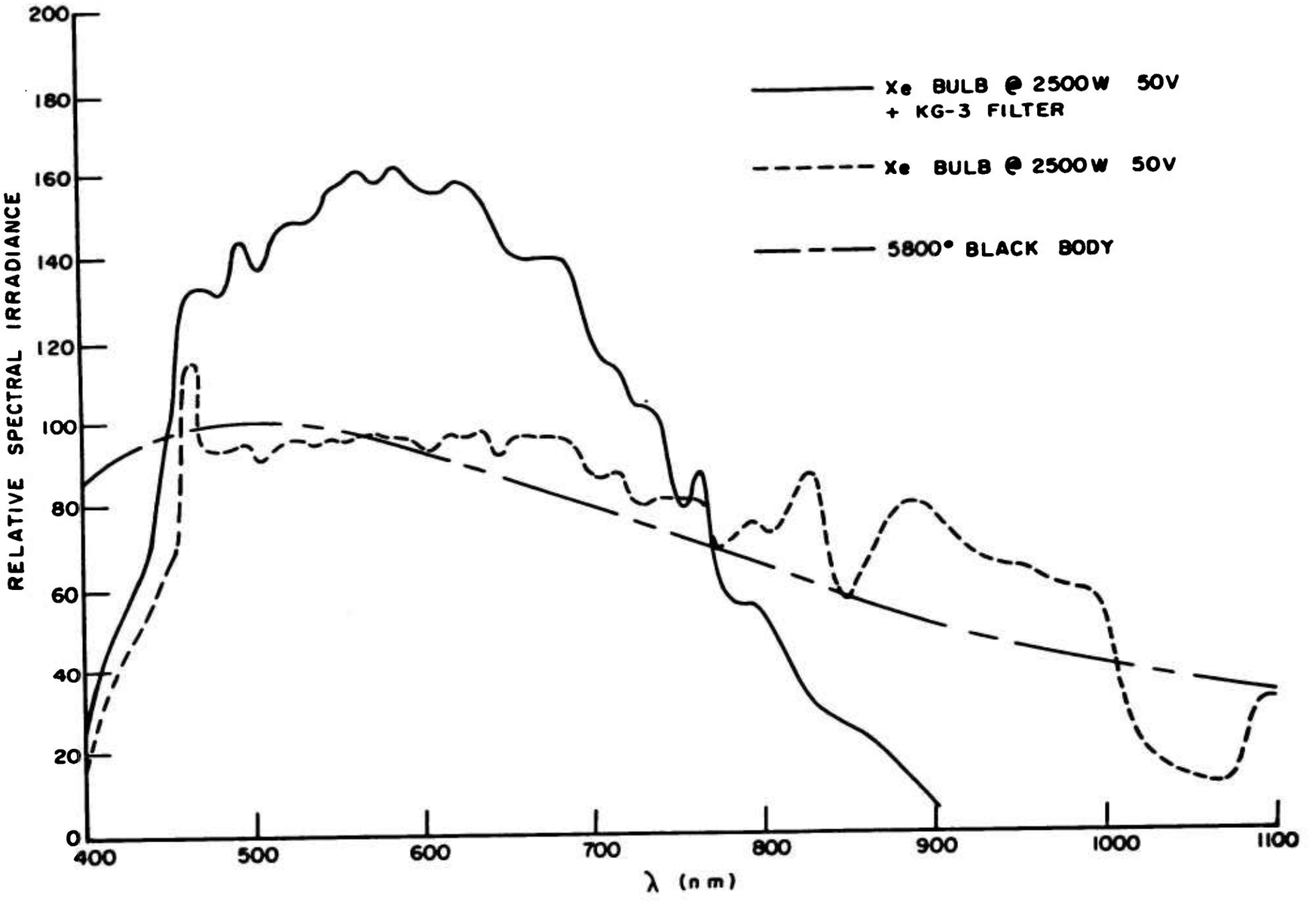

FIGURE 9. Spectral distribution of 2500 watt Xe lamp at 50V with and without KG-3 filter. Spectrum of 5800° black body.

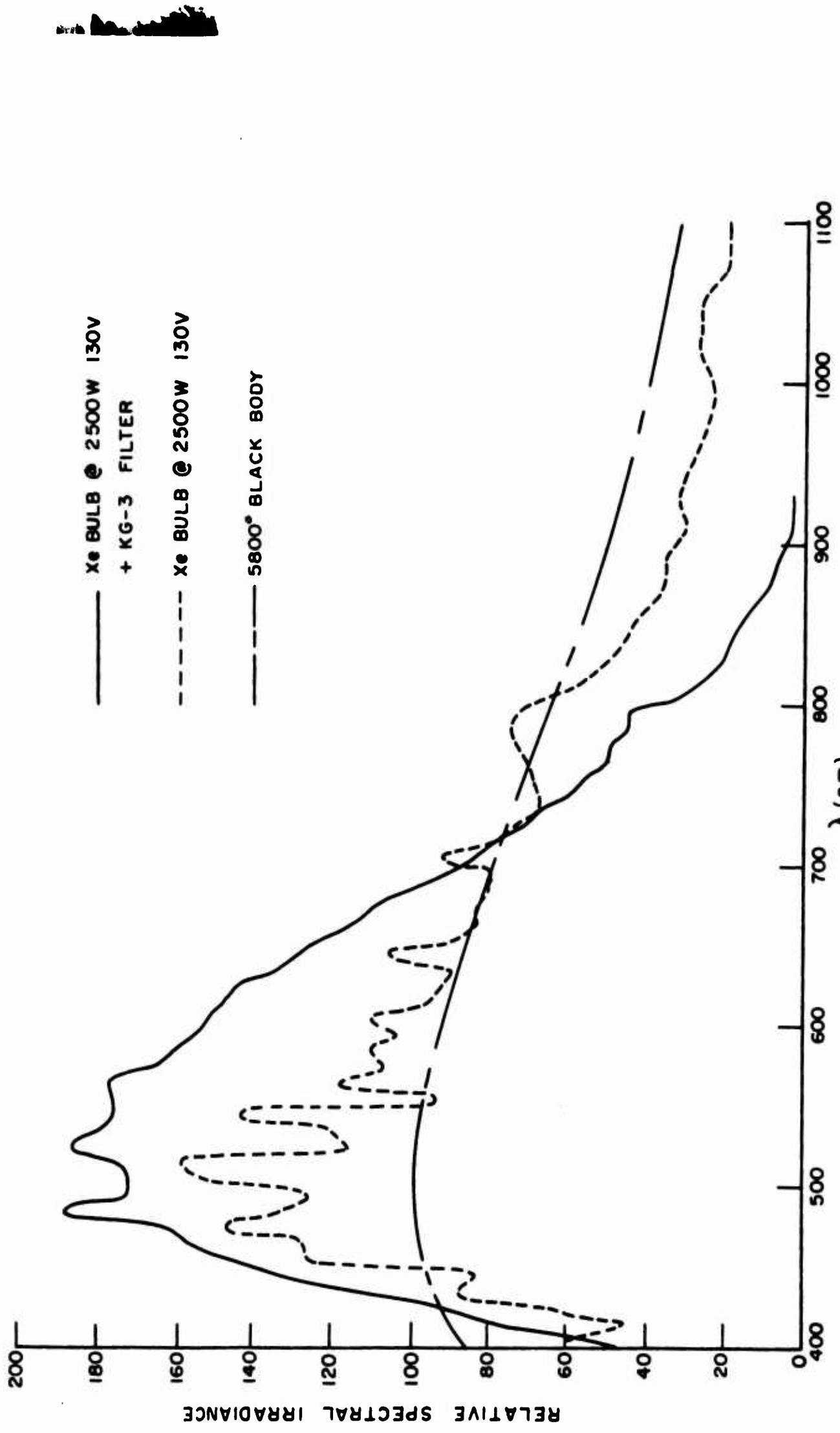

FIGURE 10. Spectral distribution of 2500 watt Xe lamp at 130V with and without KG-3 filter. Spectrum of 5800° black body.

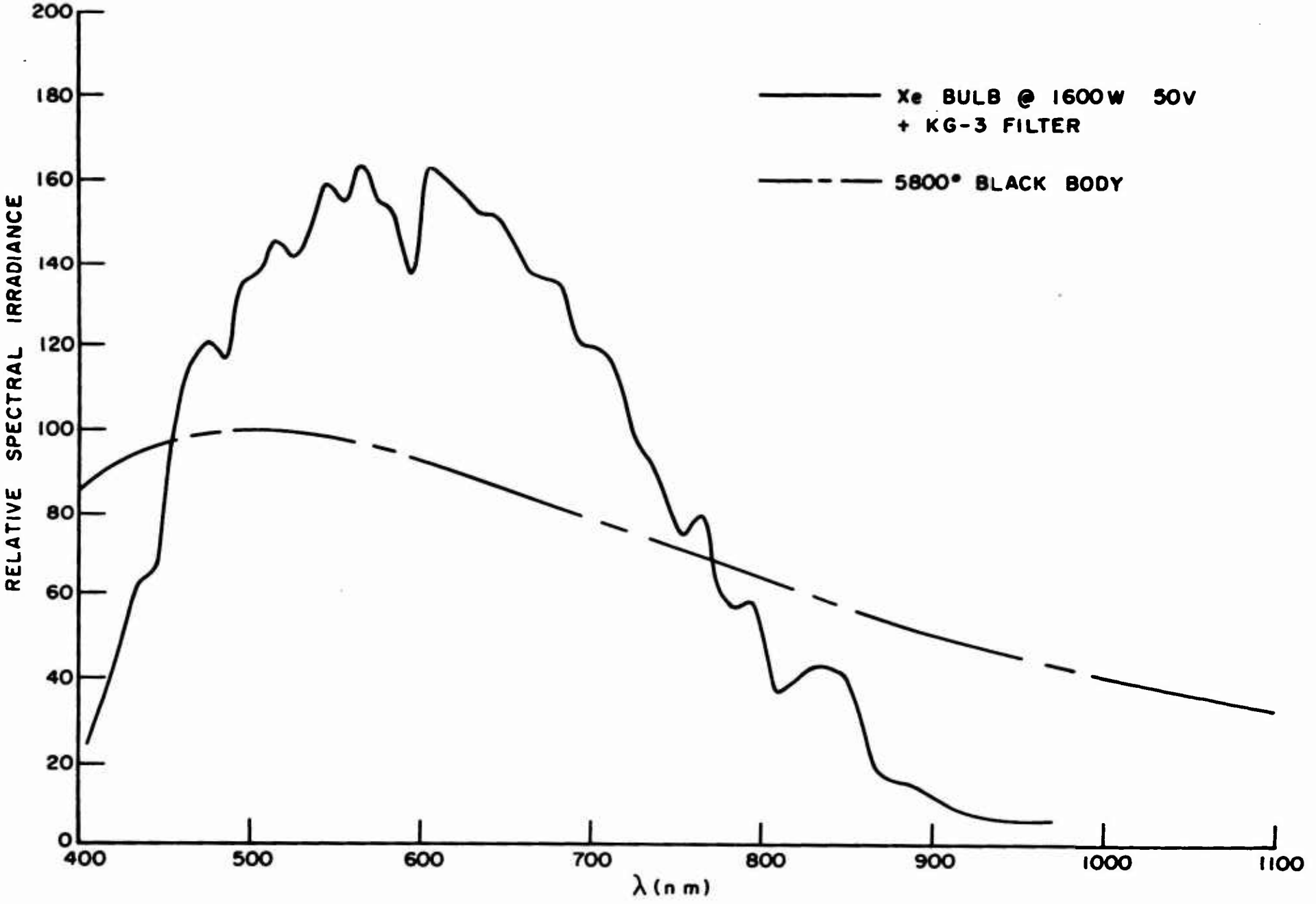

FIGURE 11. Spectral distribution of 1600 watt Xe lamp at 50V with KG-3 filter. Spectrum of 5800° black body.

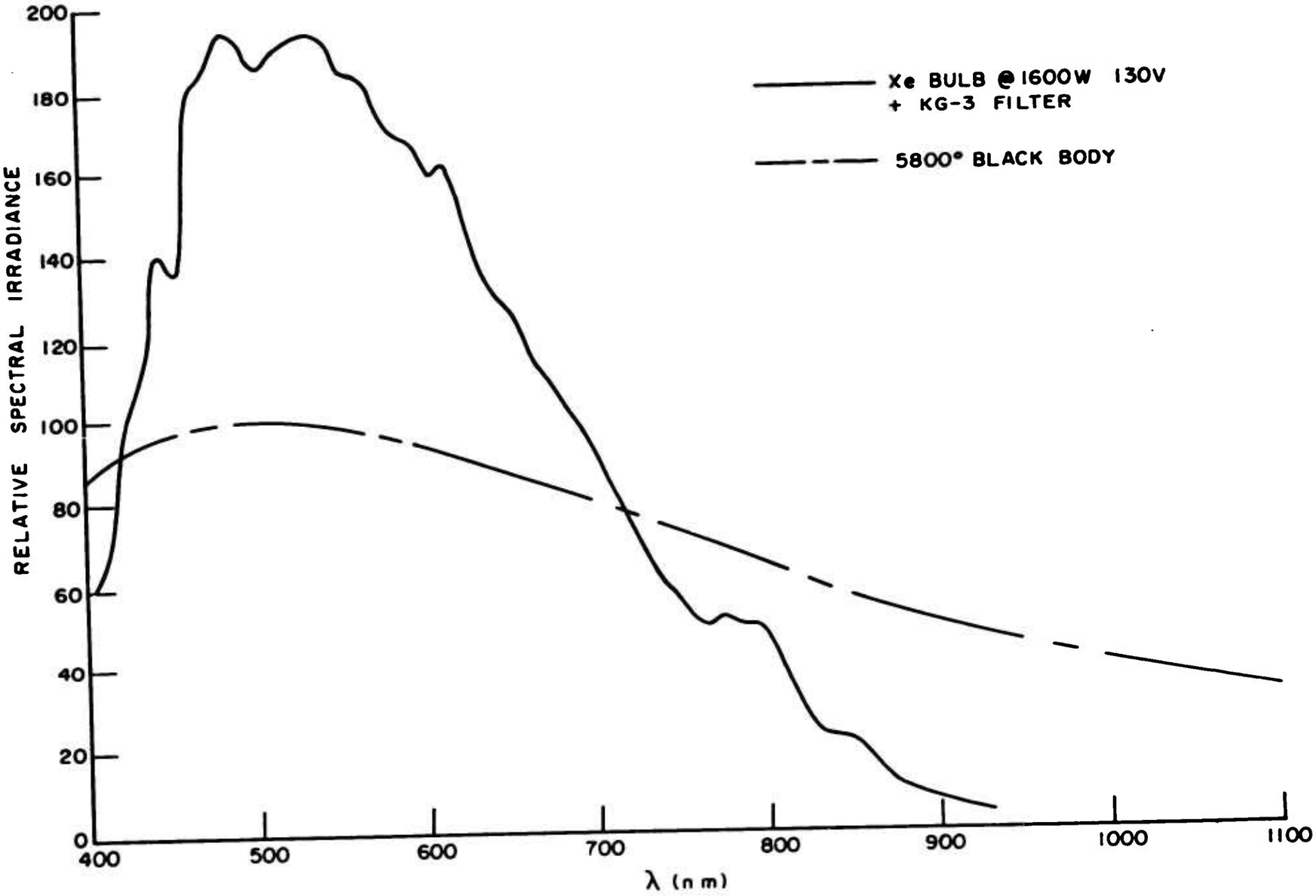

FIGURE 12. Spectral distribution of 1600 watt Xe lamp at 130V with KG-3 filter. Spectrum of 5800° black body.

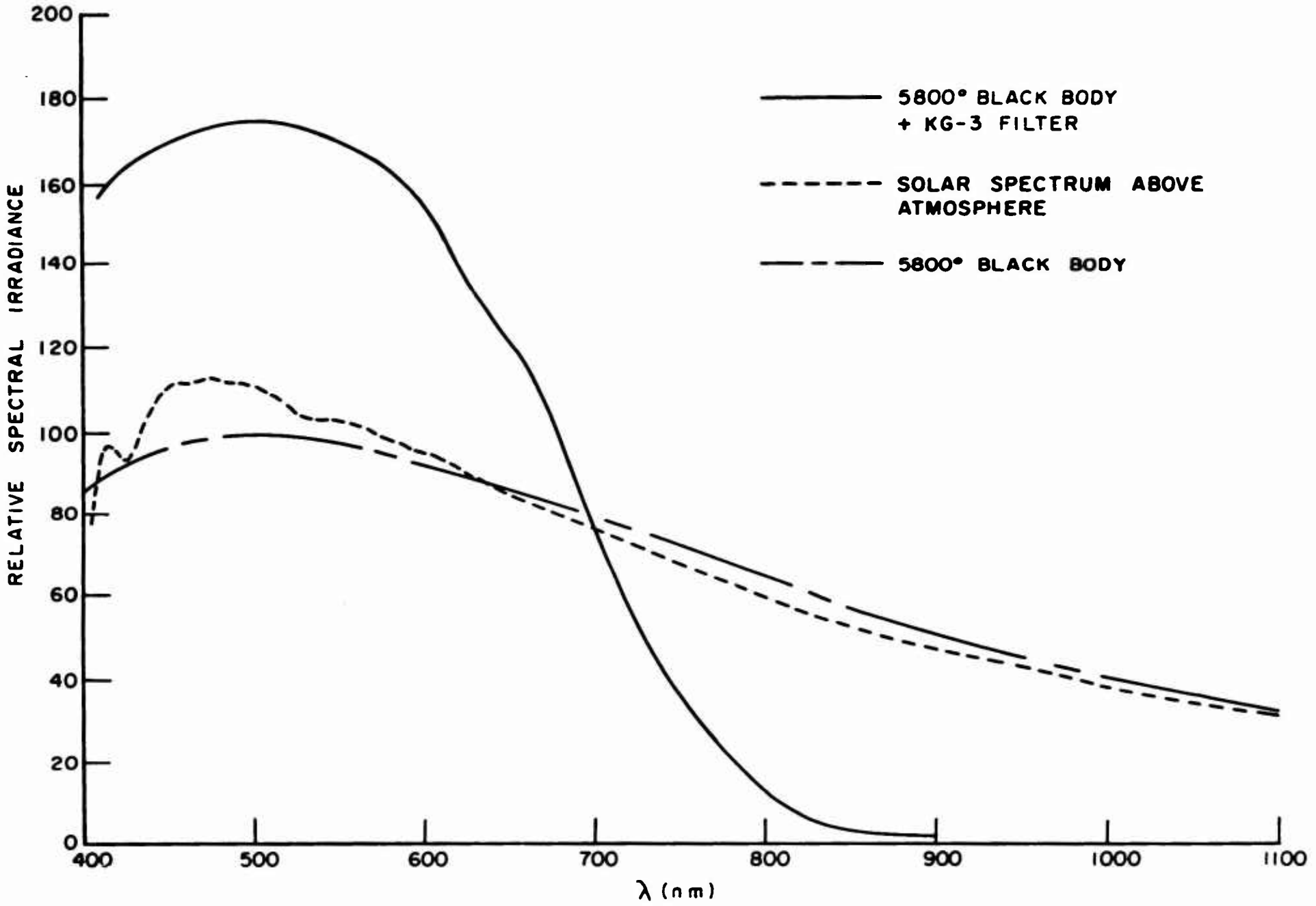

FIGURE 13. Spectrum of 5800° black body with and without KG-3 filter. Solar spectrum above atmosphere.

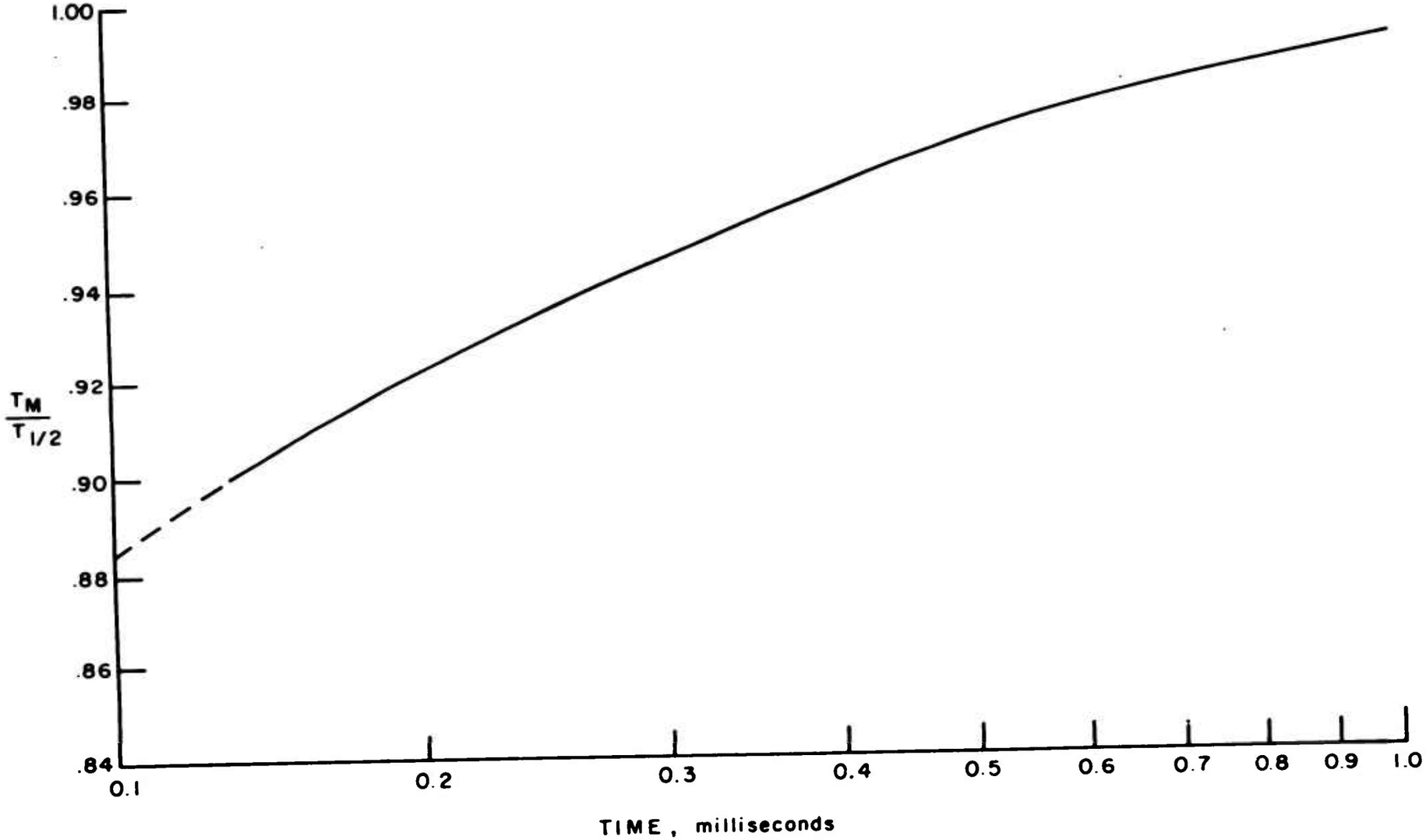

FIGURE 14. Effective pulse length $T_m/T_{1,2}$ vs. time.

BLANK PAGE

OPERATING INSTRUCTIONS FOR MODIFIED ZEISS PHOTO COAGULATOR*

Lawler, E. R., Jr. and W. R. Bruce

*This work was supported by the Department of Ophthalmology, Air Force School of Aerospace Medicine, Brooks Air Force Base, Texas and the Medical Division, Defense Atomic Support Agency, Washington, D. C.

FOREWORD

This report was prepared by personnel of the Life Sciences Division of Technology Incorporated--

Earl R. Lawler, Jr., B.S.

William R. Bruce

The effort was sponsored jointly by the Ophthalmology Branch of the United States Air Force School of Aerospace Medicine, and the Medical Division, Defense Atomic Support Agency, Washington, D. C. Mr. E. O. Richey of the Oculo-Thermal Section was the Contract Monitor during the contractual period. Grateful acknowledgement is made of the assistance provided by Lt. Col. J. F. Culver and Major D. G. Pitts of the Ophthalmology Branch.

TABLE OF CONTENTS

BLANK PAGE

OPERATING INSTRUCTIONS FOR MODIFIED ZEISS PHOTO COAGULATOR

1. GENERAL PURPOSE

The Zeiss light coagulator and associated components are used to produce a high intensity pulsed light for retinal burn studies.

2. DESCRIPTION OF COMPONENTS

The components necessary for operation and calibration of the system (figure 1) are listed below:

For Operation

Manufacturer	Equipment
Tektronix, Incorporated	Waveform generator, Type 162
	Power supply, Type 160A
	Two pulse generators, Type 161
Carl Zeiss	Coagulator
Beckman Instruments, Inc.	Eput and timer, Model 6144
Kepco, Incorporated	Power supply, Type KM255
Lambda Electronics Corp.	Power supply, Model 50
Technology Incorporated	Capacitor bank

Manufacturer	Equipment
Technology Incorporated	D. C. contactor
	Sequential control
	SCR pulse switch
Keeler Optical Products, Inc.	Ophthalmoscope, modified by addition of a control handle and moveable mirror

For Calibration

Manufacturer	Equipment
Edgerton, Germeshausen & Grier, Incorporated	Photodiode SD-100
Tektronix, Incorporated	Oscilloscope, Type 551
	Oscilloscope camera, Type C-12
Eppley Laboratory, Inc.	16 Junction Bismuth-silver thermopile
Hewlett-Packard	D. C. VTVM, Model 412A

Power Requirements

External power: (a) 115 VAC, single phase, 30 amperes, (b) 240 VAC,

3 phase Wye, 200 amperes and (c) a highly stable source of 48 VDC, 200 ampere battery power.

3. BASIC THEORY OF OPERATION

The Xenon lamp may be pulsed from a storage battery source for pulse durations of 10 seconds through 2 milliseconds or from the capacitor bank for pulse durations of 1 millisecond to 145 microseconds.

When the DC contactor is energized—"RUN" light on (green)—the capacitor bank is in parallel with the batteries. When de-energized—"OFF" light on (red)—the capacitor bank is charged from the Kepco power supply.

Pulsing is accomplished by energizing a push button switch on the ophthalmoscope handle. This energizes a relay in the sequential control (figure 2) which energizes the shutter relay in the Zeiss coagulator which in turn starts the operation of the waveform generator. The output of the waveform generator triggers the "on" and "off" pulse generators. A composite of the outputs of the pulse generators is shown in figure 3. The "on" pulse width in figure 3 has been expanded from .01 msec to 1 msec to enable both pulses to be observed. The "on" pulse (figure 4) furnishes a square wave which triggers the silicon control rectifiers, this in turn causes the capacitor to be discharged through the Xenon lamp. The "off" pulse (figure 5) furnishes a bias to turn off the Silicon control rectifiers at

the preset time of the waveform generator. The Eput Timer is triggered by the on-off pulse to give a visual readout of pulse durations.

The Kepco power supply furnishes a DC potential to charge the capacitor bank during capacitor bank operation. It also provides a trickle charge to the batteries during battery operation.

The Lambda power supply furnishes a DC potential for commutation of the SCR pulse switch to turn off the Xenon lamp.

4. CALIBRATION AND OPERATION

Turn-on Procedure

Turn off and disconnect battery charger.

Turn on main power to relay rack.

Turn on the following equipment:

Lambda, Kepco and Tektronix power supplies.

SCR pulse switch

Sequential control box

Photodiode

Oscilloscope

Vacuum tube voltmeter

Eput-timer to follow position.

On the coagulator, set the multi-stage switches for normal load and overload to R position, selector switch down (Page 15, Coagulator Instruction Manual). On the back of the coagulator, push simmer to the "UP" position and set the coagulator protective switch to position I. Press Red I, "Switch on Key". Move the knife switch, on the back of coagulator, to depress the microswitch with handle. WARNING: DEPRESS MICROSWITCH WITH KNIFE SWITCH HANDLE ONLY. When the Xenon lamp ignites, engage knife switch into slot. This bypasses the coagualtor ignitor system.

Calibration

Battery Operation

Connect the output of the photodiode to the oscilloscope; the thermopile to the vacuum tube voltmeter, and the camera shutter cable to the sequential control. Remove the ophthalmoscope handle from the optical beam director (figure 6). Disconnect the shutter cable from the coagulator and insert the dummy plug to energize the shutter relay.

Position the iris diaphram to its fully open position (zero setting) and place the image field diaphram on 6. Focus the image at 300 cm from the lens by adjusting the position of the objective lens barrel.

Check lamp electrode focusing as outlined on page 18 of the Zeiss Light Coagulator Instruction Manual.

Set the image field diaphram to 0.5. Place the thermopile in the light beam 300 cm from the objective lens. Position the thermopile at the center of the light beam with the beam reflecting to the immediate right or left of the objective lens.

Remove the dummy plug and reconnect the cable from the sequential control. Push the simmer switch down, this will maintain a low keep alive current, thus prevent excessive heating of the Xenon lamp. Adjust the "pulse interval" and "multiplier" control on the waveform generator for a pulse of 1 second--as read on the Eput-timer. Adjust the Kepco power supply to 50 VDC and the Lambda to 100 VDC. Energize the "Run" switch (green) on the DC contactor, and readjust the Kepco to 0.5 AMPS.

Push the "Reset" switch on the SCR Pulse Switch. The "Standby" light will go off and the "Ready" light on. Press the switch on the ophthalmoscope handle to pulse the coagualtor and observe the oscilloscope. It should take no more than two or three, one second pulses to properly adjust the oscilloscope. On the oscilloscope set the sweep time control to 1 second/cm and turn scale illumination

and beam intensity very low to prevent over exposure of film during the 10 second pulse.

Turn on oscilloscope camera, check film and close camera viewing door.

Set the waveform generator for 10 second pulse duration, and the scale of the VTVM to 3 mv full scale.

Reset the SCR pulse switch. While observing the VTVM, pulse the coagualtor, and record the response of the Eppley thermopile. From the film, record the amplitude of the photodiode pulse.

The Eppley thermopile is used only for the 10 second pulse and need not be observed during the remainder of the calibration.

Set the waveform generator and oscilloscope to record, on film, the response of the photodiode for each pulse width of interest. This completes the pulsing for calibration on battery operation.

Capacitor Bank Operation

Push the "OFF" switch (red) on the DC contactor. This disconnects the batteries from the capacitor bank. Set the Kepco to 100 VDC and the Lambda to 300 VDC.

During capacitor bank operation of 1 msec, allow 60 microseconds for commutation discharge by setting the waveform generator to 940 microseconds. For a 400 microsecond pulse, allow 80 microseconds for commutation by setting the waveform generator to 320 microseconds.

For a "snuff-out" or approximately 145 microsecond pulse, it is only necessary to adjust the Kepco to maximum voltage.

Pulse the coagulator and record the amplitude of each pulse as in battery operation. This completes the calibration measurements.

To prepare the coagulator for use, refocus the field lens and mount the ophthalmoscope handle. If the coagualtor is not to be used immediately, set for battery operation with a 0.5 amp charge to the batteries from the Kepco.

5. IRRADIANCE CALCULATIONS

Irradiance calculations are determined from the information recorded during calibration procedure in the following manner:

$$\overline{H}_r' = V_E \times 92.12 \ \frac{\text{cal}}{\text{cm}^2\text{-sec}}$$

V_E = Voltage reading in mv of the thermopile (at 10 seconds).

92.12 = Calibration factor of the Eppley thermopile No. 6909 at 300 cm from field lens.

H_r' = Average irradiance for the 10 second pulse.

then

$$H_r = H_r' \times \frac{V_{pd}}{V_{pd}'}$$

H_r = Average irradiance for pulse durations.

$\frac{V_{pd}}{V_{pd}'}$ = The photodiode voltage of the specified pulse divided by the photodiode voltage of the 10 second calibration pulse.

The following information is given as a guide for calibration but will vary somewhat with Xenon lamp electrode aging and positioning.

V_E (thermopile reading at 10 sec) = 4.80 mV

$$H_r' = V_E \times 92.12 \frac{cal}{cm^2\text{-sec}} = 442.2 \frac{cal}{cm^2\text{-sec}}$$

Photodiode Readings

Battery Operation

Time	10 sec	50 msec	40 msec	10 msec	4 msec
Volts	1.17V	1.35V	1.43V	1.50V	1.52V
$\frac{V_{pd}}{V_{pd}'}$	1.00	1.154	1.222	1.282	1.299

Capacitor Bank Operation

Time	1 msec	0.4 msec	0.145 msec
Volts	2.40V	3.1V	3.6V
$\frac{V_{pd}}{V'_{pd}}$	2.051	2.650	3.077

H_r = 442.2 x 1.154 = 510.3 $\frac{cal}{cm^2\text{-sec}}$ (50 msec pulse)

H_r = 442.2 x 1.222 = 540.5 $\frac{cal}{cm^2\text{-sec}}$ (40 msec pulse)

H_r = 442.2 x 1.282 = 566.9 $\frac{cal}{cm^2\text{-sec}}$ (10 msec pulse)

H_r = 442.2 x 1.299 = 574.4 $\frac{cal}{cm^2\text{-sec}}$ (4 msec pulse)

H_r = 442.2 x 2.051 = 907.0 x 0.99* = 898 $\frac{cal}{cm^2\text{-sec}}$ (1 msec pulse)

H_r = 442.2 x 2.650 = 1172 x 0.96* = 1125 $\frac{cal}{cm^2\text{-sec}}$ (0.4 msec pulse)

H_r = 442.2 x 3.077 = 1361 x 0.90* = 1225 $\frac{cal}{cm^2\text{-sec}}$ (0.145 msec pulse)

* Integrated waveform correction factor.

For a detailed explanation of the irradiance calibration procedure refer to reference (2).

6. EXPOSURE PROCEDURE

Place the animal in position and examine the fundus using the

Keeler ophthalmoscope on the Zeiss beam director. Select the cone size which corresponds to the image size desired and set pulse duration desired into the equipment. The irradiance that will produce a "5-minute" minimal retinal burn may then be determined in the following manner: Using the irradiance obtained from the calibration procedure for the particular pulse duration being investigated and the graph of H_r vs time for 5 minute minimal burns (See figure 7) select an H_r that is approximately twice the energy expected to produce a minimal burn. This irradiance is obtained by adjusting the iris diaphram--which acts as an attenuator (See table 1). An exposure at the setting is then made and should produce a definite burn. It will be used as a reference or marker burn. The irradiance may then be decreased in steps until a minimal burn is observed. For a more detailed explanation of exposure procedure and calibration, see reference (1) and (3).

7. MAINTENANCE

Preventive Maintenance

The instruction manual of the individual components should be referred to for detailed operation, maintenance and calibration (4) and (5). Xenon bulb and high voltage connectors should be checked for security of mounting once each month. Clean and lubricate knife switch pivot when

corrosion appears. Replace carbon granules in ozone filter when ozone is detected. Check mounting and security of shutter microswitch in the coagulator and burnish all points on the D. C. contactor every six months.

Troubleshooting

Symptom	Probable Cause
Xenon lamp fails to turn OFF on battery Operation.	PUSH RED "OFF" BUTTON ON DC CONTACTOR. Lambda voltage set too low.
Double pulsing of Xenon lamp	Microswitch on the coagulator shutter out of adjustment.
Xenon lamp output irregular	Dirty or corroded DC contactor, battery connections, high voltage interconnect cables.
Xenon lamp premature turn-off at 400 microseconds and 1 msec.	Kepco power supply voltage too high.
Xenon lamp fails to commutate on capacitor bank operation.	Lambda voltage set too low.
Standby and ready light on SCR Pulse Switch both stay on after pulsing.	Turn off 28V supply for 10 seconds then turn on. Check Lambda and Kepco voltages.
Ophthalmoscope mirror sticks in "up" position.	Turn off sequential control, check cables, and turn on.

REFERENCES

1. Alexander, T. A., R. L. Bessey, and E. R. Lawler, Jr. Ocular Effects of Thermal Radiation. Final Report of Air Force Contract AF 41(609)-2464, Task No. 630103, 1965.

2. Bessey, R. L. and R. G. Allen, Jr. Calibration of Zeiss Photo Coagulator. Technical Report, Technology Incorporated, 1966.

3. Alexander, T. A., et al. A Study of the Production of Chorioretinal Lesions by Thermal Radiation. Progress Report of Air Force Contract AF 41(609)-2906, 1966.

4. Alexander, T. A., E. R. Lawler, Jr., P. W. Wilson, Jr., and R. I. McDonald. High D. C. Power, Solid-State Switch for Pulsing an Arc Lamp. Review of Scientific Instruments, 36, pp. 1707-1709, December 1965.

5. Operating and Service Manuals for:

   Hewlett-Packard - 412A Vacuum Tube Voltmeter

   Tektronix - 160 Series Equipment

   Zeiss Light Coagulator

   Lambda - Model 50 Regulated Power Supply

   Kepco - Model KM-255 Power Supply

   Beckman - Model 6144 Eput and Timmer

Storage Batteries - Type MA-2, Sec. T. O. 8D2-3-1

Tektronix - Type 551 Dual Beam Oscilloscope and Power Supply

Tektronix - Type C-12 Oscilloscope Camera

TABLE 1

Iris settings vs. attenuations

0	.1	.2	.3	.4	.5
100%	100%	100%	100%	100%	99.6
	.6	.7	.8	.9	1
	96.7	93.8	90.6	87.5	84.4
	1.1	1.2	1.3	1.4	1.5
	81.8	79.5	77.0	74.5	71.7
	1.6	1.7	1.8	1.9	2.0
	69.7	67.4	65.2	62.8	60.5
	2.1	2.2	2.3	2.4	2.5
	58.4	56.5	54.6	52.8	51.0
	2.6	2.7	2.8	2.9	3.0
	49.1	47.5	45.7	44.0	42.5
	3.1	3.2	3.3	3.4	3.5
	40.6	39.3	37.8	36.3	35.0
	3.6	3.7	3.8	3.9	4.0
	33.4	31.9	30.4	28.8	27.5
	4.1	4.2	4.3	4.4	4.5
	26.2	25.0	23.5	22.2	21.0
	4.6	4.7	4.8	4.9	5.0
	20.0	18.8	17.7	16.7	15.6
	5.1	5.2	5.3	5.4	5.5
	14.5	13.5	12.5	11.1	10.5
	5.6	5.7	5.8	5.9	6.0
	9.75	8.90	8.00	7.30	6.50

TABLE 1 (Cont'd)

Iris settings vs. attenuations

	6.1 5.80	6.2 5.20	6.3 4.50	6.4 3.80	6.5 3.20
	6.6 2.70	6.7 2.20	6.8 1.70	6.9 1.40	7.0 1.00
	7.1 0.60	7.2 0.50			

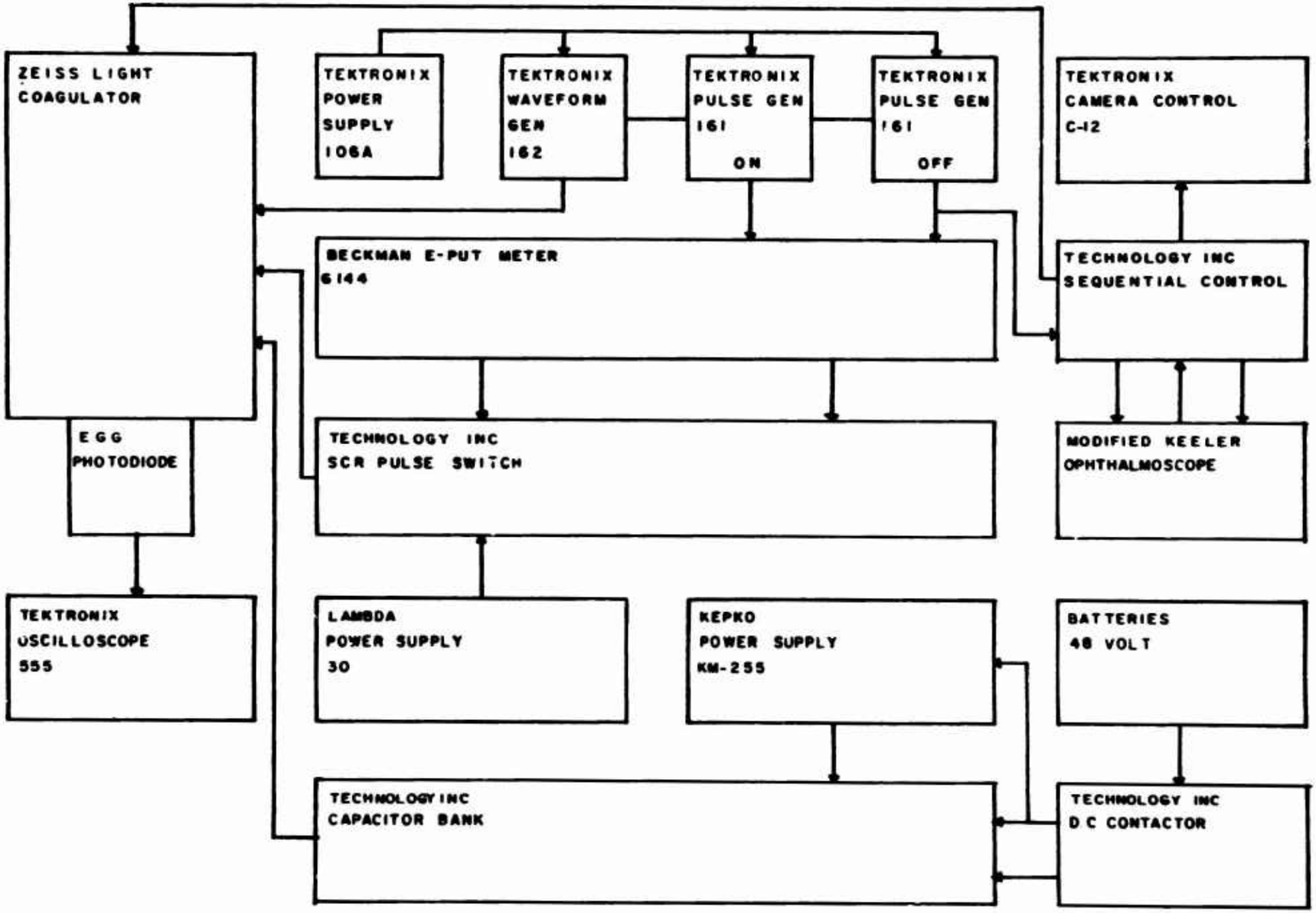

HIGH INTENSITY PULSED LIGHT SYSTEM

FIGURE 1. High intensity pulsed light system, block diagram.

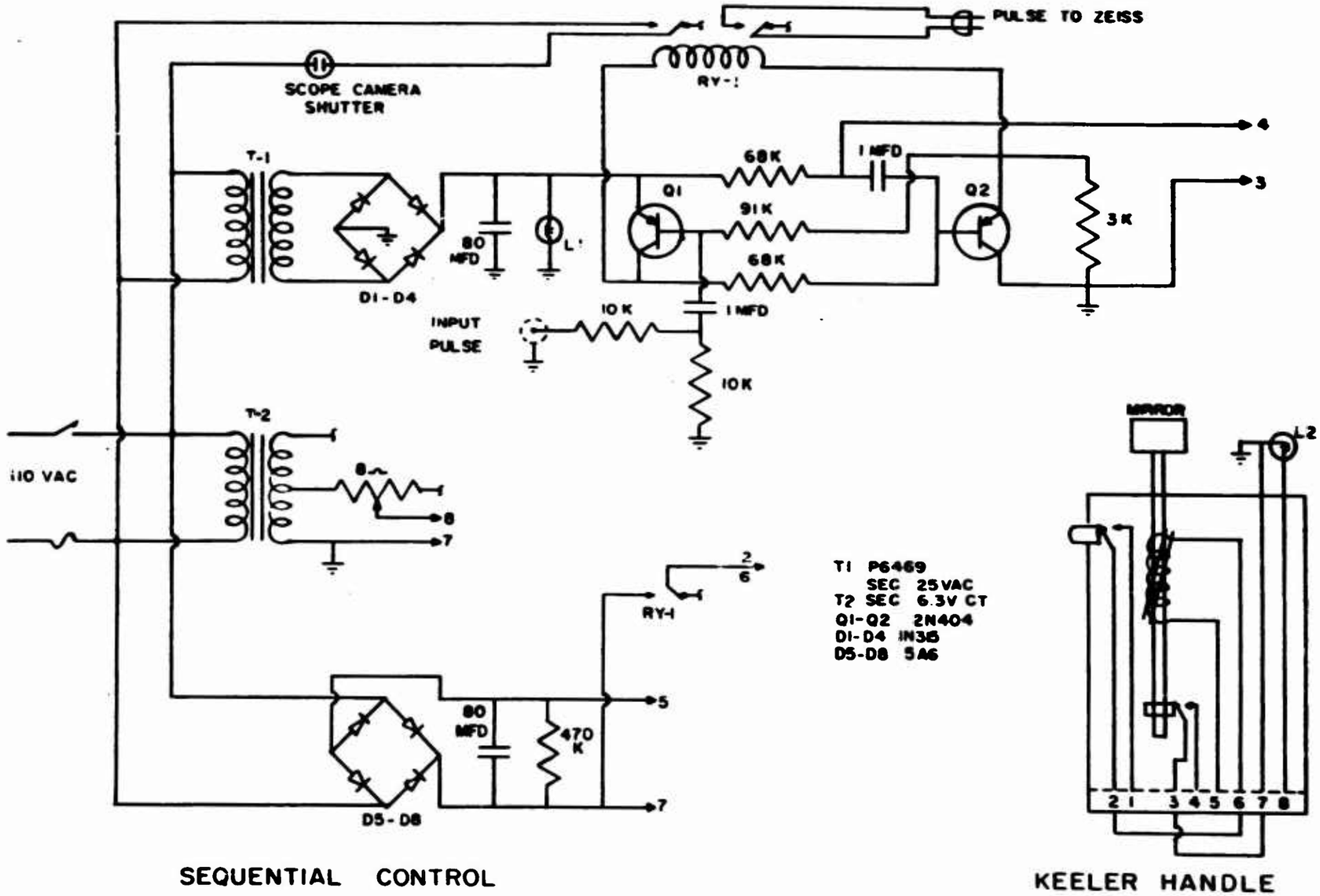

FIGURE 2. Sequential control and Keeler handle circuit diagram.

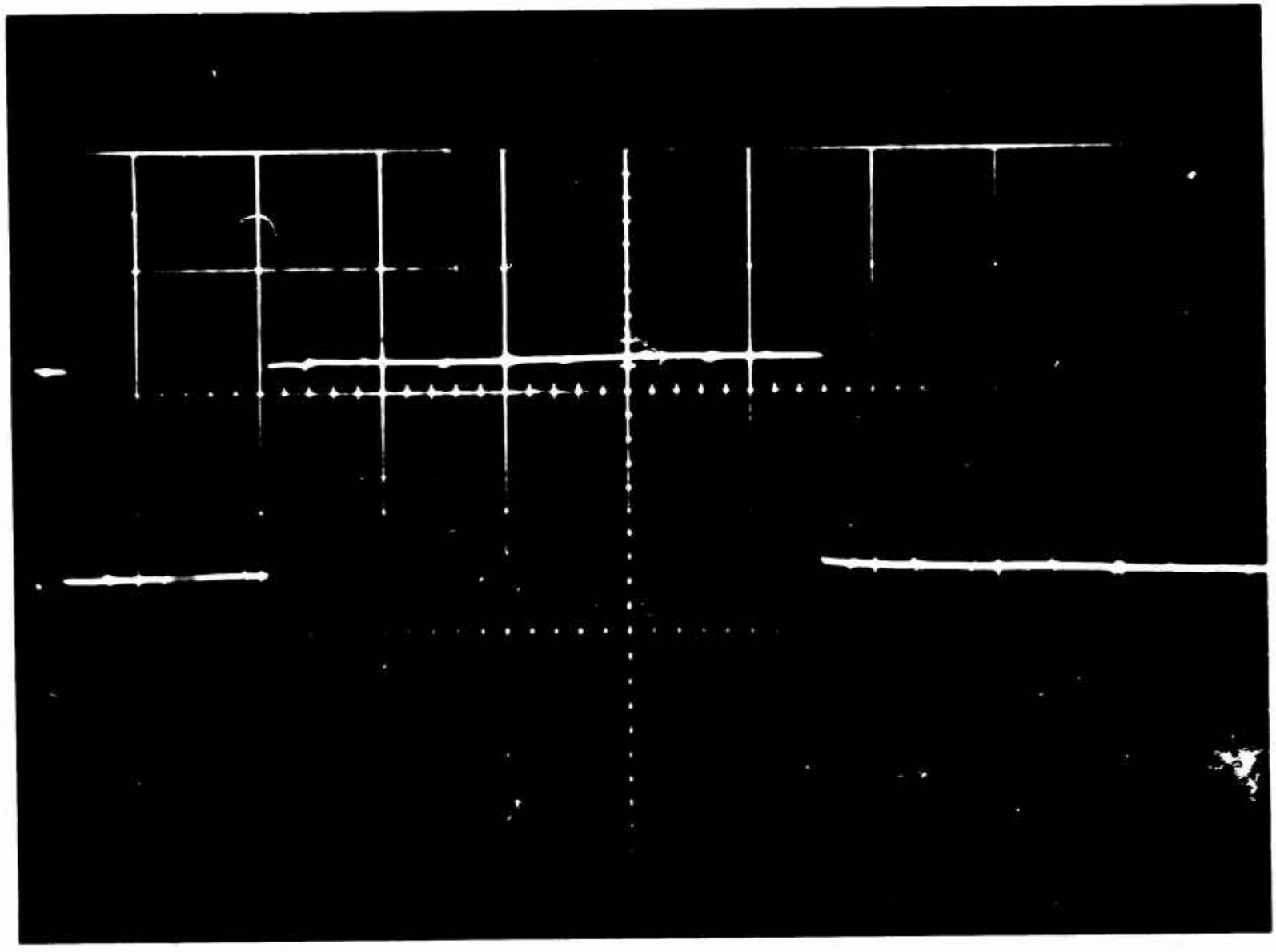

FIGURE 3. Composite turn "on" and "off" pulse. Oscilloscope set at 5 msec/cm and 10 v/cm.

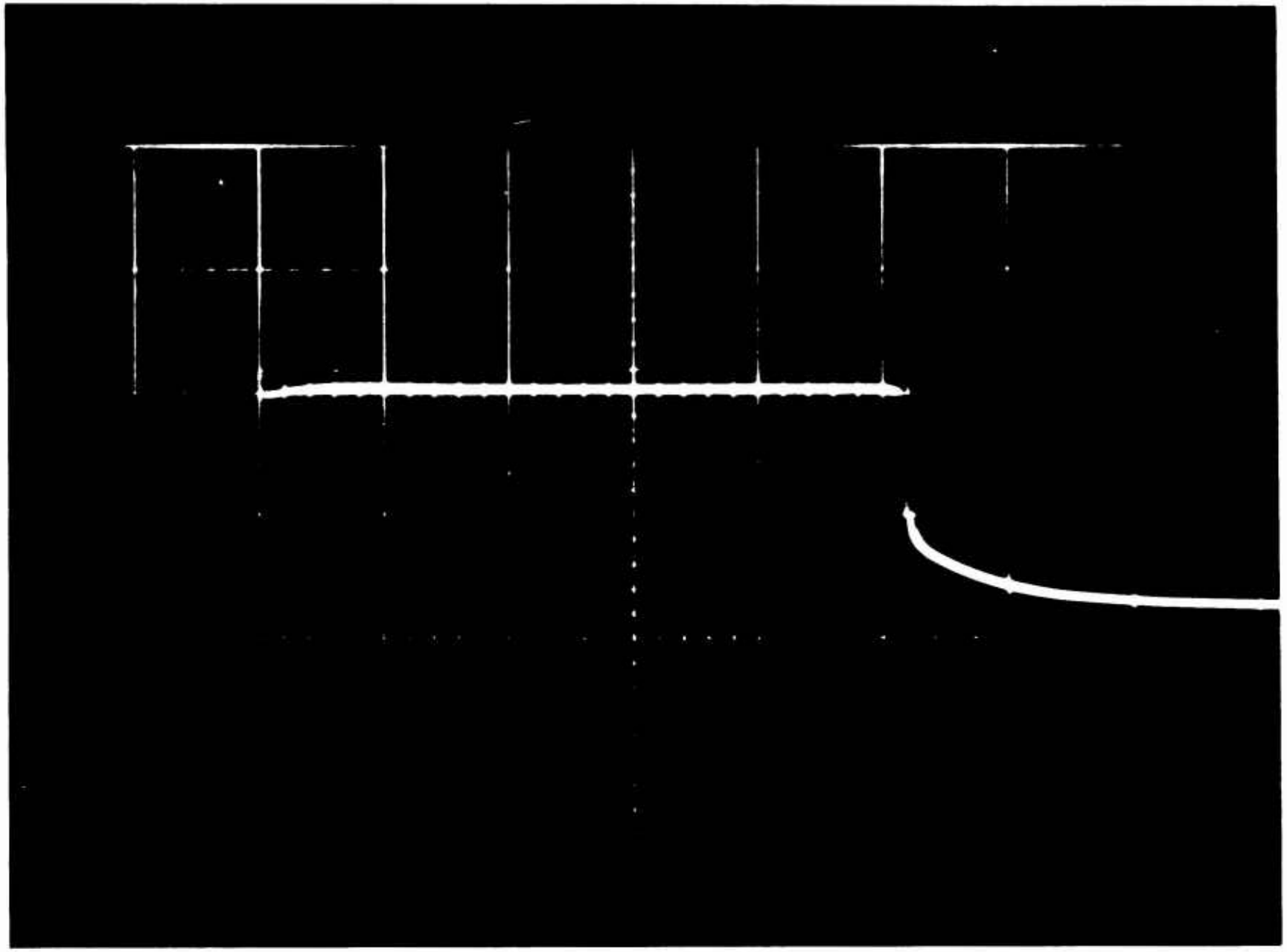

FIGURE 4. Turn on pulse. Oscilloscope set at 2 microsec/cm and 10 v/cm.

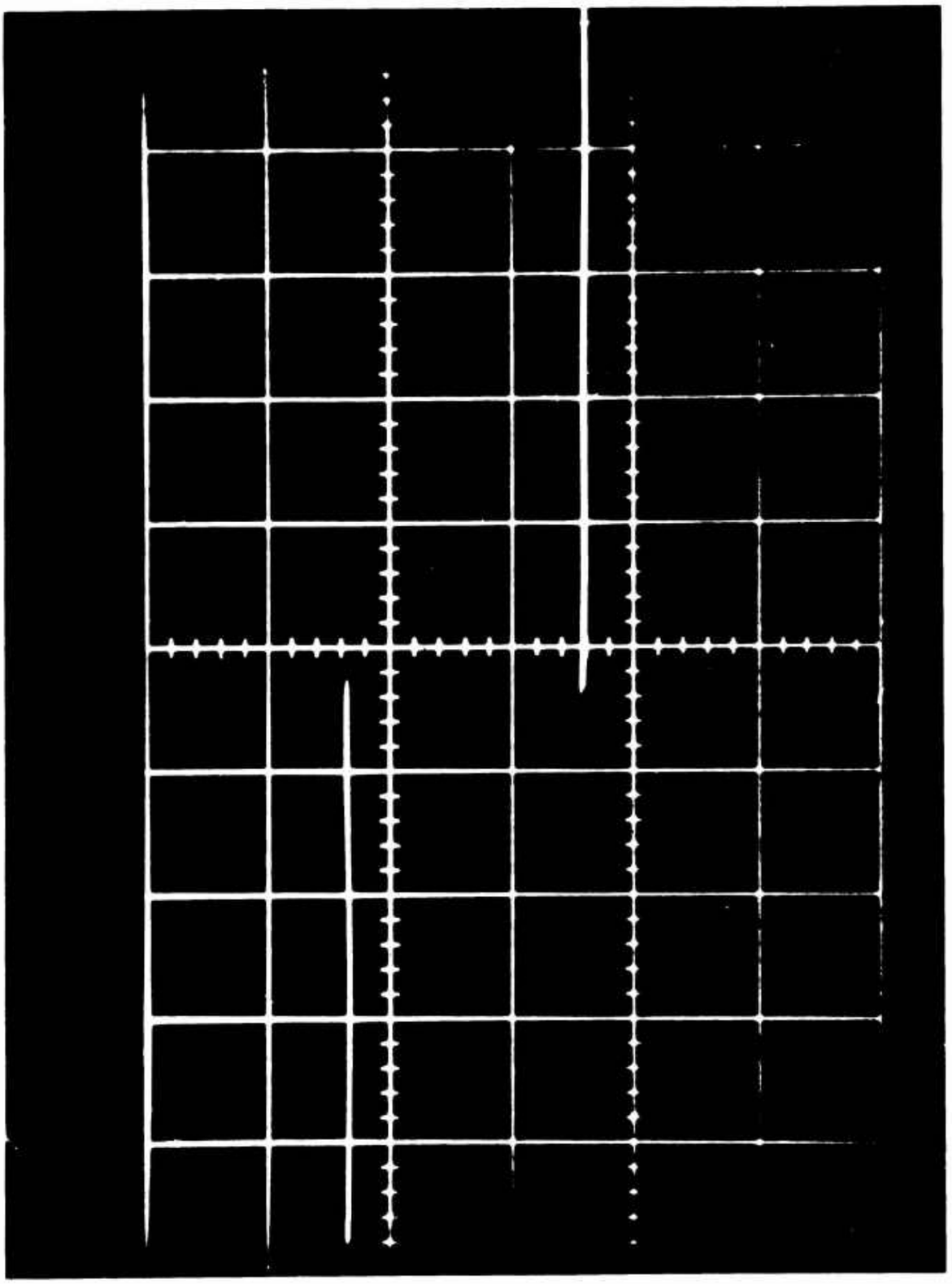

FIGURE 5. Turn off pulse. Oscilloscope set at 5 msec/cm and 10 v/cm.

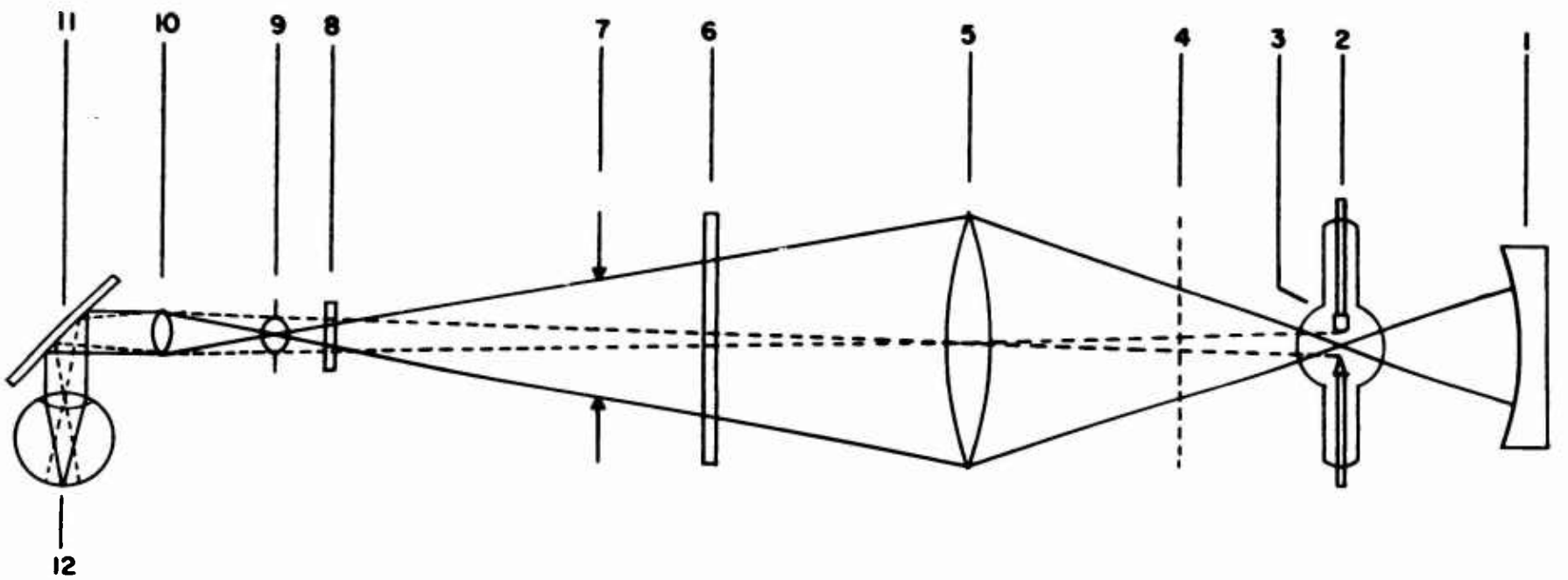

1. CONCAVE MIRROR
2. XENON LAMP
3. LUMINOUS PLASMA
4. PERFORATION DIAPHRAM
5. CONDENSER
6. KG-3 FILTER
7. IRIS DIAPHRAM
8. FILTER DISC
9. IMAGE FIELD DIAPHRAM
10. OBJECTIVE
11. POP-UP MIRROR
12. EYE OF RABBIT

FIGURE 6. Optical beam director.

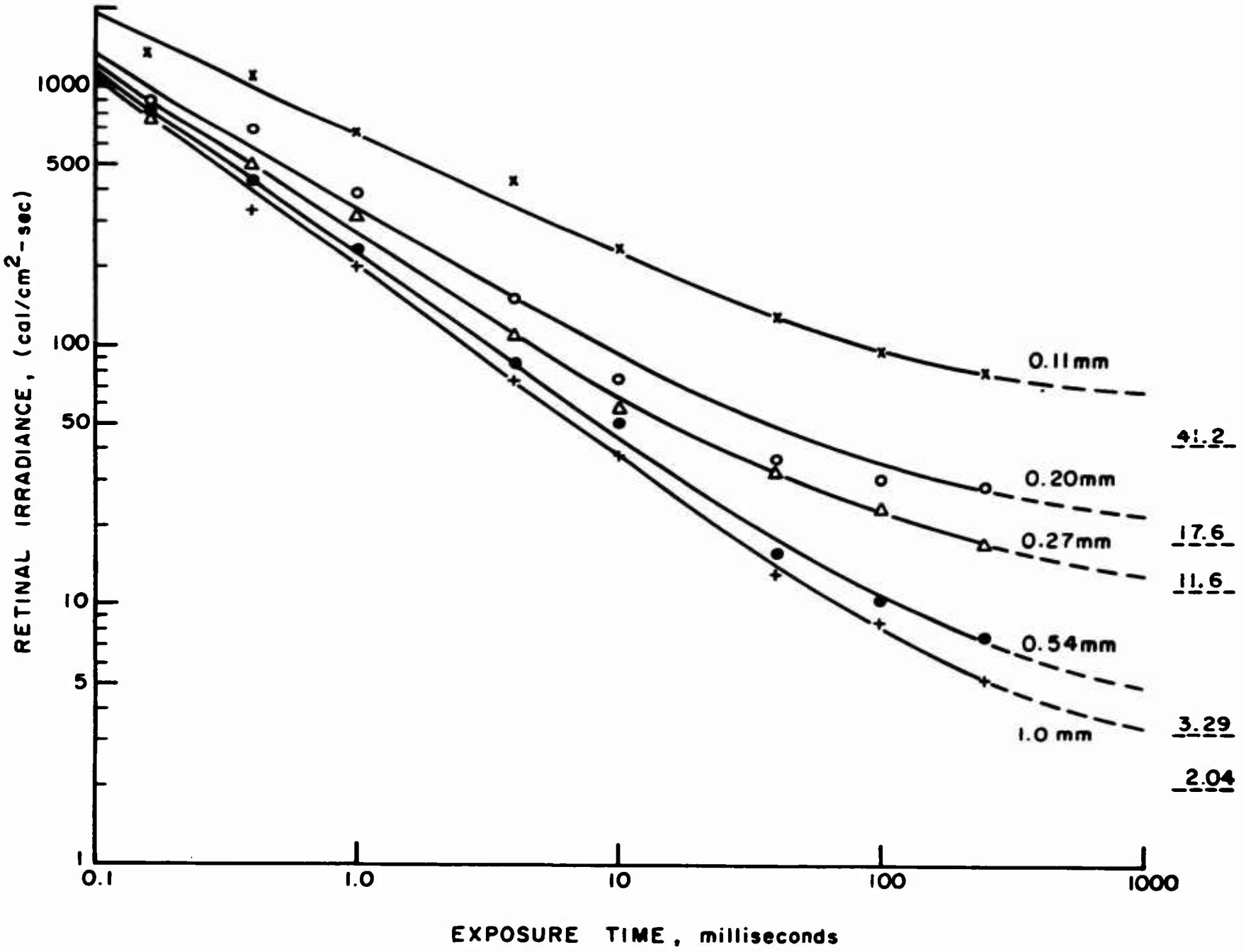

FIGURE 7. Plot of H_r vs. time for 5 minute burns.

BLANK PAGE

A STUDY OF THE PRODUCTION OF CHORIORETINAL LESIONS BY THERMAL RADIATION*

Alexander, T. A., R. L. Bessey, E. R. Lawler, Jr.,
W. R. Bruce, and R. G. Allen, Jr.

*This work was supported by the Department of Ophthalmology, Air Force School of Aerospace Medicine, Brooks Air Force Base, Texas and the Medical Division, Defense Atomic Support Agency, Washington, D. C.

FOREWORD

This investigation was accomplished by personnel of the Life Sciences Division of Technology Incorporated--

Thomas A. Alexander, M. S.

Roger L. Bessey, M. S.

Earl R. Lawler, Jr., B. S.

William R. Bruce

Ralph G. Allen, Jr., Ph. D.

The effort was sponsored jointly by the Ophthalmology Branch of the United States Air Force School of Aerospace Medicine, and the Medical Division, Defense Atomic Support Agency, Washington, D. C. Grateful acknowledgement is made of the assistance provided by personnel of the School of Aerospace Medicine--Mr. E. O. Richey, the Contract Monitor; Lt. Col. J. F. Culver, consulting ophthalmologist; and Major's A. V. Alder and D. G. Pitts who provided advice and assistance generously throughout the investigation.

ABSTRACT

Chorioretinal burns have been systematically produced in pigmented rabbits under carefully controlled laboratory conditions. Lesions were produced by high-intensity light flashes ranging in duration from 165 microseconds to 250 milliseconds and with image diameters which ranged from 1.0 mm to 0.11 mm. From these measurements relationships were obtained between exposure duration and threshold irradiance for the production of "5-minute" minimal lesions.

BLANK PAGE

A STUDY OF THE PRODUCTION OF CHORIORETINAL LESIONS BY THERMAL RADIATION

1. INTRODUCTION

The production of chorioretinal burns has been of interest for a number of years--particularly since the advent of nuclear weapons. However, the problem is such that it has not yet yielded to a theoretical approach. Progress has been made in this direction, but the prediction of chorioretinal burns still depends primarily upon threshold data collected in the laboratory using rabbits as subjects. In view of the importance of laboratory threshold data to the prediction problem, it was imperative that more complete and extensive data be obtained. Acquisition of more reliable and complete threshold data was the objective of this study. The work was carried out during the period 15 October 1965 to 15 March 1966.

Threshold data were obtained on the production of 5-minute minimal retinal lesions in rabbits for image sizes of 1.0, 0.54, 0.27, 0.20 and 0.11 mm with exposure times ranging from 165 μseconds to 250 mseconds. Thermal energy, primarily in the visible, was generated with a Meyer Schwickerath photo coagulator which had been modified for pulsed operation under a previous contract (1), (2).

The criteria used to define a 5-minute minimal retinal lesion were as follows: (1) appearance of an area of disturbance with a grey

or whitish center within five minutes after the end of exposure, and (2) non-appearance of a similar lesion within five minutes at an irradiance approximately 5-10% lower.

The irradiance level associated with the production of a minimal lesion was arbitrarily taken as the average of the lowest irradiance that produced a lesion as described, and the highest value of irradiance that would not produce such a lesion--where the difference between the two levels was required to be less than 10% of the value of the higher irradiance.

2. EQUIPMENT

The basic instrument used in this study was a Meyer-Schwickerath Light Coagulator manufactured by the Carl Zeiss Company. For the purpose of studying chorioretinal burns, this machine was modified as follows: (a) a Keeler ophthalmoscope with a pop-up mirror replaced the standard pinhole-mirror, (b) a KG-3 phosphate glass filter was added to the optical system to reduce the infrared energy in the beam, (c) one of the beam-size apertures was changed from 0.8 mm (4.5° light cone) to 0.2 mm (1° light cone), (d) the maximum opening of the iris was increased in order to obtain a 200-to-1 intensity control of the beam in 72 graded steps, (e) the lamp holder was modified to permit use of an Osram 2500W xenon lamp, and (f) an auxiliary light control unit was added for accurate

and automatic control of the length of the light pulse. Figure 1 shows the modified machine with its auxiliary equipment and figure 2 shows the optical system in schematic.

Light pulses of specified durations were obtained by controlling the power applied to the lamp. To accomplish this, a solid state switch was used to connect the xenon lamp to a source of power--either a set of aircraft batteries or a capacitor bank. With the batteries, pulses could be obtained with durations of 2 mseconds to 10 seconds. For shorter pulses, 165 μseconds to 1 msecond, the capacitor bank was used in place of the batteries. Current through the lamp was approximately 200 amps for battery operation and 2000 amps for capacitor operation.

Both total wavelength integrated irradiance measurements and spectral irradiance measurements were made on the light produced by the Zeiss coagulator. Total irradiance measurements were made with a calibrated Eppley Thermopile, and spectral measurements were made, in 10 mμ bandwidths, using a Jarrell-Ash Ebert Monochromator and a National Bureau of Standards calibrated 1000 W lamp (3). The measured spectral distributions are shown in figures 3 and 4 with total energy, between 400 mμ and 1200 mμ, normalized to the energy radiated by a 5800° black body in the same wavelength region.

The results of the integrated intensity measurements agreed with

the values obtained from integration of the spectral distributions within 5 percent. It is seen from these figures that the spectrum shifts toward shorter wavelengths at higher currents and that the spectrum without the KG-3 filter may be considered as a rough approximation of the spectrum of a 5800° black body.

3. EXPERIMENTAL PROCEDURES

All rabbits were baselined by Air Force ophthalmologists, and only rabbits with medium homogeneous pigmentation of the fundus and uniform unclouded clear media were used.

In preparation for exposure, hair was shaved from around the eyes of the animals, the animals were tranquilized with 2 cc of Demerol, I. M., and their pupils dilated with 1% Cyclopentolate Hydrochloride Ophthalmic Solution. After a pre-exposure examination with an AO Giantscope, the animal was positioned in front of the photo coagulator--shown in figure 1.

In making exposures, a marker burn was first placed on the fundus using an irradiance approximately twice that expected to produce a minimal burn for the particular image size concerned. This burn was placed in the central region of the fundus, about 5 mm below the medullated nerve fibers, and served as a reference for subsequent

exposures. The flash duration desired for the first test exposure was then set into the electronic pulse control unit, an irradiance level selected that would produce a burn, and an exposure made at a position located with respect to the marker burn. Immediately following exposure, the fundus was examined with the AO Giantscope or the Keeler ophthalmoscope attached to the beam director. After determining that a burn had been produced, the rabbit's head was turned slightly to bring an adjacent area of the fundus into view, the iris diaphragm reset to decrease the irradiance, and another exposure made. This process was continued, with exposures placed in a horizontal row, until the irradiance level for the production of a 5-minute minimal burn was identified (figure 5). This procedure was repeated for different exposure durations, different image sizes, and different subjects, until approximately 10 (or more) values were obtained at each of the image size and exposure duration combinations selected for investigation. Ordinarily, a sufficient number of exposures could be placed in a single eye to establish several points on a threshold irradiance versus time curve; however, the number of exposures actually placed in one eye depended upon the image size.

The procedure of placing exposures in a horizontal row was adopted after inconsistencies were observed in the results obtained from placing exposures in a circle around the marker burn. The rather large variations observed in circling the marker burn were attributed to variations in the

distribution of pigment. It was found that the irradiance required to produce a minimal burn at the 12 o'clock position was generally about 50% higher than that required to produce a minimal burn at the 6 o'clock position (a position further from the medullated fibers). Variations in the horizontal direction were found to be much smaller. The dependence of threshold irradiance on retinal position was taken into account (averaged) by establishing threshold irradiances with exposures placed in horizontal rows and by systematically varying the positions of rows in the subjects.

4. RESULTS AND DISCUSSION

Values of individual threshold irradiances for various image sizes are given in tables I through V. Average threshold irradiance, $\overline{H}_r$, standard deviation (σ), and average retinal exposure, $\overline{Q}_r$, are also given. These results are summerized in table VI.

Figure 6 presents the average measured threshold irradiances along curves of "best fit"--obtained through consideration of the entire set of data. To obtain these "best fit" curves, average values of threshold irradiance were graphed versus burn diameter--for a fixed value of the exposure time. Smooth curves were fitted to these points by eye. Values of $\overline{H}_r$ corresponding to the exposure times actually employed were then taken from these curves and used to determine the curves which best fit the expression $\overline{H}_r = At^B + C$, where A, B, and C are constants and t is expressed in milliseconds. The

constants were determined for each curve by a machine program using Newton's iterative process and are given in table VII. From figure 6 it is seen that the burn data can be approximated reasonably well by equations of this form for times greater than approximately 100 μseconds. The method used to generate these expressions rules out their use for times less than about 100 μseconds. On the other hand, it is believed that some credence can be attached to values computed for relatively long exposures, exposures longer than one second--for example. In this scheme, the value for C has special significance in that it represents the lowest value of $\overline{H}_r$ that is capable of producing a burn for a given image size--regardless of exposure duration.

Figure 7 presents values of $\overline{Q}_r$ as a function of exposure time since it has been found that in many instances this presentation facilitates the solution of prediction problems.

It is known that a five-minute minimal lesion does not represent the threshold of permanent injury since visible lesions have been observed to develop several hours after exposure--and result from exposures at significantly lower irradiances. This situation is under investigation and efforts are being made to relate the production of these late developing lesions to the production of five-minute minimal lesions.

REFERENCES

1. Alexander, T. A., R. L. Bessey, E. R. Lawler, Jr.. Research for Ocular Effects of Thermal Radiation, Final Report on Contract AF 41(609)-2464.

2. Alexander, T. A., E. R. Lawler, Jr., P. W. Wilson, Jr., and R. I. McDonald. High D. C. Power, Solid State Switch for Pulsing an Arc Lamp, Review of Scientific Instruments, Vol. 36, No. 12, pp. 1707-1709, December 1965.

3. Bessey, R. L. and R. G. Allen, Jr.. Calibration of Zeiss Photo Coagulator, Technical Report, Technology Incorporated.

TABLE I

Retinal irradiance (H_r) for production of 5 minute minimal burns in rabbits using Zenon arc light source filtered with a 1.5 mm KG-3 (phosphate glass) filter

A. 1.0 mm image diameter (6° light cone from Zeiss coagulator)

	H_r (cal/cm^2-sec)						
Exposure Time (msec) / Rabbit No.	250	100	40	10	1	.4	.165
G-79	4.80		10.5		242.		
Q-15	5.00	7.73			211.		
N-03	5.40	9.88			211.		
L-78	6.11	8.45			17o.		
Q-21	5.32	8.99		41.7		328.	
Q-39	4.38	7.40		32.6		302.	1010.
Q-43	5.78	9.52		33.6		324.	590.
S-96	5.27	8.66		36.5		374.	
T-16	5.37	8.81	15.4	39.6		367.	
T-18	4.76	8.05		37.7		287.	797.
Avg $\bar{H}_r$	5.22	8.61	13.0	37.0	210.	330.	799.
Standard Deviation (σ) for H_r	0.51	0.81	3.47	3.48	26.9	34.6	210.
Avg $\bar{Q}_r$	1.31	0.86	0.52	.37	.21	.13	.13

TABLE II

Retinal irradiance (H_r) for production of 5 minute minimal burns in rabbits using Zenon arc light source filtered with a 1.5 mm KG-3 (phosphate glass) filter

B. 0.54 mm image diameter (1.5° light cone)

H_r (cal/cm^2-sec)

Exposure Time (msec) / Rabbit No.	250	100	40	10	1	.4	.165
G-79	8.43		15.8		306.		
P-97	5.78	5.78	12.0	27.9	179.	482.	
Q-15	7.73	10.6		52.9	220.		
N-03	7.16	12.2			219.		
L-78	9.70	12.4					
Q-21	7.60	10.5		49.6		454.	
Q-39	6.25	8.66					869.
Q-43	8.12	12.0		47.3		380.	760.
S-96	7.40	10.9		57.0		483.	
T-16	6.36	9.97	19.6	58.0		506.	
T-18	8.05	11.9		58.9		313.	
Avg $\bar{H}_r$	7.51	10.5	15.8	50.2	231.	436.	815.
Standard Deviation (σ) for H_r	1.11	2.02	3.8	10.8	46.4	74.6	77.1
Avg $\bar{Q}_r$	1.88	1.05	.63	.50	.23	.17	.13

TABLE III

Retinal irradiance (H_r) for production of 5 minute minimal burns in rabbits using Zenon arc light source filtered with a 1.5 mm KG-3 (phosphate glass) filter

C. 0.27 mm image diameter (1.5° light cone)

H_r (cal/cm^2-sec)

Exposure Time (msec) / Rabbit No.	250	100	40	10	1	.4	.165
G-79	12.1	18.2	28.9	70.8	357.	979.	
G-79	13.9				363.		
P-97	6.9	9.5	18.2	41.7	190.	564.	
Q-15	16.7	21.4			220.		
N-03	22.0	29.0	54.8		534.		
Q-21	15.0	16.6		55.6		429.	792.
Q-39	13.7	16.2	25.4	46.9		292.	603.
Q-43	18.2	23.1	27.5	41.8		502.	
Q-43		21.8					
S-96	20.2	26.8	30.0	63.2		376.	
T-16	21.5	24.6	34.1	71.9		473.	
T-18	16.9	19.8	25.1	44.1		268.	603.
K-37		22.8				520.	
M-10	21.3		30.6	63.2		537.	
Q-23			36.0	76.1		593.	952.
Q-27	22.7	24.7					
Q-17		29.2	39.3	55.7			
Q-47		31.0					
Q-51		37.8					
Avg $\bar{H}_r$	17.0	23.3	31.9	57.4	333.	503.	738.
Standard Deviation (σ) for H_r	4.65	6.74	9.54	12.6	137.	190.3	168.5
Avg $\bar{Q}_r$	4.25	2.33	1.28	0.57	0.33	0.20	0.12

TABLE IV

Retinal irradiance (H_r) for production of 5 minute minimal burns in rabbits using Zenon arc light source filtered with a 1.5 mm KG-3 (phosphate glass) filter

D. 0.20 mm image diameter (1.0° light cone)

	H_r (cal/cm^2-sec)						
Exposure Time (msec) / Rabbit No.	250	100	40	10	1	.4	.165
G-79	31.4		41.0		697.		
P-97	15.0	18.2	25.5	70.0	211.		
Q-15	65.0	49.0			239.		
Q-21	23.5	30.3		74.3		808.	
Q-21						676.	
Q-39	25.4	28.5	39.1	64.8		365.	670.
Q-43	21.8	27.5	30.9	48.4		584.	
S-96	30.0	33.6	45.4	99.7		820.	
T-16	27.4	34.1	41.4	91.7		753.	
T-18	22.4	22.4	31.2	79.1		831.	1090.
Avg $\bar{\bar{H}}_r$	29.1	30.5	36.4	75.4	382.	691.	880.
Standard Deviation (σ) for H_r	13.5	9.22	7.19	17.0	273.	169.	297.
Avg $\bar{Q}_r$	7.28	3.05	1.46	.75	.38	.28	.15

Retinal irradiance (H_r) for production of 5 minute minimal burns in rabbits using Zenon arc light source filtered with a 1.5 mm KG-3 (phosphate glass) filter

E. 0.11 mm image diameter (0.5° light cone)

H_r (cal/cm^2-sec)

Exposure Time (msec) / Rabbit No.	250	100	40	10	4	1	.4	.165
G-79	65.2		102.					
P-97	69.9	80.2	75.7					
P-97			130.					
Q-21	103.	150.		181.				
Q-21	54.6	76.0						
Q-39	69.1	74.1	89.0	177.			1160.	
Q-43	58.3	67.5	87.0	173.			1150.	
S-96	83.6	94.3	190.					
T-16	91.7	108.	155.					
T-18	79.1	109.	216.	376.				
Q-93		117.	131.	230.	431.	726.		
Q-93		89.0	119.	222.	447.	619.	1010.	
R-03	59.1	89.6	117.	230.	411.	740.	1110.	
R-03	50.1	63.4	84.8	209.	423.	490.	883.	1030.
R-17	62.5	82.3	105.	217.	472.	586.	985.	1150.
R-17	77.9	92.7	142.	275.	438.	690.	1240.	1330.
R-31	126.	149.	201.	343.		666.	1110.	1240.
R-31	97.5						1280.	1280.
W-007								1610.
W-007	116.							1610.
Avg $\bar{H}_r$	79.0	96.1	130.	239.	437.	685.	1100.	1320.
Standard Deviation (σ) for H_r	22.48	26.42	43.94	66.54	21.14	138.1	125.8	219.6
Avg $\bar{Q}_r$	19.8	9.61	5.20	2.39	1.75	.685	.440	.191

TABLE VI

Average retinal irradiance (cal/cm^2-sec)

(For 5-minute Burn)

IMAGE DIAMETER (mm)	Exposure Time (msec)						
	0.165	0.4	1.0	10	40	100	250
1.0	799 [3]	330 [6]	210 [4]	37.0 [6]	13.0 [2]	8.61 [9]	5.22 [10]
0.54	815 [2]	436 [7]	231 [5]	50.2 [7]	15.8 [3]	10.5 [9]	7.51 [10]
0.27	738 [3]	503 [8]	333 [5]	57.4 [8]	31.9 [8]	23.3 [11]	17.1 [11]
0.20	880 [2]	691 [7]	382 [3]	75.4 [7]	36.4 [7]	30.5 [8]	29.1 [9]
0.11	1320 [7]	1100 [9]	685 [7]	239 [11]	130 [15]	96.1 [15]	79.0 [16]

Note: The numbers in the small boxes give the number of animals used in obtaining the average retinal irradiance listed.

TABLE VII

Calculated constants for the equations for threshold retinal irradiance vs. time

Burn size mm	A $cal/cm^2/sec^2$	B	C $cal/cm^2/sec$
0.11	597	-0.511	41.18
0.20	315	-0.626	17.60
0.27	255	-0.683	11.62
0.54	219	-0.730	3.29
1.00	197	-0.750	2.04

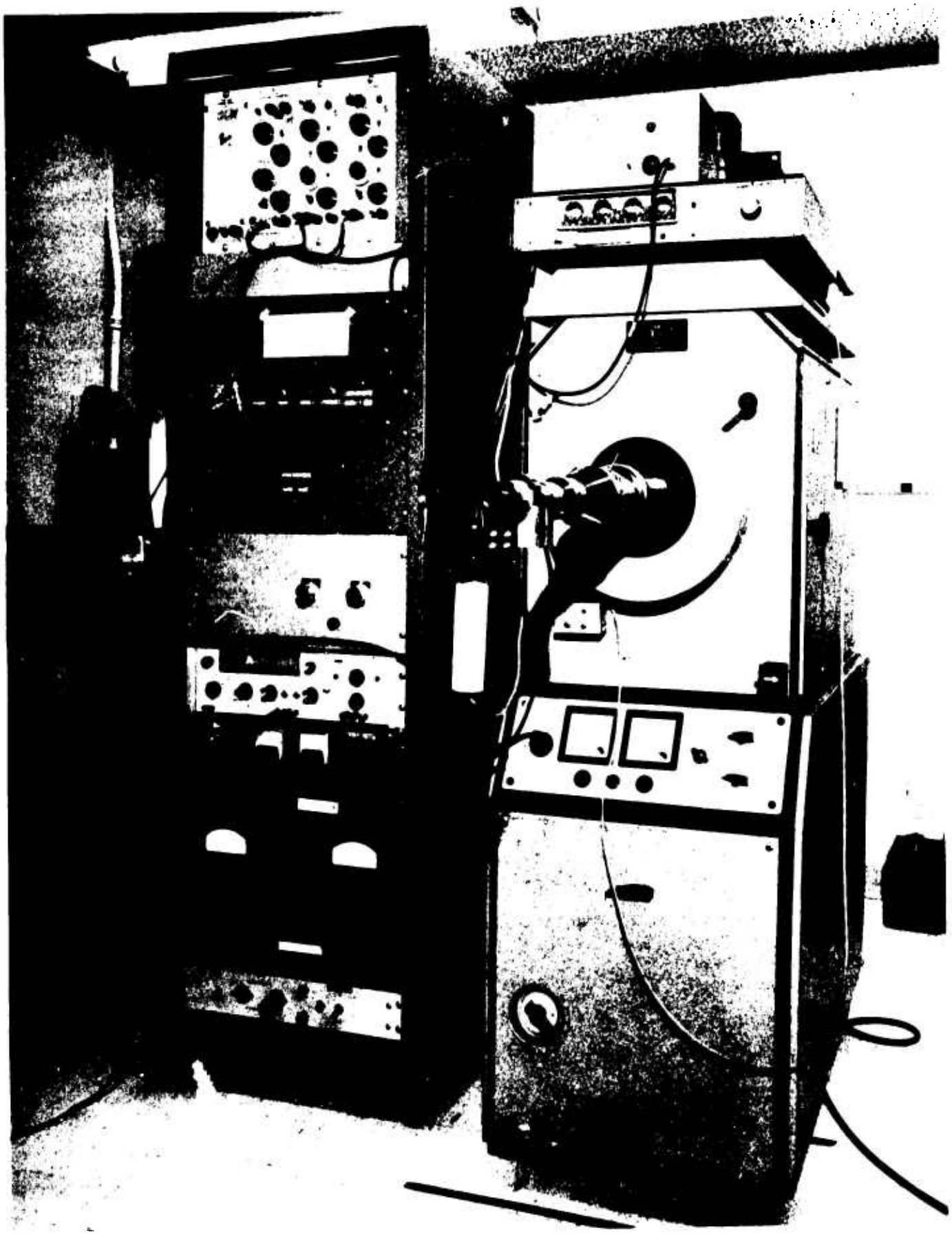

FIGURE 1. Modified Zeiss photo coagulator with auxiliary equipment.

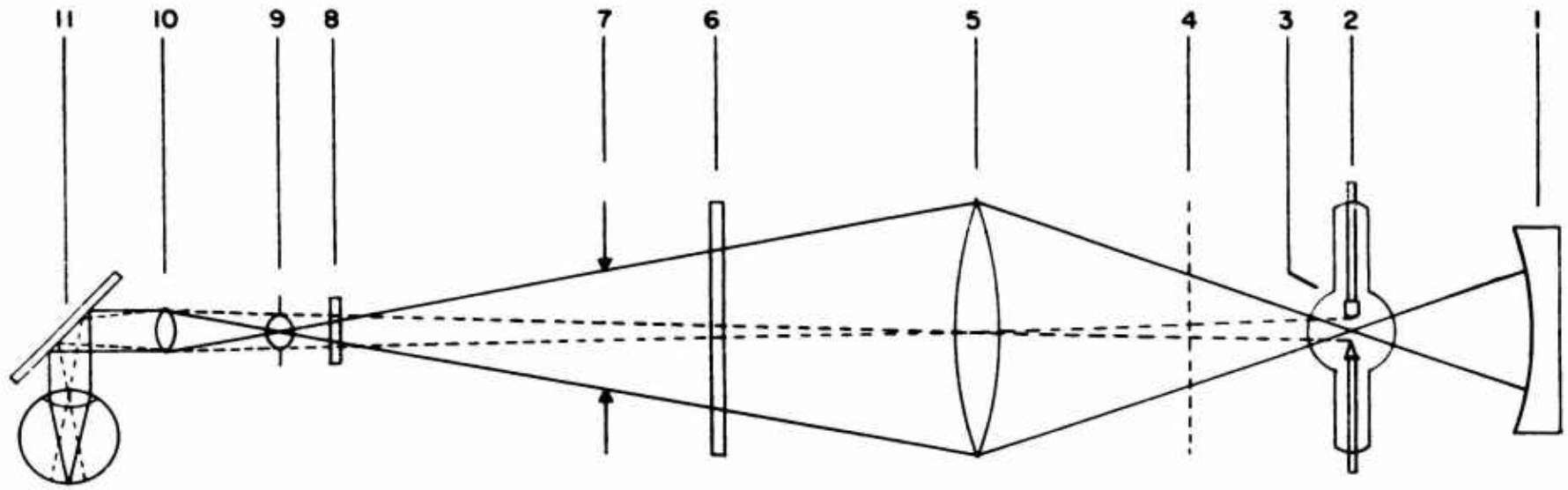

1. CONCAVE MIRROR
2. XENON LAMP
3. LUMINOUS PLASMA
4. PERFORATION DIAPHRAM
5. CONDENSER
6. KG-3 FILTER
7. IRIS DIAPHRAM
8. FILTER DISC
9. IMAGE FIELD DIAPHRAM
10. OBJECTIVE
11. POP-UP MIRROR
12. EYE OF RABBIT

FIGURE 2. Optical beam director.

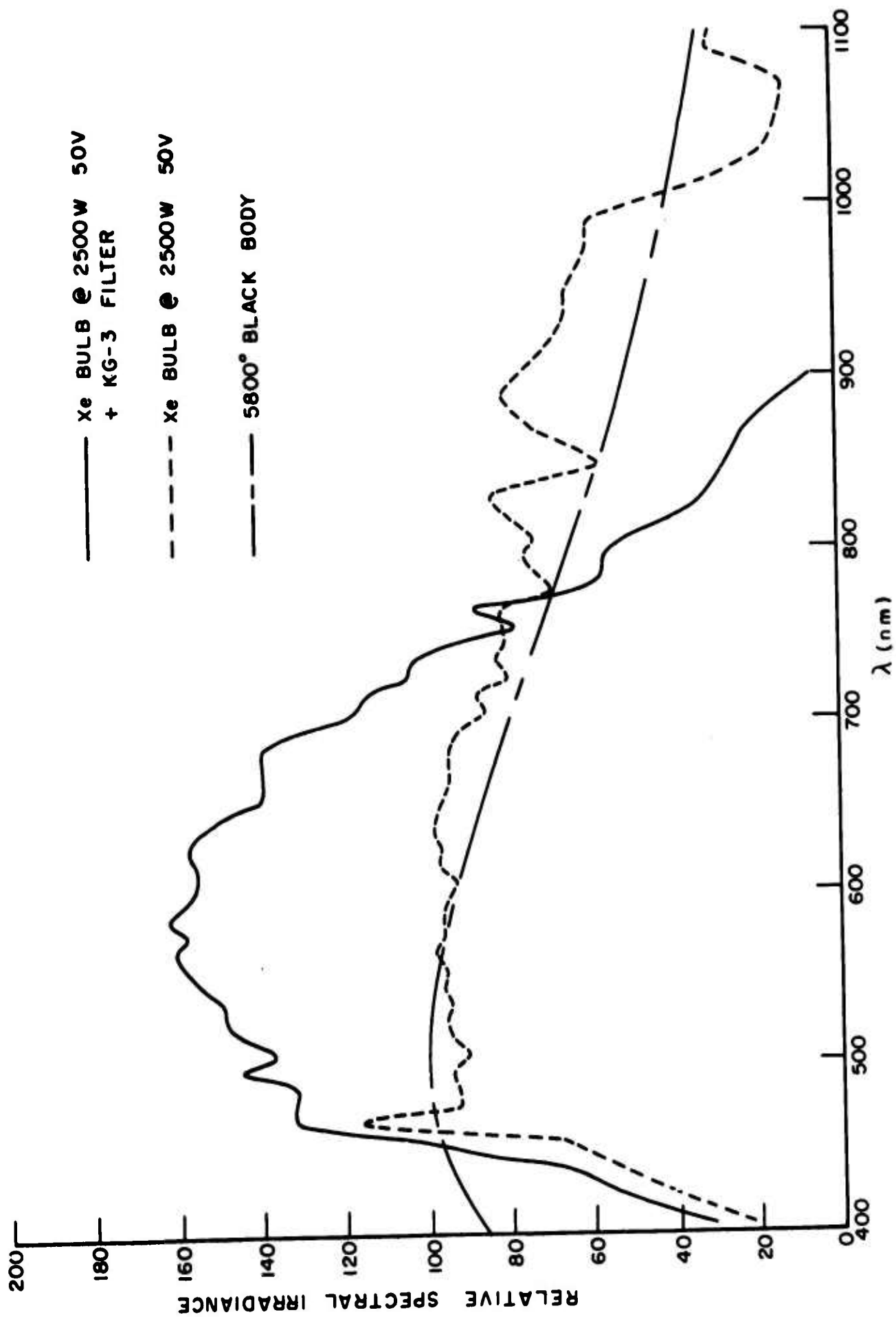

FIGURE 3. Spectral distributions of Xe bulb at 50V with and without KG-3 filter.

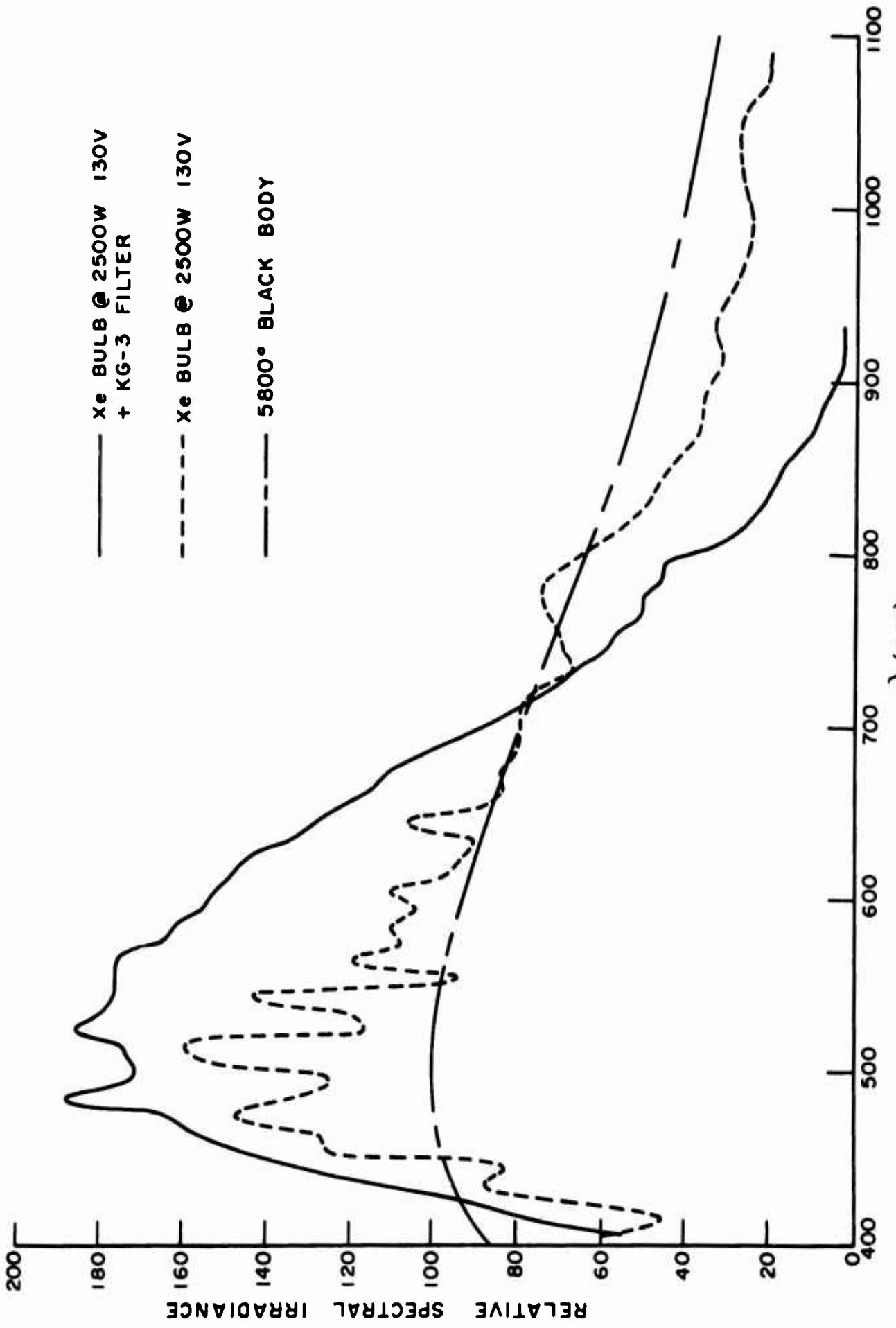

FIGURE 4. Spectral distributions of Xe bulb at 130V with and without KG-3 filter.

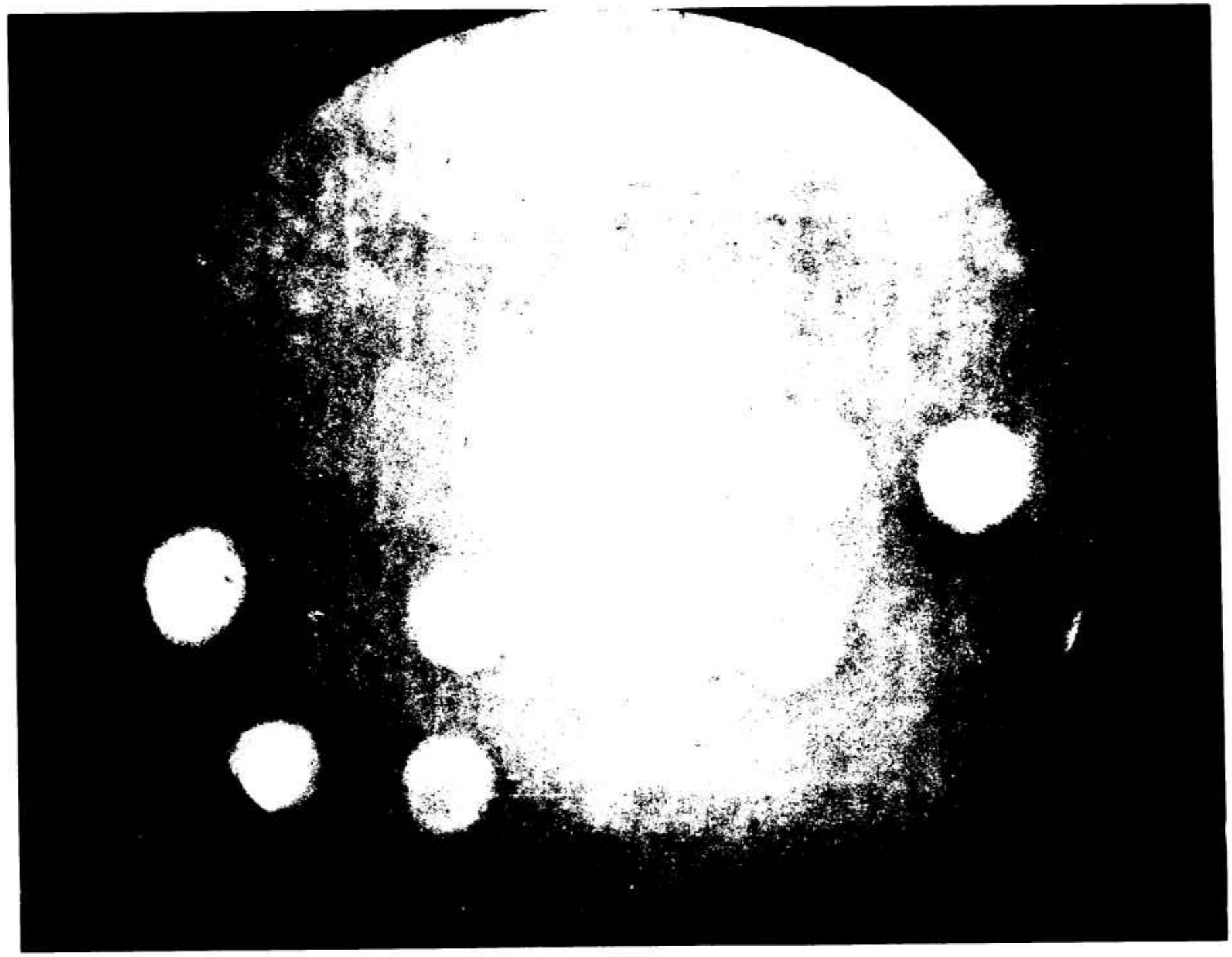

FIGURE 5. Fundus photograph of burns placed in horizontal rows.

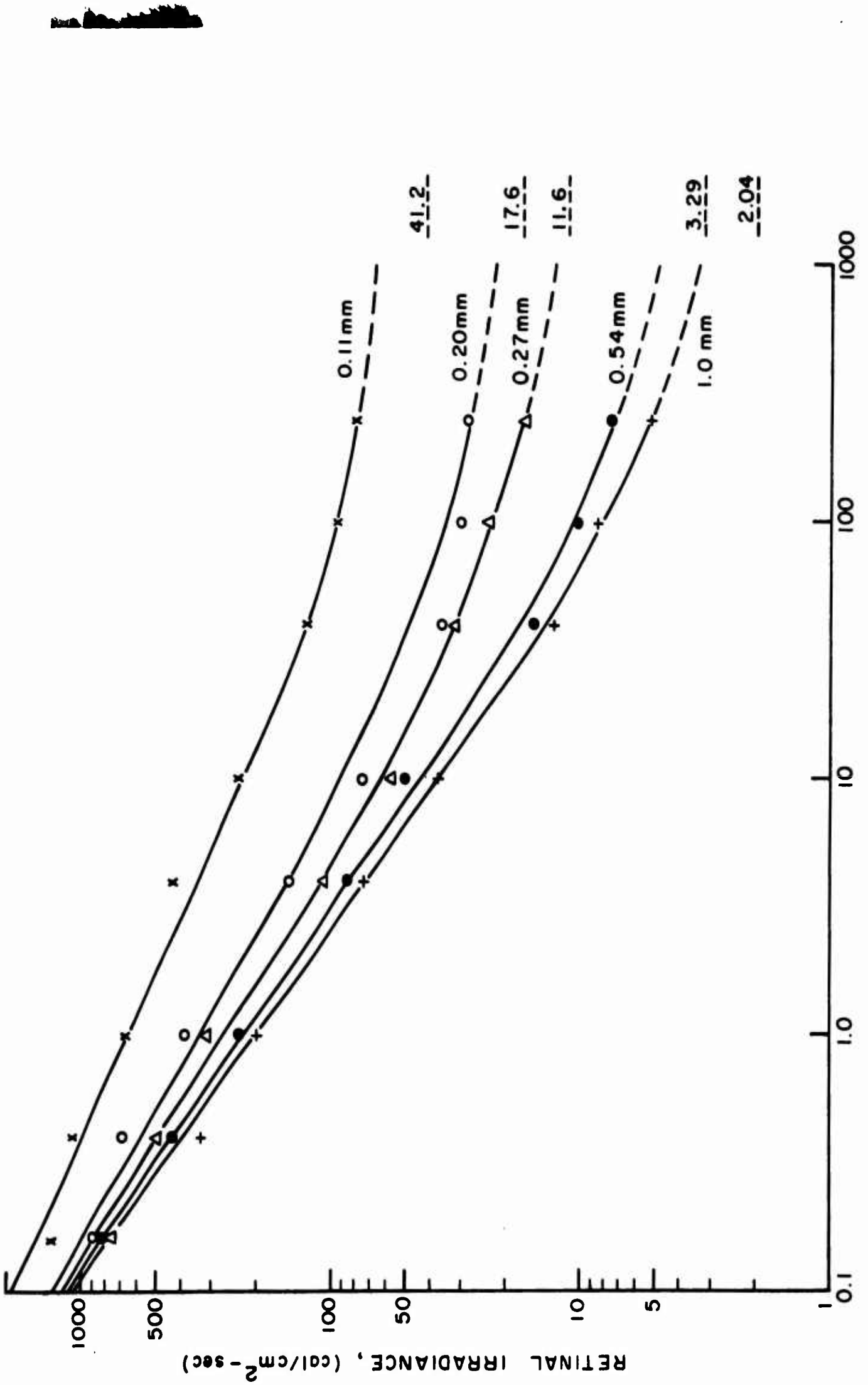

FIGURE 6. Average threshold irradiance ($\bar{H}_r$) vs. time for five image sizes. Asymptotic values (c in the equation) are shown at right.

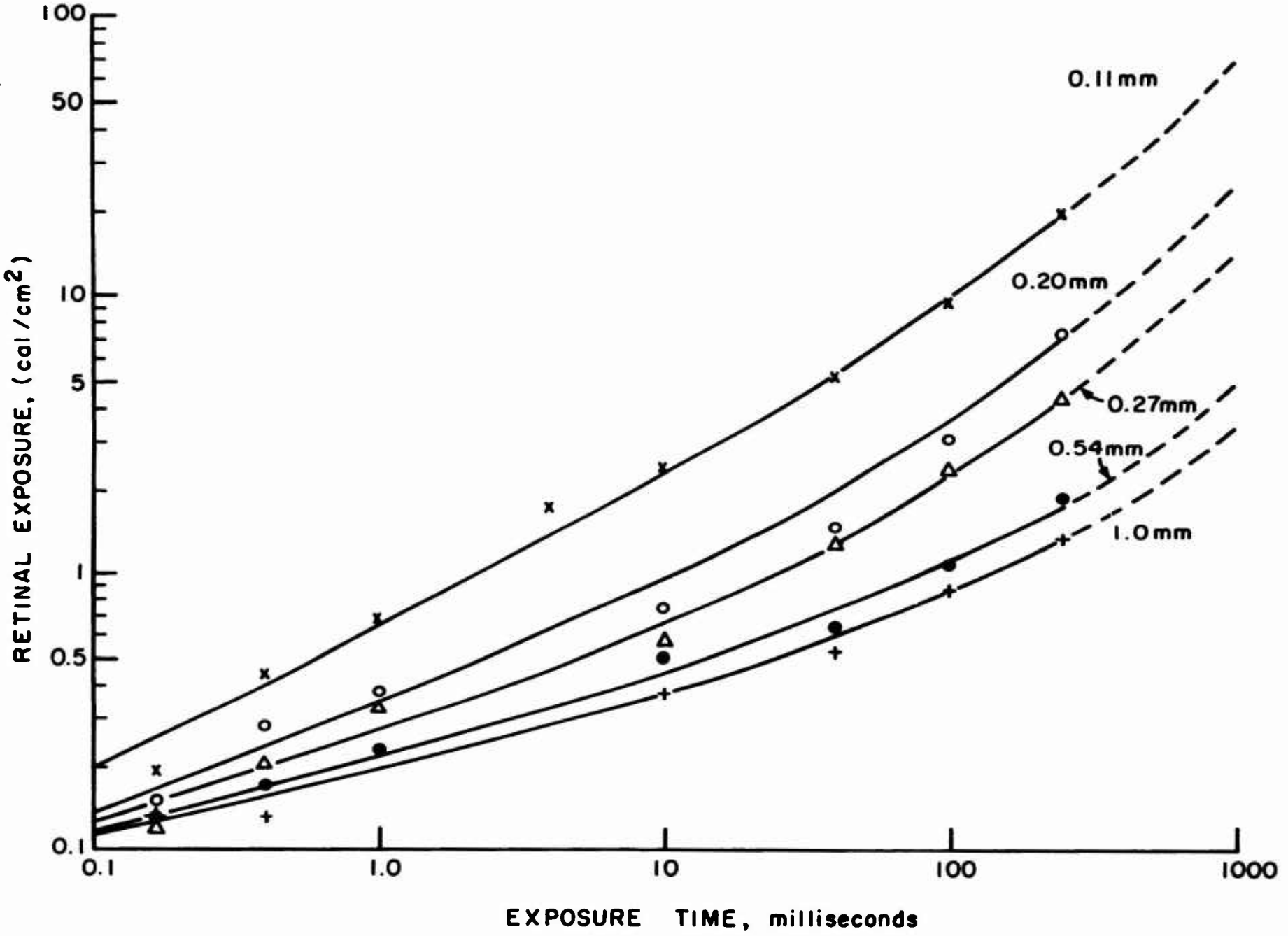

FIGURE 7. $\bar{Q}_r$ vs. time for five image sizes.

AN EXAMINATION OF THE PRODUCTION OF CHORIORETINAL BURNS IN TERMS OF TEMPERATURE DISTRIBUTIONS*

Ralph G. Allen, Jr., Ph. D., Arthur F. Muller, M. S.
Earl R. Lawler, Jr., B. S., William R. Bruce
Technology Incorporated, San Antonio, Texas

*This work was supported by the Oculo-Thermal Section, Department of Ophthalmology, Air Force School of Aerospace Medicine, Brooks Air Force Base, Texas.

BLANK PAGE

AN EXAMINATION OF THE PRODUCTION OF CHORIORETINAL BURNS IN TERMS OF TEMPERATURE DISTRIBUTIONS*

Ralph G. Allen, Jr., Ph. D , Arthur F Muller, M. S.
Earl R. Lawler, Jr., B. S., William R. Bruce
Technology Incorporated, San Antonio. Texas

It has been generally agreed that, in the case of retinal burns, permanent injury stems from the production of elevated temperatures in the retina and choroid as a result of the absorption of radiant energy--primarily energy in the visible spectrum. Although the injury has been associated with elevated temperatures--applicable retinal temperatures have not been obtained experimentally with any degree of success because of the difficulty inherent in such measurements.

Even though experimentally determined temperatures are not available, temperature distributions in the retina and choroid can be estimated in many cases by applying the 3-dimensional heat conductivity equation. This has been done in connection with a series of well-controlled exposures using rabbits, and calculated temperature distributions compared with ophthalmoscopic examinations in an effort to relate observed changes to the temperatures produced. Visible changes were

*This work was supported by the Oculo-Thermal Section, Department of Ophthalmology, Air Force School of Aerospace Medicine, Brooks Air Force Base, Texas.

associated with a calculated temperature rise exceeding 15-20°C for a 20 msecond exposure and a 0.52 mm image. However, the adequacy of the model or a simple temperature criterion for predicting the spacial extent of visible changes is questionable.

INTRODUCTION

It has been known for many years that damage to the eyes can occur as a result of viewing a very bright light, and that this damage could result in a permanent loss of visual acuity. The early evidence of retinal damage produced in this way was observed in individuals who had viewed a solar eclipse without adequate eye protection (10). The resulting loss in vision was called "eclipse blindness", and even now, despite frequent warning to the public, injuries from viewing eclipses are still reported (9).

The development of the atomic bomb introduced a new and potentially more hazardous source of radiation capable of producing eye injuries. The first experiments dealing with the effects of a nuclear flash on the eyes were conducted by the Air Force School of Aviation Medicine in 1951 during Operation Buster. It appears, however, that this problem was not discussed in the open literature until 1953 when it was pointed out that, because of the focusing of energy by the eye, injury could be sustained at extremely long distances--much longer distances than those at which injury could be produced by any other direct effects (4). Following Operation Buster came a series of field experiments to

study the effects of nuclear detonations on vision. This series of field studies culminated with an extensive experiment conducted during Operation Dominic and Operation Fishbowl in 1962 (2).

Today, there are several sources of radiant energy that are capable of producing retinal damage, and most of these sources possess a much greater capacity for producing damage than does the sun. With the exception of the Q-switched laser--an ultra high power mode of laser operation that apparently introduces a new spectrum of biological damage (12, 5)--the mechanism by which injury to the eye is produced appears to be the same in all cases, viz., the production of regions of elevated temperatures in the retina and its vicinity as a result of absorption of energy. If the temperatures generated exceed the tolerances of the biological systems involved, physical damage (chorioretinal burns) and associated permanent loss of visual function result. If tolerances are not exceeded, the ordinary visual mechanism operates and normal vision, or perhaps a temporary impairment of vision (flashblindness) is experienced.

Since permanent injury appears to be a direct consequence of the temperatures created in the retina and adjacent structures, a knowledge of the time history and spatial distribution of the temperature is important to understanding and predicting the effects produced by exposure to high intensity light sources. No matter if the source be the sun, a nuclear detonation, a normally operated laser, a pulsed

xenon tube, an incandescent plasma, or some other high intensity source, results will be similar--differing only as a result of variations in the conditions of exposure, differences in the characteristics of the light sources, and differences in the subjects themselves.

The ultimate significance of chorioretinal burns depends upon the loss of visual function and the importance of the affected function(s) to the individual and to the performance of his job. The particular function and extent of loss depends upon the location, size, and severity of the lesion. The importance of the loss to the individual depends upon his actual use of this function, and perhaps the possibility of overcoming the loss by training, etc.

There are still other factors which become significant under certain circumstances--for example, during nuclear testing in the atmosphere, or in testing laser devices. These situations can involve philosophical, political, and legal considerations pertaining to responsibility for public safety, protection of test personnel, and the medico-legal questions of injury, liability and compensation.

Perhaps the situation is unduly complicated, but the importance of vision, man's primary sensory contact with the physical world, the complex psycho-physiological nature of visual perception, and a lack of knowledge concerning human thresholds and injury criteria, combine frequently with inadequate information concerning the light source to produce situations in which speculation, large margins of

safety, and personal opinion dominate.

THE PROBLEM

The general problem of the production of chorioretinal burns concerns three phenomena which, combined, make up the overall problem. These three parts are (1) the radiating source, (2) transmission through the atmosphere and other intervening material, and (3) interaction of the radiant energy with the eye. Since each of these phenomena is wavelength dependent, the entire problem is spectrally sensitive.

Considering the source to be a plane radiating surface, the irradiance, H_C, at a point in space at time t due to radiation originating from an element of the source dA_S (Figure 1) is:

$$1) \quad H_c(A, B, t) = \int_\lambda N(A, B, \lambda, t)\, T(\lambda) \sin B \cos B \, dA \, dB \, d\lambda$$

where $N(A, B, t, \lambda)$ = spectral radiance in the direction B

$T(\lambda)$ = transmission of the atmosphere and intervening media

λ = wavelength

Treating the lens of the eye as a simple thin lens, the irradiance (H_r) at a position in the image on the retina corresponding to the position of the element of area, dA_s, on the source (Figure 2) may be expressed as

$$2) \quad H_r(A, B, t) = \frac{\cos^4 B}{[2 f(t)]^2} \int_\lambda \pi N(A, B, \lambda, t)\, T(\lambda)\, T_e(\lambda)\, d\lambda$$

where $f(t) = \dfrac{F \text{ (focal length of the eye)}}{d_p(t) \text{ (diameter of pupil which may undergo a change with time)}}$

$T_e(\lambda)$ = transmission of the clear media of the eye

The corresponding retinal exposure will be

3) $$Q_r(A, B) = \int H_r(A, B, t)\, dt$$

The rate of absorption of energy in the eye depends primarily upon the amount of pigment present. The most heavily pigmented, thus the most highly absorbing regions, are the retinal pigmented epithelium and the choroid.

Making the simplifying assumption that the absorbing materials are distributed in homogeneous layers characterized by individual absorption, conduction, and reflection properties, the rate of absorption, $E_j(A, B, Z, t)$, per unit volume in the j^{th} layer will be approximately

4) $$E_j(A, B, Z, t) = \int_{\lambda} \left[1 - R_{j+1}(\lambda) T_j(\lambda, l_j)\right]\left[1 - R_j(\lambda)\right] H_r^j(A, B, t, \lambda) \cdot \left[-\frac{dT_j(\lambda, Z)}{dZ}\right] d\lambda$$

where $T_j(\lambda, Z)$ = transmission of the j^{th} retinal layer at Z

Z = depth in chorioretinal region along optical axis

$R_j(\lambda)$ = reflection from the j^{th} layer--taken as if reflection occurred at the front surface of the j^{th} layer

If conduction is considered to be the primary method by which heat is dissipated, i.e., if re-radiation and cooling by convection resulting from the blood flow in the choroid are considered to be negligible--

reasonable assumptions for short times and/or when rates of absorption of energy are large (6)--the temperature distribution in the j^{th} layer as a function of time can be obtained from the heat conduction equation.

Thus,

$$5) \quad \nabla^2 U_j + \frac{E_j}{k_j} = \frac{\rho_j c_j}{k_j} \frac{\partial U_j}{\partial t}$$

where $\nabla^2 = \frac{1}{r} \frac{\partial}{\partial r} + \frac{\partial^2}{\partial r^2} + \frac{\partial^2}{\partial Z^2} + \frac{1}{r^2} \frac{\partial^2}{\partial A^2}$ (cylindrical coordinates)

U_j = temperature at time t in the j^{th} retinal layer and

$U_j(A, r, Z, \lambda, t)$ is a function of position in the retina,

wavelength of the radiation, and time.

ρ_j = density of material in the j^{th} layer

k_j = thermal conductivity of j^{th} layer

c_j = specific heat of the j^{th} layer

t = time

j = 1, 2, 3, ---n (number of retinal layers)

r = radial distance from the center of the image

The temperature distribution throughout the volume concerned can be obtained by a simultaneous solution of the set of n conduction equations--using appropriate boundary conditions. However, uncertainties in available data associated with the various phenomena involved

justify further simplification of the model. This may be accomplished if:

a. The source is taken to be a plain circular disc with a uniform radiance over its surface, and the distance from the source to the eye is assumed to be large relative to the diameter of the source, i.e., angle B is small.

b. Diffraction effects and image defects produced by lens system aberrations are not considered.

c. Only four regions are delineated in the eye--the clear media, the pigmented epithelium, the choroid, and the sclera (Figure 3). Each is considered to be homogeneous and characterized by its particular absorption coefficient. Absorption in the pigmented epithelium is taken to be uniform, absorption in the choroid is taken to decrease exponentially with Z, and the clear media and sclera are considered to be non-absorbing. The spectral absorption in the retina and choroid are treated according to the results reported by Geeraets, et al. [7] with the assumption that essentially all of the energy is absorbed in these two regions, leaving no energy for absorption in the sclera.

d. The density, specific heat, and thermal conductivity of these retinal regions are taken to be constants--independent of location, direction, and temperature, and in first approximation to have values corresponding to those for water. (ρ = 1.00 gms/cm^3, c = 1.00 cal/gm - ^{o}C, k = 1.4 x 10^{-3} cal/sec - ^{o}C - cm).

e. No account is taken of the latent heat of vaporization for

situations in which temperatures exceed 100° C.

f. The absorbing volume of the retina is taken to be a right circular cylinder lying directly behind a circular image of the source.

g. Reflections from the retinal regions are neglected.

h. Exposure is assumed to be completed before pupillary changes can occur.

Equation 5 is still applicable; however, for the laboratory experiment reported here, the expression for absorption of energy in the j^{th} layer (Equation 4) becomes:

$$6) \quad E_j(Z,t) = \frac{A_c}{A_i} \int_{\lambda} H_c(\lambda,t) \cdot \left[\prod_{m=1}^{m=j-1} \cdot T_m(\lambda) \right] \cdot \left[- \frac{dT_j(\lambda, Z)}{dZ} \right] d\lambda$$

where A_c = cross sectional area of the light beam at the position of the rabbit's eye ($A_c \ll A_{pupil}$)

A_i = area of the image on the retina

$H_c(\lambda, t)$ = measured spectral irradiance at the position of the rabbit's eye.

$T_m(\lambda)$ = transmission of the m^{th} layer

j = 2, 3

The initial and boundary conditions assumed for this model are:

1. At time equal zero, temperature is taken to be zero. Thus, the temperatures that are calculated are temperature rises rather than total temperatures.

2. All of the energy remains within a finite cylindrical volume which has dimensions large with respect to the volume irradiated. At the external boundary, the temperature gradient is taken to be zero.

3. The temperature at an interior boundary is independent of the direction in which the boundary is approached.

4. The temperature gradient at an interior boundary is independent of the direction in which the boundary is approached.

If the energy source is viewed long enough for the rate of dissipation of energy in the fundus to equal the rate of absorption, temperature equilibrium will be reached. The situation at equilibrium is described by Equation 5 with $\frac{\partial U_j}{\partial t} = 0$ for all j, i.e.:

$$7) \quad \nabla^2 U_j + \frac{E_j}{k_j} = 0$$

After extinction of the source, temperatures will be given by Equation 5 (using appropriate initial conditions) with $E_j = 0$, i.e.:

$$8) \quad \nabla^2 U_j = \frac{\rho_j \, c_j}{k_j} \frac{\partial U_j}{\partial t}$$

These equations can be solved by relaxation methods (11) to give temperature distributions in the retina and adjacent structures for sources of essentially any radiance and size desired.

EXPERIMENTAL PROCEDURE

Although chorioretinal injury has been associated with elevated temperatures--retinal temperatures have not been obtained experi-

mentally with any degree of success due to the difficulties inherent in such measurements. Thus, to compare observed effects with temperature distributions, it is necessary to use a calculative technique, such as that described, or to construct a two-dimensional analog simulator (5). In this investigation, a series of carefully controlled exposures using rabbits was carried out and temperature distributions calculated to correspond to the actual exposure conditions.

A. Equipment. The instrument used tc produce retinal burns was a modified Meyer-Schwicherath light coagulator manufactured by Carl Zeiss, Incorporated. This machine used an Osram XBO 2500 watt high pressure xenon gas arc bulb (Figure 4). The duration of the light pulse was controlled with a high current solid state switching circuit (1) that permitted pulsing of the xenon bulb between 145 μsec and 10 seconds. Figure 5 shows a 400 μsecond pulse and Figure 6 shows a typical 100 msecond pulse. The light was filtered with a 1.5 mm KG-3 phosphate glass filter to remove the infrared. Total irradiance was measured with an Eppley 16-junction bismuth-silver thermopile, and these measurements were related to the voltage response of an EG&G SD-100 photodiode mounted just inside the eye piece of the Zeiss where it responded to light that was not collected by the eye piece. In addition to the total irradiance measurements, the spectral irradiance was measured in 10 mμ bands using a Jarrell-Ash monochromator and an RCA 7102 photomultiplier tube. These

spectral measurements were interpreted in terms of the spectral irradiance from a GE DXW, 120V, 1000 watt tungsten filament standard lamp obtained from the National Bureau of Standards. Integration of the spectral irradiance over wavelength yielded agreement with the total irradiance measurements to within 5% (3). Figure 7 shows the filtered spectrum that was actually obtained--normalized to the spectrum of a 5800° K black body at 550 mμ for comparison.

B. Procedures for Exposing Rabbits. A single adult New Zealand rabbit was the subject in this study. This rabbit was selected for homogeneous medium pigmentation of the fundus and uniform, unclouded, clear-media. The hair was clipped away from both eyes, and during exposure, the rabbit was tranquilized with 2 cc of Demerol, IM, and pupils dilated with 1% cyclopentolate hydrochloride ophthalmic solution. The animal was placed in a restraining box so that its eye could be positioned in the light beam emerging from the Zeiss coagulator. A Keeler ophthalmoscope mounted on the arm of the coagulator was used to position the image on the fundus as desired. The cornea was kept moist during the procedure and no corneal or lens clouding was observed during the period of irradiation.

The aperature which defines the image size was adjusted to produce an image on the retina calculated to be 0.54 mm in diameter. Actual measurements of the diameter of the image from photographs of the image reflected from the fundus yielded a value of 0.52 mm.

This value was obtained by comparing fundus photographs of the image of the beam with fundus photographs showing an object of known size--in this case a dual probe with precisely 1 mm spacing introduced posterially into the fundus. A hand-held Nikon fundus camera was used for all photographs.

Placement of burns was accomplished as follows:

a. A reference burn was produced in the central region of the fundus about 1 mm below the myelinated fibers.

b. Exposures of decreasing irradiances were placed around the reference burn to establish the irradiance that, for a 20 msec exposure, would produce a 5-minute lesion--i.e., a lesion that appeared within 5 minutes and had a small grey or whitish color in its central region. This procedure was repeated until a decrease in irradiance by about 10% did not produce a lesion of this description. Irradiance for a minimal lesion was then arbitrarily taken to be the average of the last two values. The value of irradiance for a 20 msec - 5-minute burn for this rabbit was 24.5 cal/cm^2 -sec.

c. Holding the irradiance constant at this value and using an image diameter of 0.52 mm, exposures were made in the right eye for pulse durations of 0.145, 0.4, 1, 2, 4, 10, 20, 40, 60, 100, and 200 milliseconds. The eye was examined immediately after each exposure and photographed at 2, 24, and 48 hours post exposure.

d. Retinal exposures were made in the left eye to duplicate the

exposures (cal/cm^2) delivered to the right eye. However, time was fixed at 20 milliseconds for exposures in the left eye and irradiances were varied to give the desired exposure. Fundus photography was again accomplished at 2, 24, and 48 hours post-exposure.

RESULTS

Approximately 25 burns were placed in each eye in an area of about 15 mm^2 centered on the posterior pole. These exposures were delivered at about 5-minute intervals--a period long enough, according to calculations, to permit the fundus to return to its pre-exposure temperature. In each instance, immediate post-exposure observation of the exposed area was carried out and visible changes noted. The average sizes of the burns and their individual characteristics were obtained from the photographs that were taken at 2 and 24 hours post-exposure. Figure 8, drawn to scale, shows the position of each exposure and the outline of each of the visible lesions produced in the right eye. Figure 9 presents the same information for the left eye. Features used to describe the visible lesions are shown graphically in Figure 10. Conditions for the individual exposures and observed results are tabulated in Tables I and II. Figures 11, 12, 13, and 14 present typical results of the temperature calculations made for comparison with observed results. Only the results for exposures 6L, 8L and 10L have been examined in detail since these exposures appeared to

present the best possibility for correlating temperature distributions with observations.

DISCUSSION

Examination of Tables I and II shows that consistently observable changes were noted for calculated temperature rises greater than 25° C. The observed effects were immediate, i.e., occurred within 5 minutes. In two instances (exposures 16, 17 right and 12, 13 left) visible effects were recorded for less than a 25° C rise. However, these changes took longer than 5 minutes to mature, and even under carefully controlled laboratory conditions, were minimally detectable by ophthalmoscopic examination. In view of the variables involved and the subjective nature of the determination of visible change, it was concluded that minimal observable effects could be considered to accompany temperature rises in the pigment epithelium of 15-20° C--for a 0.52 mm image and a 20 msec exposure--as calculated with the model described here. From earlier work, it appears that correspondingly higher temperature rises are required for minimally visible effects from shorter exposures.

Looking at the temperature distribution histories calculated for a specific exposure (6, 7 left) shown in Figure 12, a temperature rise of 20° C or greater is indicated out to a radius of 260 to 270 microns at the center of the pigment epithelium--the plane of maximum temperature. This condition extends throughout a considerable

region--from 20 microns anterior to the pigment epithelium to at least the center of the 100 micron thick choroid of this model. On this basis, a visible lesion of the same size as the image, or somewhat greater, would be expected--and was observed (Table II and Figure 15). Actually, a visible disturbance with radius of 310 microns was measured 2 hours after irradiation. At 24 hours post exposure the radius of comparable disturbance had receded to 280 microns. The maximum temperature rise at the 310 micron radial distance was only about 7° C--too small, according to the criterion selected, for the occurrance of visible effects. Thus, for this exposure, correlation of visible changes with calculated temperatures leads only to qualitative agreement insofar as the size of the lesion produced is concerned.

Similar examination of the temperature distributions calculated for exposure 8, 9 left eye (Figure 13) leads to expectation of a visible disturbance, characterized as pale greyish-white, of about the same size as the image, or perhaps slightly smaller. In this case, agreement between observed effects and calculated temperatures was quite acceptable considering the nature of the correlation being attempted.

Treating exposure 10, 11 left in the same way disclosed an apparent discrepancy between observation and prediction. The calculated temperature distributions for this exposure (Figure 14) would require observable effects extending over an area with radius of approximately 200 microns, whereas the observed disturbance had

a radius of only 40 microns. The temperature calculations indicate a lesion of much less depth than that indicated for either 6, 7 left or 8, 9 left, and this is certainly a factor for consideration. Still, the model predicts a temperature distribution across the image that exceeds 20° C and that is essentially flat out to a distance of 180 microns. This is much flatter than would be anticipated on the basis of the observed results and the simple temperature criteria assumed.

An explanation in terms of inhomogeneity of the incident beam is not credible since prior examination of the beam showed that, although the beam was not completely uniform, it did not contain localized "hot spots". The possibility of small isolated regions of the fundus having much higher sensitivities cannot be ruled out. However, there is no evidence to indicate that this situation existed, and even if it did, it would not remove the discrepancy which apparently exists between observation and theory.

In an effort to test the sensitivity of the model to the numerical values assumed for the constants ρ, c, and k, temperature distributions were calculated for exposure 10, 11 left using the values suggested by Felstead (5). These values are: $\rho = 1.03$ gms/cm^3, C = 0.86 cal/gm °C, k = 2.4×10^{-3} cal/sec -°C - cm. Using these numbers, temperatures about 25% lower than those calculated using the corresponding values for water were obtained; however, the shapes of the temperature distribution curves were not affected

appreciably. Thus, it does not appear that the observations associated with exposure 10, 11 left can be reconciled with predictions of the model by a better choice of numerical values for these particular properties of the absorbing media.

It seems that a simple temperature criterion, such as that applied, is inadequate for a description of the extent of visible effects. It is also possible that the model, as constructed, is not adequate for the degree of precision searched for in this investigation. Additional correlations between visible effects and calculated temperature distributions are needed to clarify the relationships that exist.

SUMMARY

1. The eyes of an adult New Zealand rabbit were subjected to a series of carefully controlled exposures to investigate the relationship between ophthalmoscopically visible results and the temperature rise produced in the chorioretinal region.

2. Minimally visible effects were associated with a temperature rise in the pigment epithelium of 15-20^{o} C--for the exposure condition investigated (20 msecond exposure, 0.52 mm image diameter).

3. For increases in temperatures considerably above 20^{o} C. lesions appeared almost immediately and were approximately the size of the image on the retina--or somewhat larger. The region of high temperature extended well into the choroid for exposures of 20 milliseconds or more. The area of observable changes increased with time

such that at 24 hours the area of disturbance was measurably larger than that of the early lesion.

4. For temperature increases of the order of 15-20° C, the appearance of visible change was delayed several hours and the size of the disturbed area was considerably less than the image size.

5. Temperature rises less than 15° C, maintained for several 10's of milliseconds, did not produce any visible changes.

6. A simple temperature criterion seems to be inadequate for a quantitative description of the extent of visible changes and/or the model used for calculating the temperature distributions may not be adequate.

7. Further correlations of observed effects with temperature histories are needed for clarification of the relationships that exist and for refinement of the mathematical model.

REFERENCES

1. Alexander, T. A., Lawler, E. R. Jr., Wilson, P. W. Jr., McDonald, R. I.: High D. C. power, solid-state switch for pulsing an arc lamp. Review of Sci. Inst., 36, 1707-1709, Dec. (1965).

2. Allen, R. G., Jr., et al.: The production of chorioretinal burns from high altitude nuclear detonations. POR DASA Rpt. No. 2014, March (1965). Secret F. R. D.

3. Bessey, R. L.: Unpublished report on calibration of the Zeiss coagulator. Technology Incorporated, Texas Division (1965).

4. Buettner, K. and Rose, H. W.: Eye hazards from an atomic bomb. Sight-Saving Rev., 23, 1, (1953).

5. Felstead, E. B. and Cobbold, R. S. C.: Analog solution of laser retinal coagulation. Med. Electron. Biol. Engng. 3, 145-155, Pergamon Press, (1965).

6. Geeraets, W. J., Williams, R. C., Ham, W. T., Jr., and Guerry, D. III.: Rate of blood flow and its effect on chorio-retinal burns. A. M. A. Arch. Ophth. 68, 58-60, (1962).

7. Geeraets, W. T., Williams, R. C., Chan, G., Ham, W. T., Guerry, D., and Schmidt, F. H.: The relative absorption of thermal energy in retina and choroid. Invest. Ophthal., 1, 340-347, (1962).

8. Ham, W. T., Jr., et al.: Ocular effects of laser radiation. Acta Ophthalmologica 43, 390-409, (1965).

9. Penner, R.: Personal communication. Dept. of Ophthal. Walter Reed Army Hospital, Washington, D. C.

10. Verhoff, F. H. and Bell, L.: The pathological effects of radiant energy on the eye. Proc. Am. Acad. Arts and Sci. 51, 630, (1916).

11. Wray, J. L.: Model for prediction of retinal burns. DASA Rpt. No. 1282, Washington, D. C., (1962).

12. Zaret, M. M., Ripps, H., Siegel, I. M. and Breinin, G. M. Laser coagulation of the eye. Arch. Ophthal. 69, 97-104, (1963).

BLANK PAGE

TABLE II

LEFT EYE EXPOSURES

Exposure Number	Duration msec	Irradiance (cal/cm^2-sec)	Exposure (cal/cm^2)	Temperature Rise* (^oC)
1, 2, 3	20	50.9	1.02	53.5
4, 5	20	123	2.46	129
6, 7	20	74	1.48	77.8
8, 9	20	49	0.98	51.5
10, 11	20	24.5	0.49	25.7
12, 13	20	12.5	0.25	13.1
14, 15	20	4.9	0.10	5.1
16, 17	20	2.45	0.05	2.6
18, 19	20	1.20	0.024	1.3
20, 21	20	0.93	0.019	1.0
22	151	23.6	3.56	40.1
23	20	185	3.70	195

2 Hours Post Irradiation						24 Hours Post Irradiation				
Average Radius (mm)					Exposure	Average Radius (mm)				
A	B	C	D	E	Number	A	B	C	D	E
- -	0.16	0.24	- -	0.48	1, 2, 3	- -	0.18	0.24	0.31	0.58
0.21	0.27	0.34	- -	0.52	4, 5	0.22	0.24	0.30	0.37	0.77
0.16	0.24	0.31	- -	0.47	6, 7	0.15	0.22	0.28	0.33	0.64
- -	0.18	0.27	- -	0.36	8, 9	- -	0.11	0.23	0.28	0.52
- -	- -	0.04	- -	- -	10, 11	- -	- -	0.04	- -	- -
- -	- -	- -	- -	- -	12, 13	- -	- -	~0.02	- -	- -
- -	- -	- -	- -	- -	14, 15	- -	- -	- -	- -	- -
- -	- -	- -	- -	- -	16, 17	- -	- -	- -	- -	- -
- -	- -	- -	- -	- -	18, 19	- -	- -	- -	- -	- -
- -	- -	- -	- -	- -	20, 21	- -	- -	- -	- -	- -
0.22	0.28	0.34	- -	0.64	22	0.21	0.25	0.33	0.38	0.75
0.23	0.29	0.36	- -	0.70	23	0.20	0.24	0.31	0.40	0.81

*Maximum ΔT at the center of the pigmented epithelium (PE)

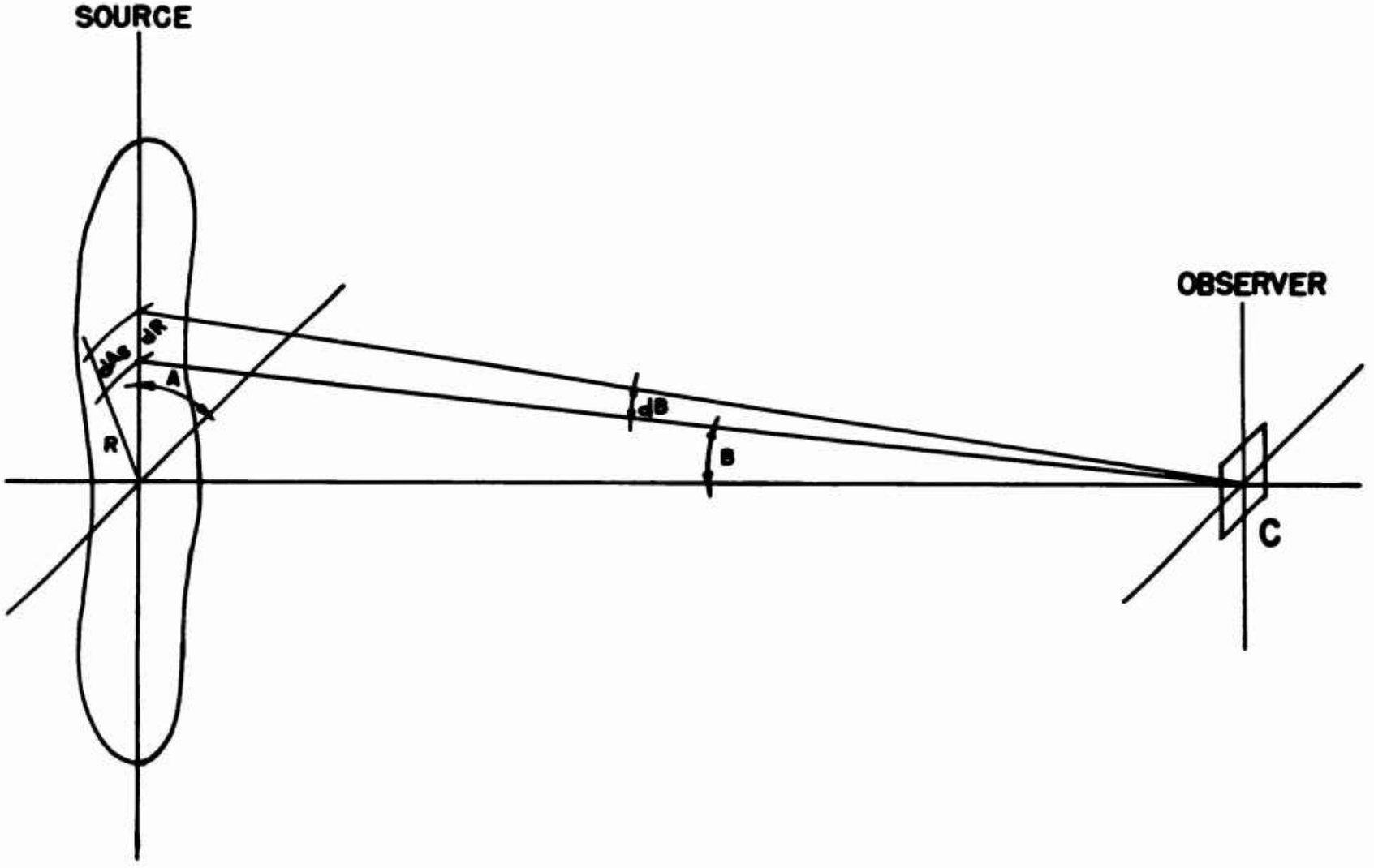

FIGURE 1. Irradiance from a plane source.

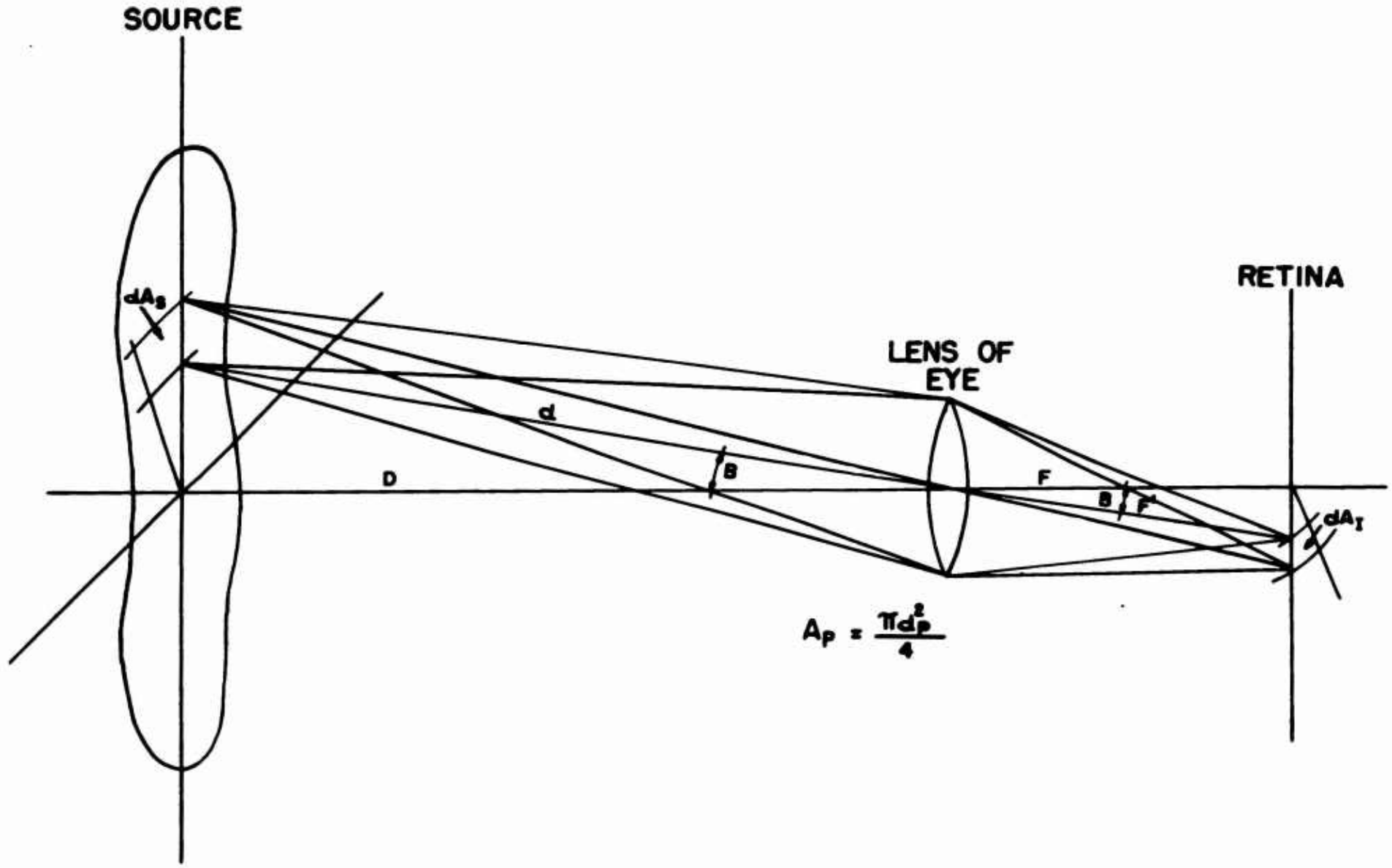

FIGURE 2. Retinal irradiance from a plane source.

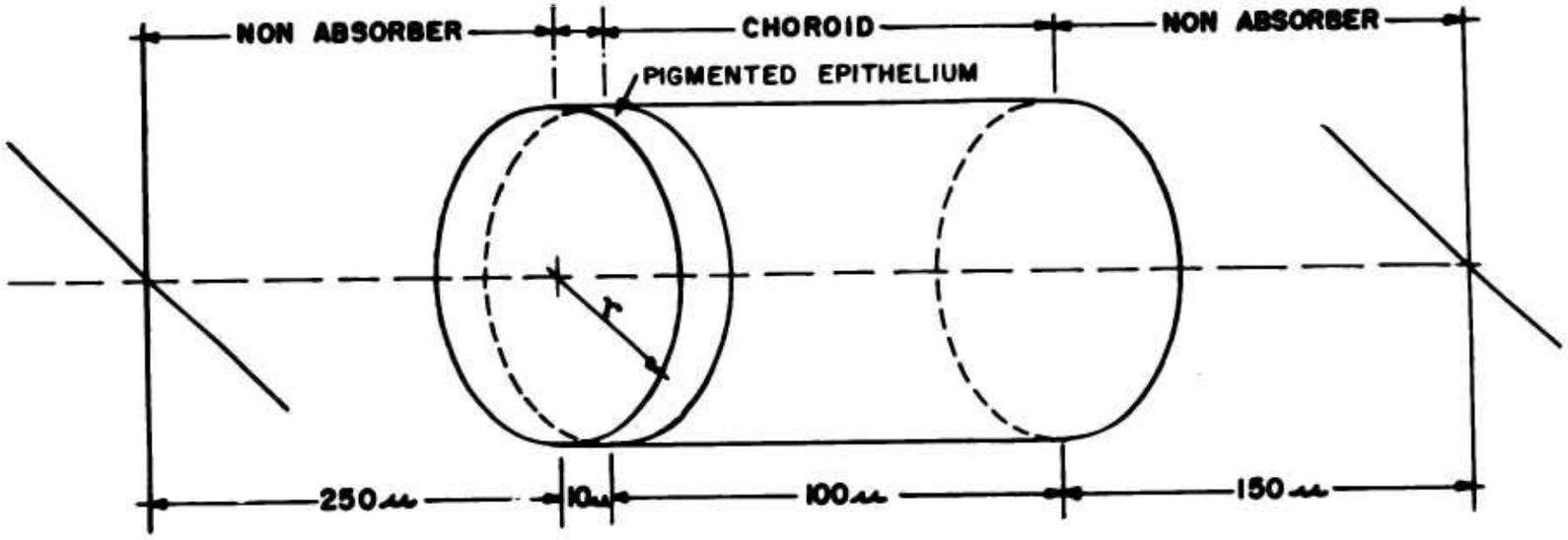

FIGURE 3. Simplified geometry of the chorioretinal region used in calculating temperature distributions.

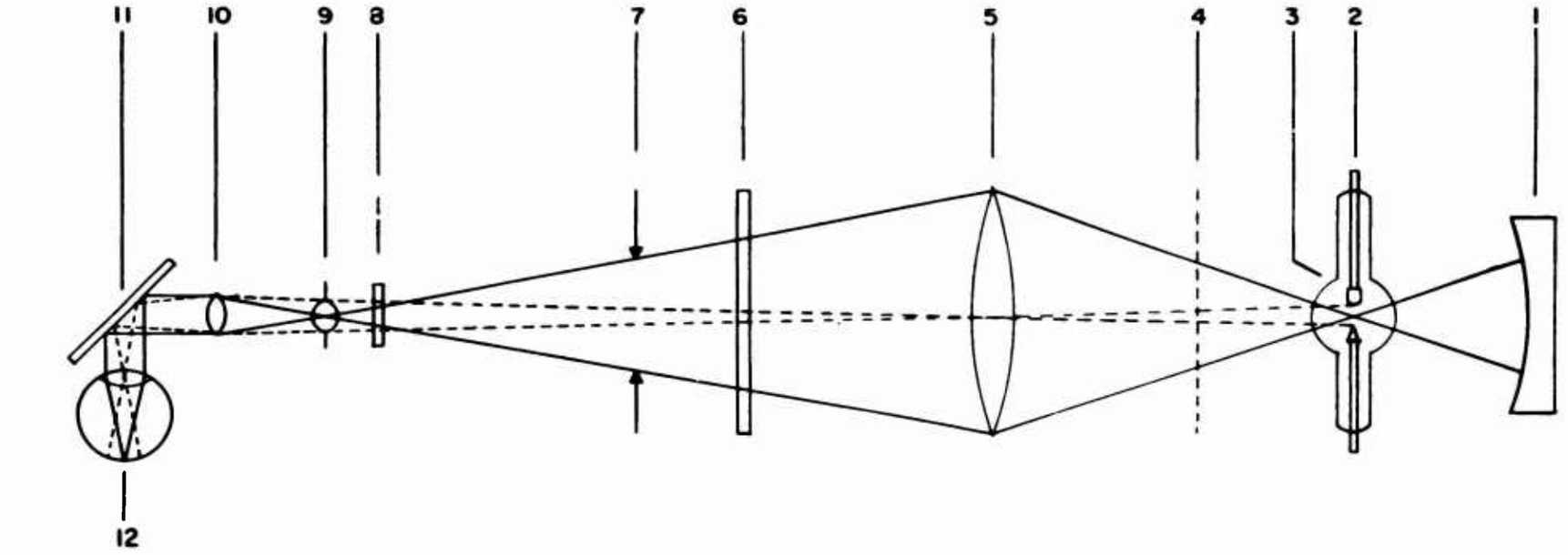

FIGURE 4. Modified Meyer-Schwickerath coagulator.

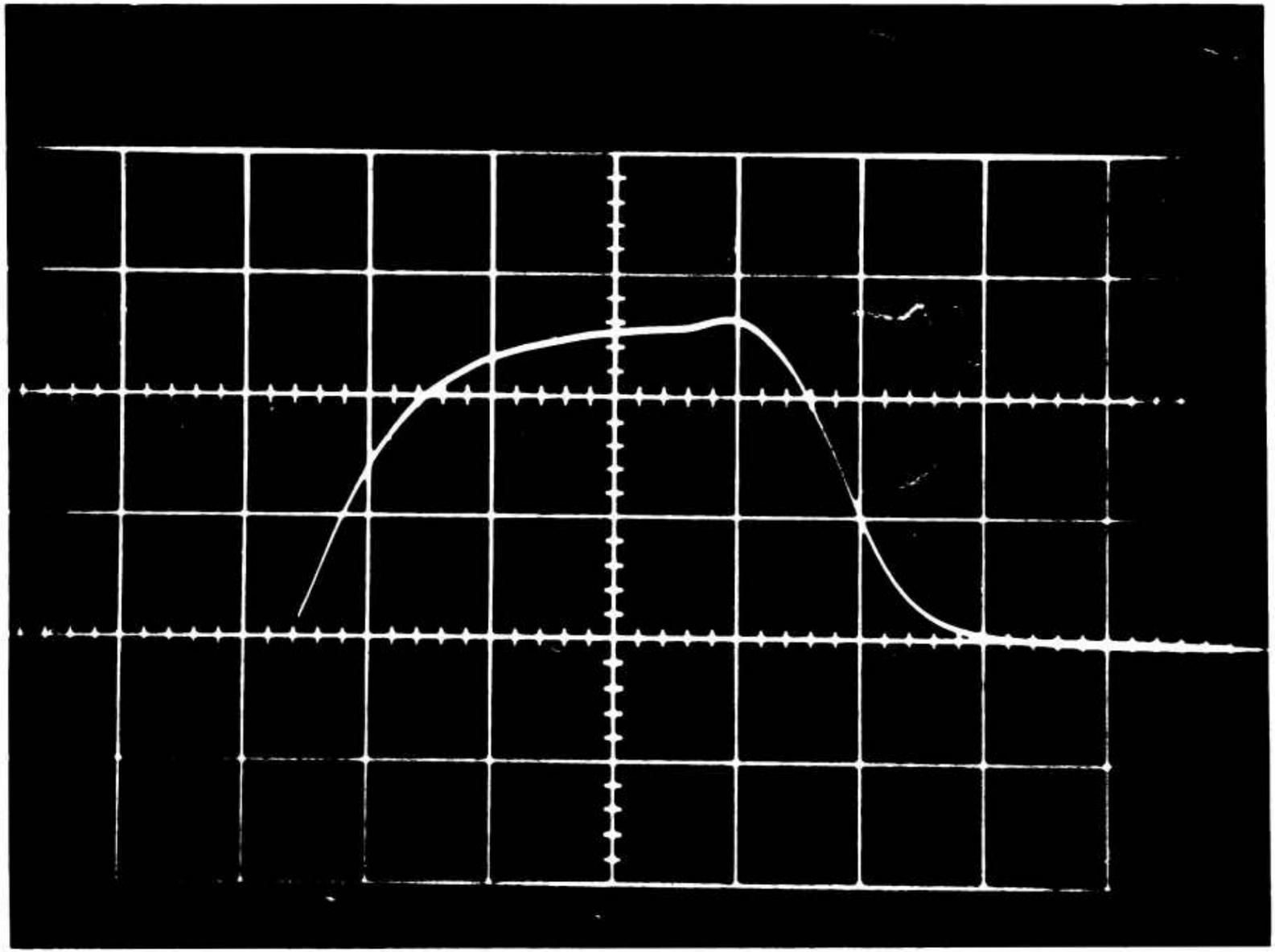

FIGURE 5. Shape of the 400 μsecond light pulse from the modified coagulator. (100 μseconds per division).

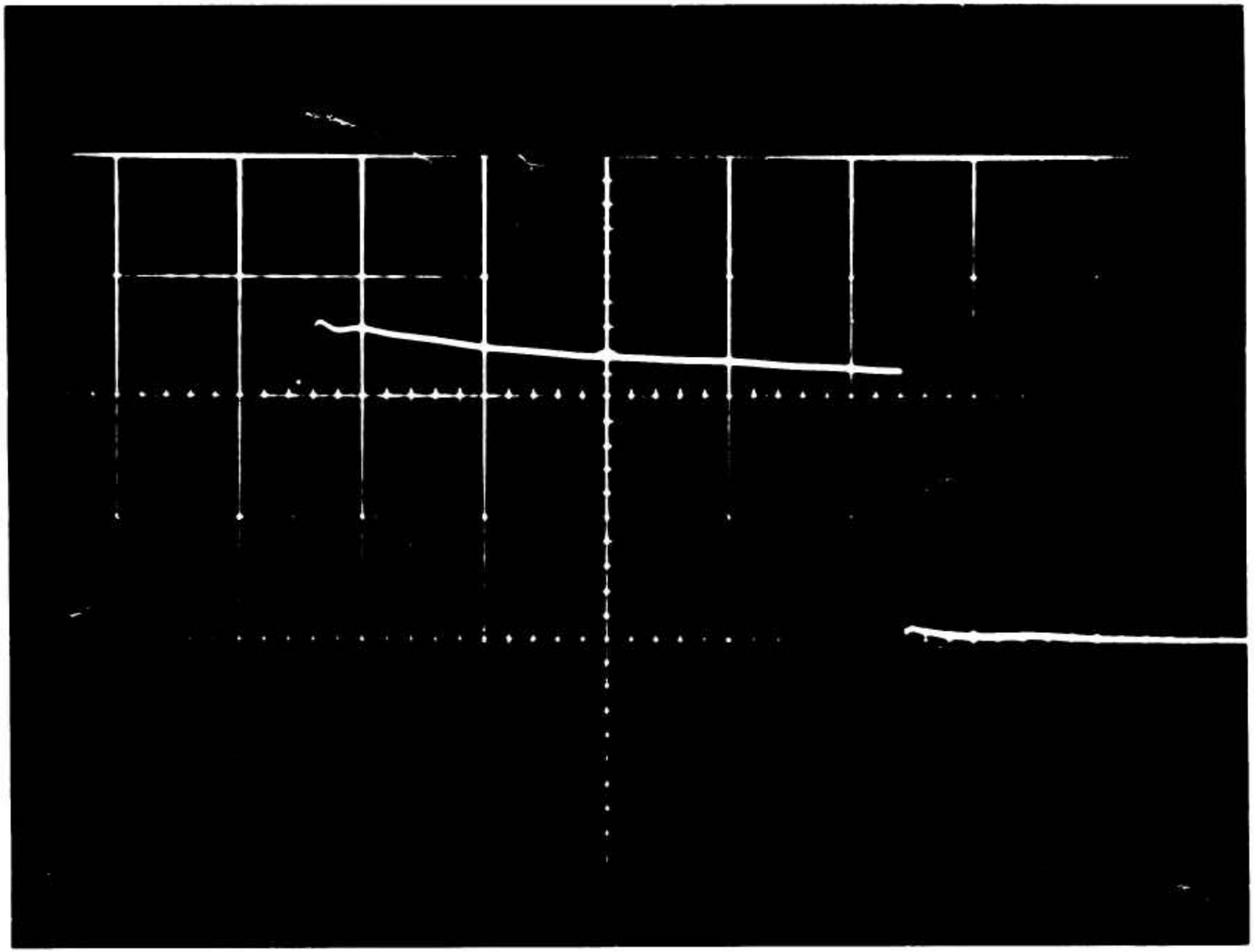

FIGURE 6. Shape of the 100 msecond light pulse from the modified coagulator. (20 mseconds per division).

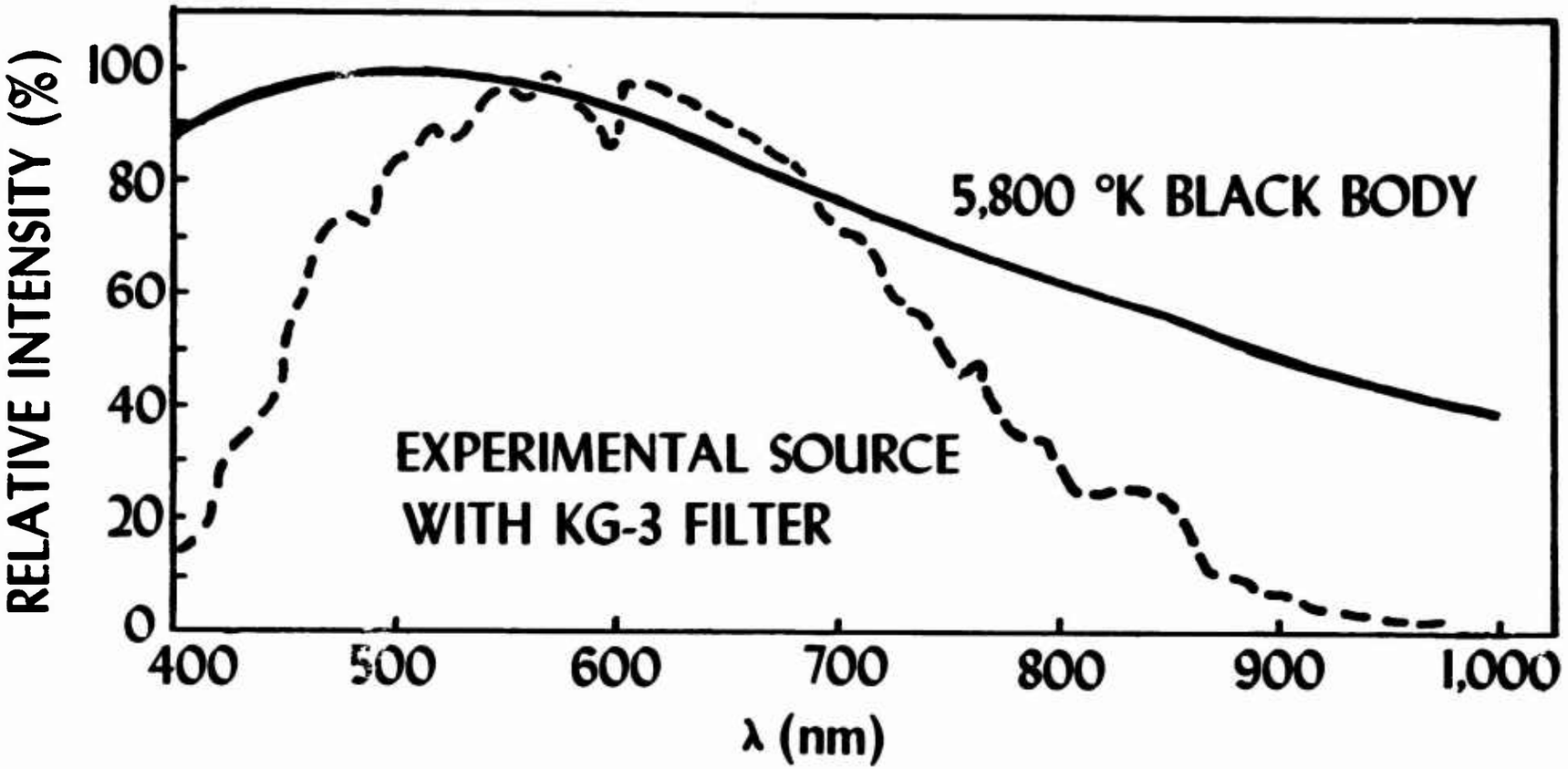

FIGURE 7. KG-3 filtered xenon spectrum from the modified coagulator—normalized to the spectrum of a 5800° K black body.

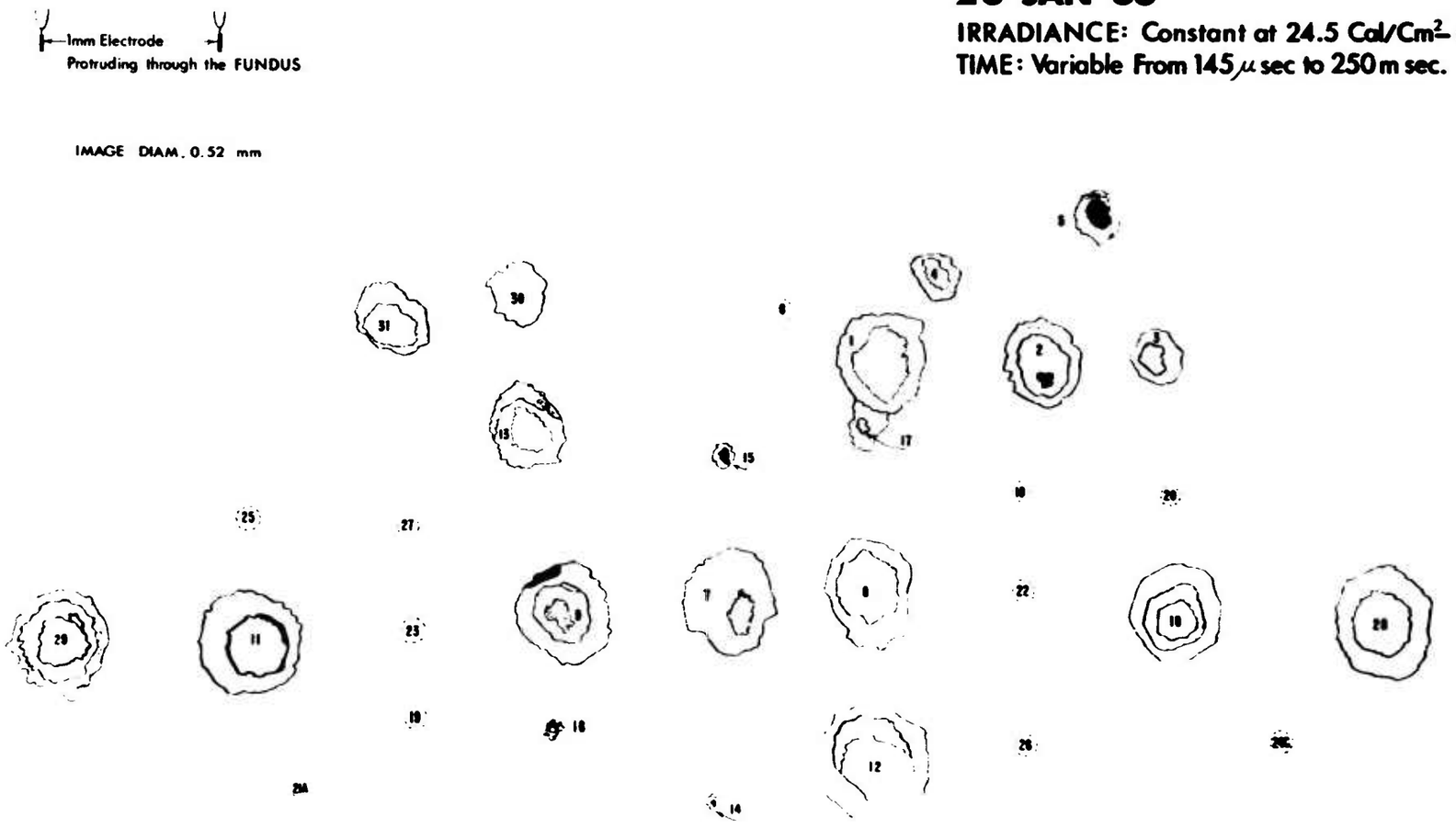

FIGURE 8. Composite, drawn to scale, of the results produced by exposures in the right eye.

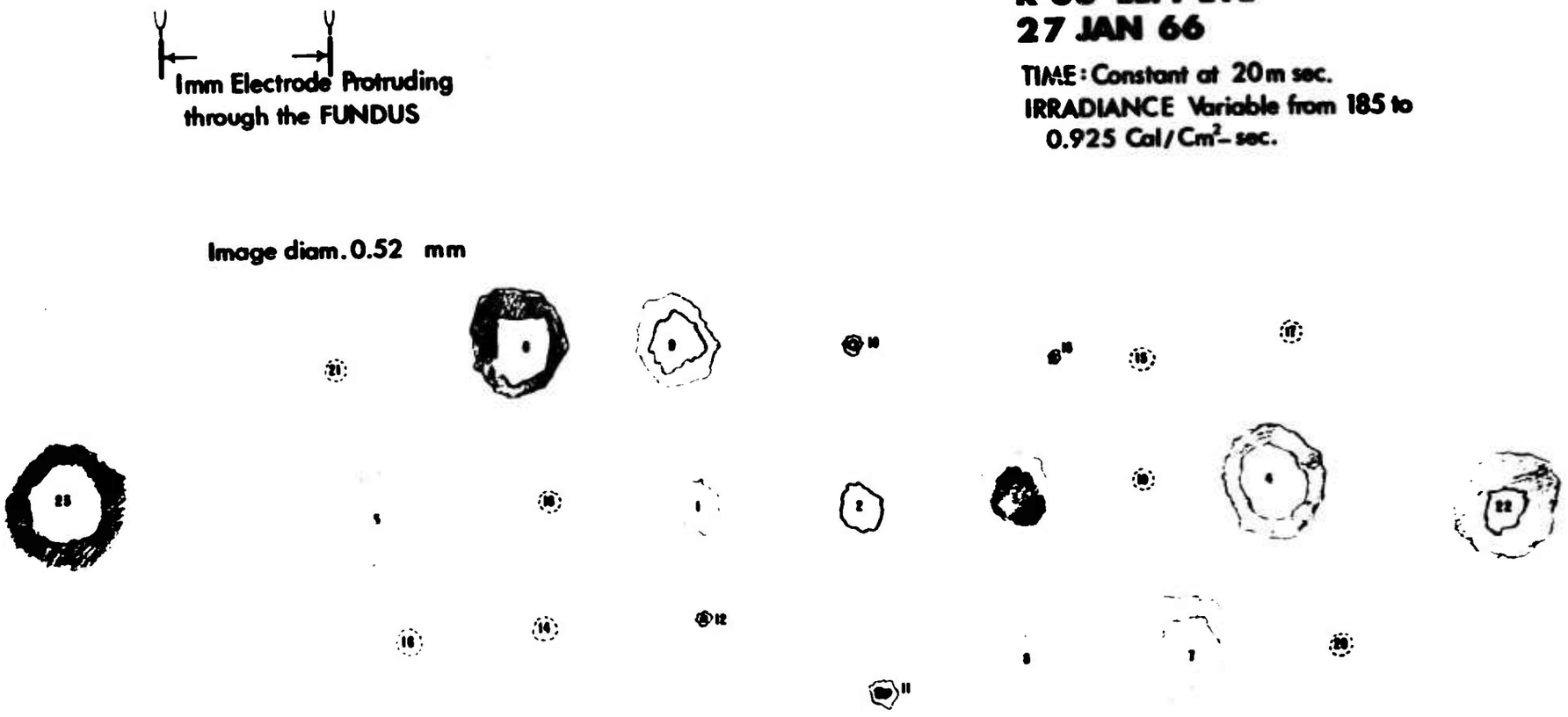

FIGURE 9. Composite, drawn to scale, of the results produced by exposures in the left eye.

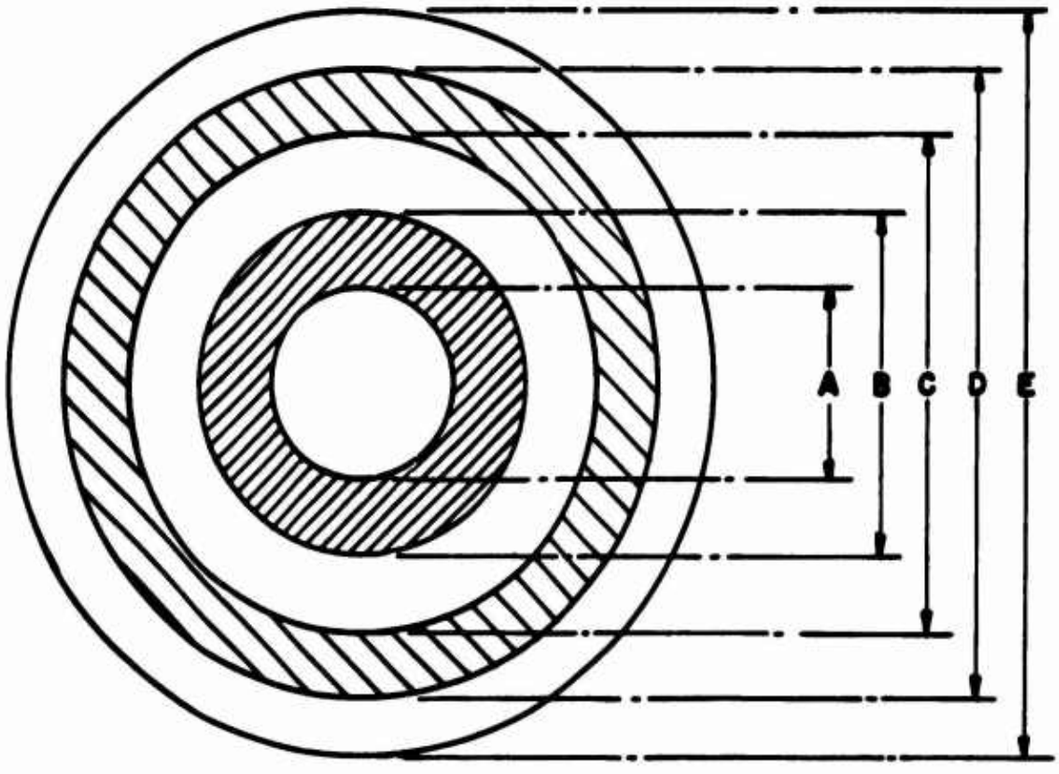

A = DEEP YELLOWISH - WHITE
B = DARK GREY
C = PALE GREYISH - WHITE
D = PALE PINKISH - WHITE
E = ERYTHEMA

FIGURE 10. Characteristic visible features of chorioretinal lesions.

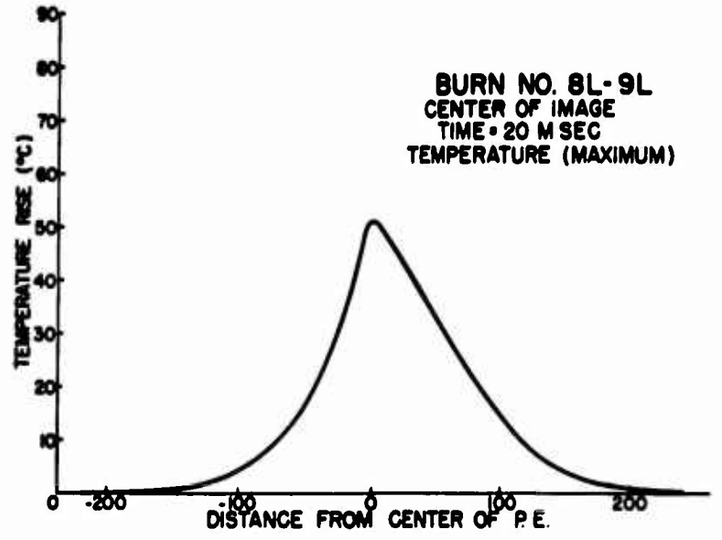

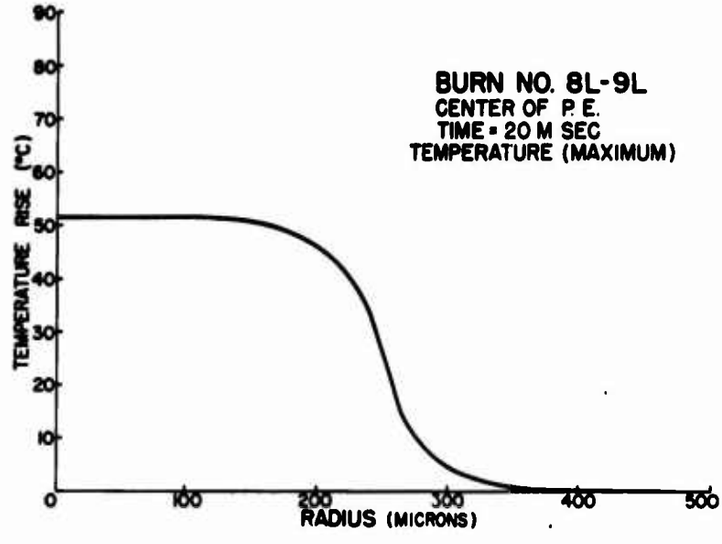

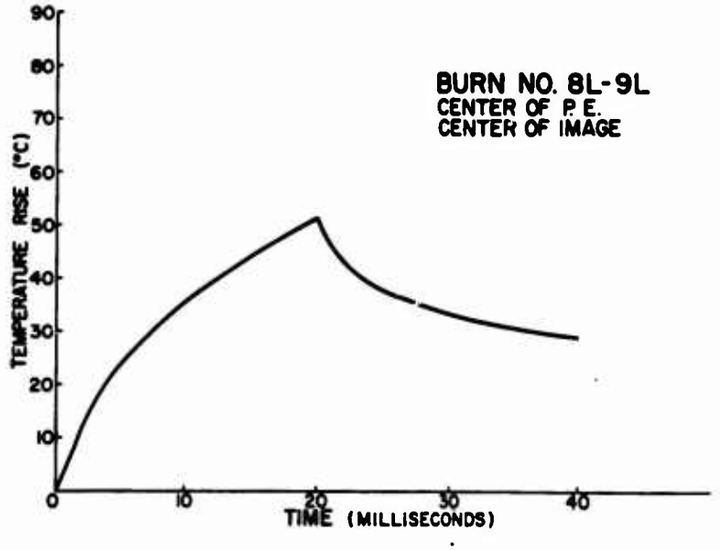

FIGURE 11. Calculated temperature distributions for exposure 8, 9 left eye.

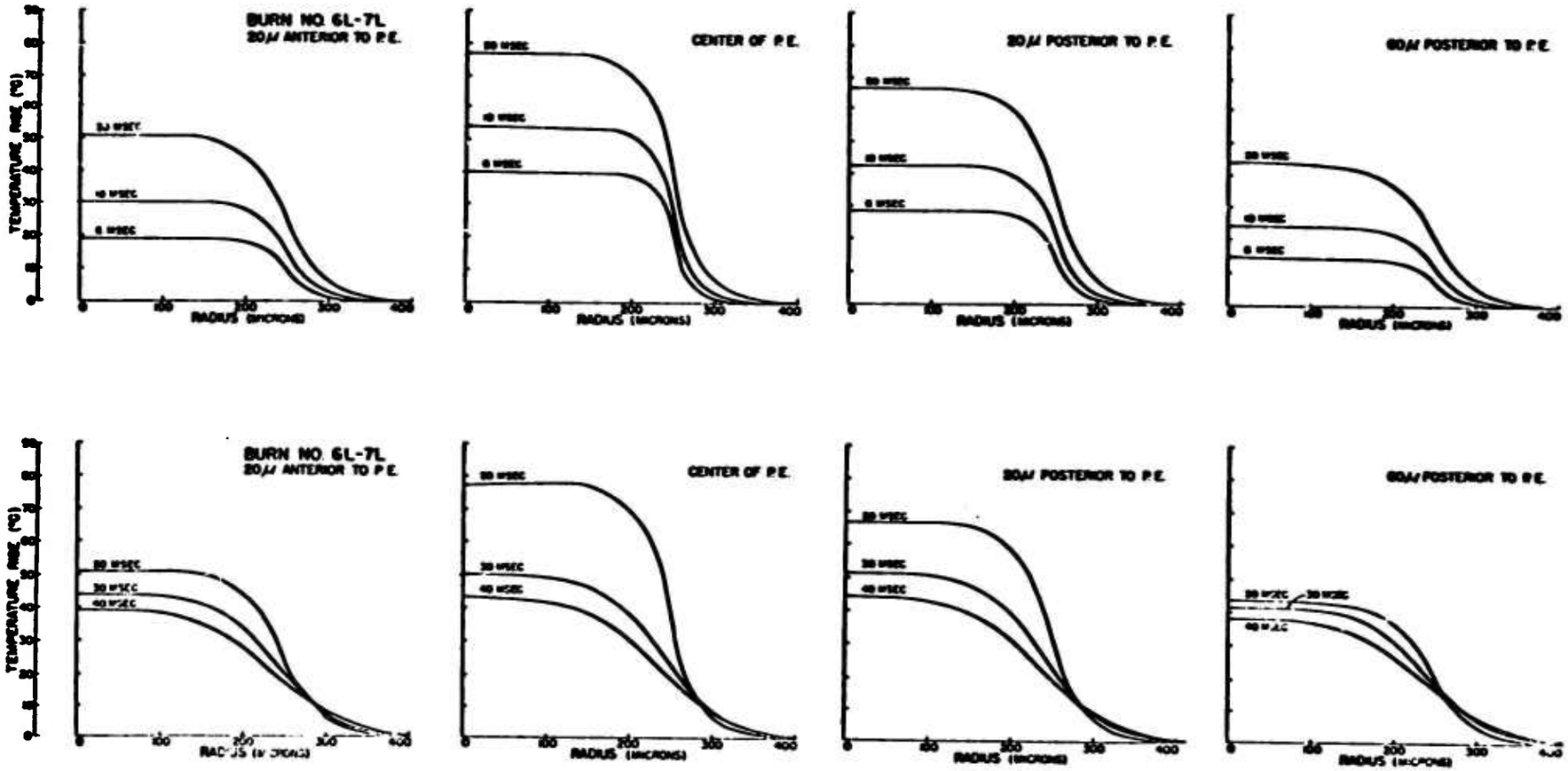

FIGURE 12. Calculated radial temperature increase at various times and depths for exposure 6, 7 left eye.

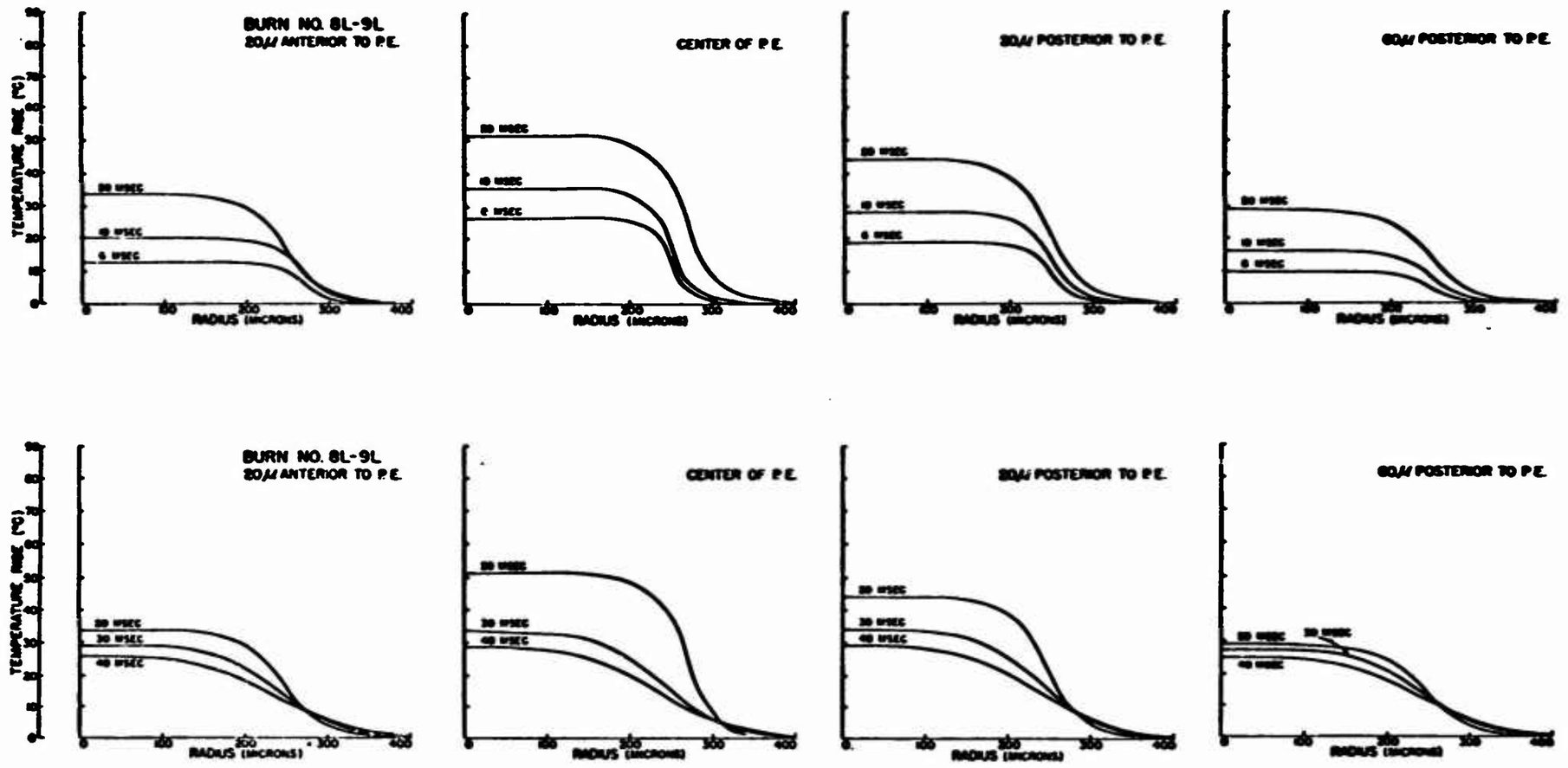

FIGURE 13. Calculated radial temperature increase at various times and depths for exposure 8, 9 left eye.

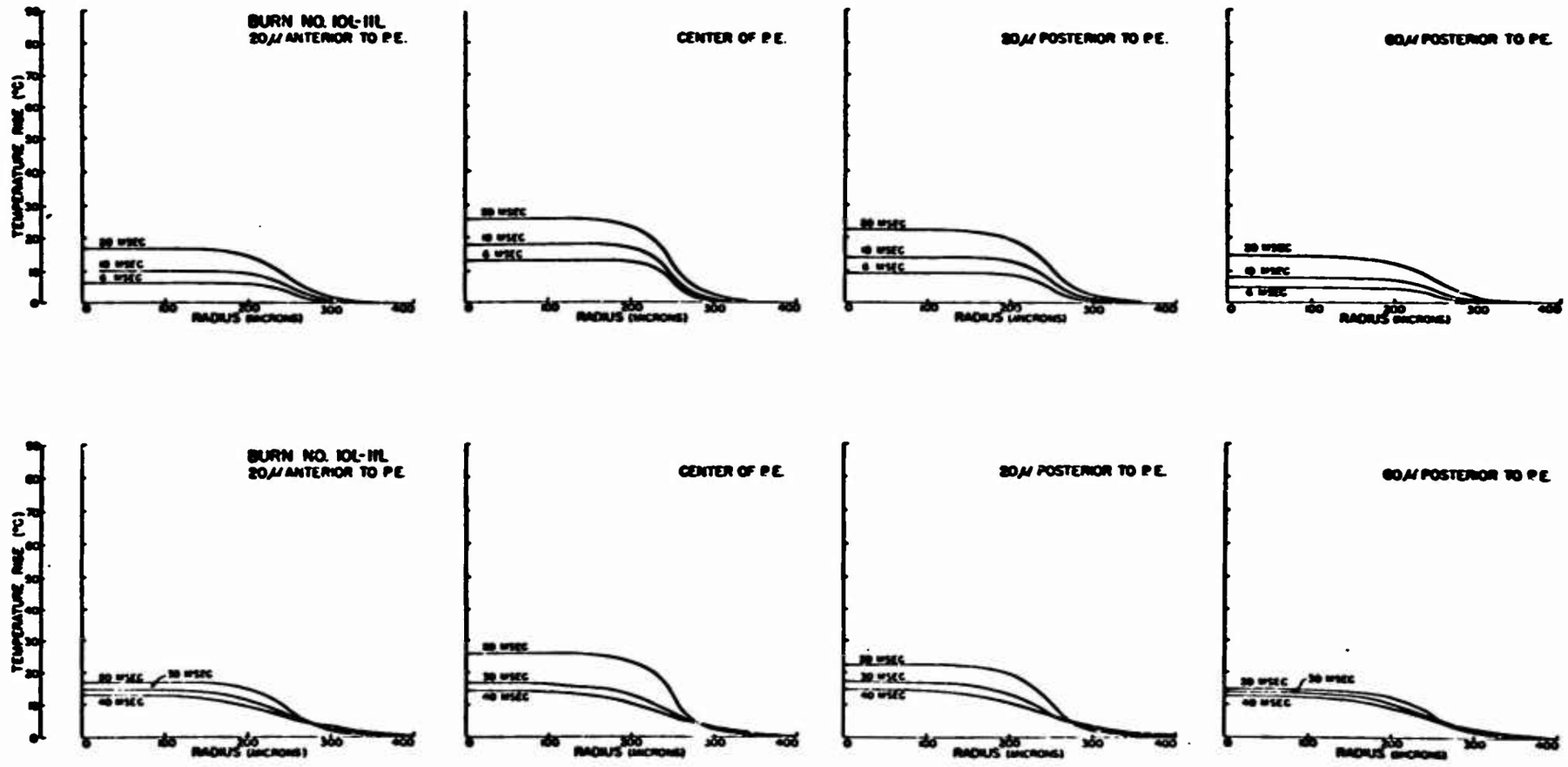

FIGURE 14. Calculated radial temperature increase at various times and depths for exposure 10, 11 left eye.

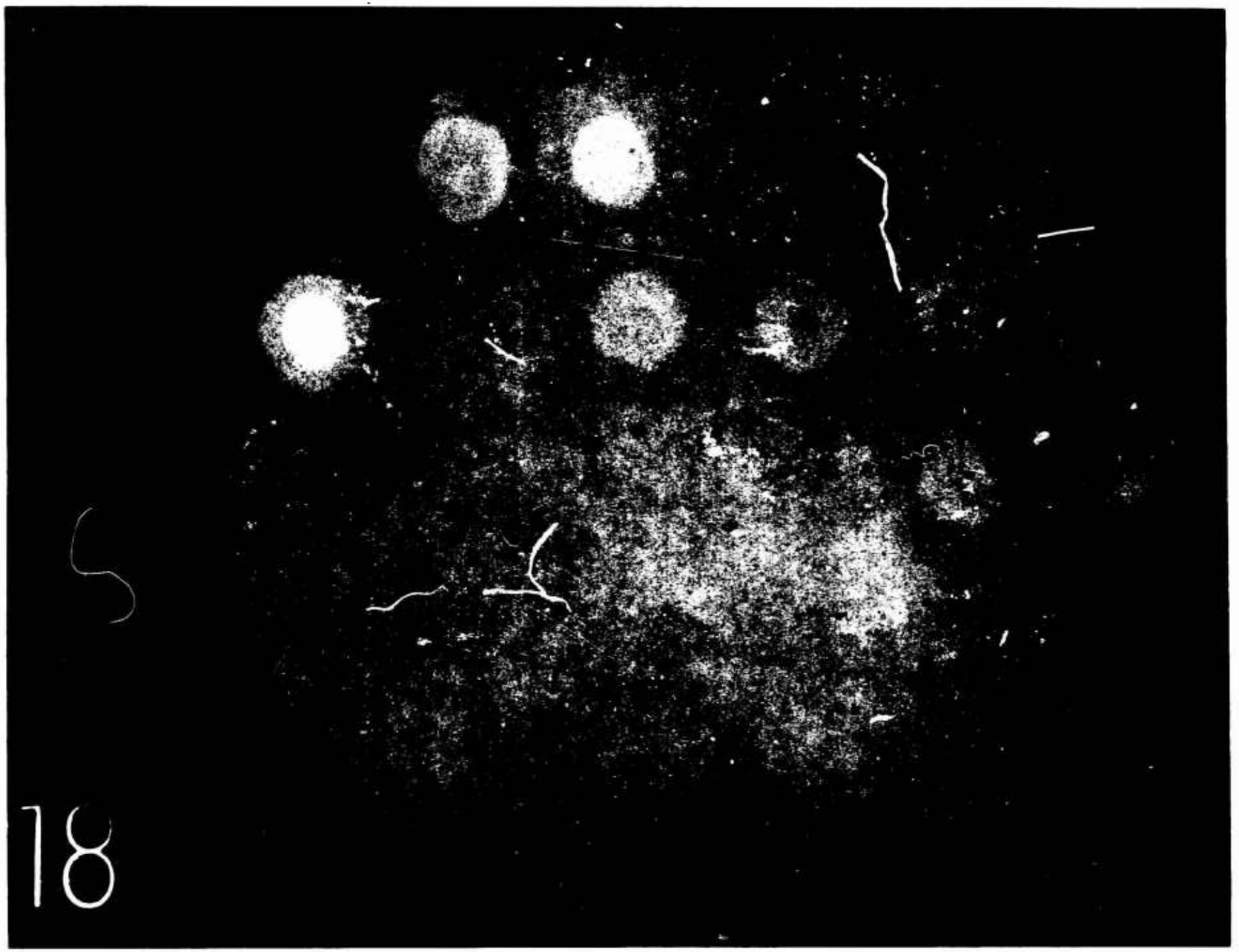

FIGURE 15. Photograph of exposures 6, 7; 8, 9; and 10, 11 left eye.

MEASUREMENTS OF THE TOTAL LUMINOUS ENERGY OUTPUT OF TWO HONEYWELL STROBONAR FLASH UNITS*

Polaski, C. A., and R. G. Allen, Jr.

*This work was supported by the Department of Ophthalmology, Air Force School of Aerospace Medicine, Brooks Air Force Base, Texas and the Medical Division, Defense Atomic Support Agency, Washington, D. C.

FOREWORD

This report was prepared by personnel of the Life Sciences Division of Technology Incorporated--

Charles A. Polaski, M.E.

Ralph G. Allen, Jr., Ph.D.

The effort was sponsored jointly by the Ophthalmology Branch of the United States Air Force School of Aerospace Medicine, and the Medical Division, Defense Atomic Support Agency, Washington, D. C. Mr. E. O. Richey of the Oculo-Thermal Section was the Contract Monitor during the contractual period. Grateful acknowledgement is made of the assistance provided by Lt. Col. J. F. Culver and Major D. G. Pitts of the Ophthalmology Branch.

ABSTRACT

The luminous and radiant emittance of Honeywell Strobonar flash units (Model 65C and Model 600) were measured indirectly by measuring the illuminance and irradiance at a point 100 cm from these light sources. The spectral distribution of the Model 600 was also measured in the range of 400 to 700 millimicrons.

The total luminous emittance of the Model 600 was found to be 74.4 $\frac{\text{lumen-sec}}{\text{cm}^2}$ on battery operation and 72.7 $\frac{\text{lumen-sec}}{\text{cm}^2}$ on A. C. operation. The total luminous emittance of the Model 65C was found to be 63.3 $\frac{\text{lumen-sec}}{\text{cm}^2}$ on A. C. operation.

The total radiant emittance of the Model 600 was found to be 0.463 cal/cm^2 on battery operation 0.453 cal/cm^2 on A. C. operation. The total radiant emittance of the Model 65C was found to be 0.394 cal/cm^2 on A. C. operation.

BLANK PAGE

MEASUREMENTS OF THE TOTAL LUMINOUS ENERGY OUTPUT OF TWO HONEYWELL STROBONAR FLASH UNITS

1. INTRODUCTION AND OBJECTIVE

Experiments were undertaken to measure the irradiance and illuminance of two Honeywell Strobonar Flash Units, Model 65c and Model 600. These measurements were then used to determine the total luminous and radiant emittance of these devices. This was done using a SD-100 photodiode that had been calibrated in terms of physical and photometric units. In addition, limited measurements were made of the spectral distribution of the Model 65c strobe unit in the range 400 to 700 mu. These measurements were made using interference filters and the calibrated SD-100.

2. THEORY

A photodiode in an appropriate circuit produces a voltage output that is proportional to the total irradiance (illuminance) at the diode, i. e.

$$V \propto H\ (\text{cal/cm}^2\text{-sec}) \quad \propto \quad E(\text{ft-candles}) \tag{1}$$

or:

$$E_s = cV_s$$

where

c = proportionality constant appropriate to the particular spectrum concerned

V_s = photodiode output voltage for a steady state light

E_s = light meter reading in ft-candles for a steady state light

Thus

$$c = \frac{E_s}{V_s} \quad \left(\frac{\text{ft-candles}}{\text{volt}}\right)$$

Similarily in physical units:

$$H_s = kV_s$$

where

k = proportionality constant for the particular spectrum concerned

H_s = thermopile reading in cal/cm^2-sec for a steady state light

Therefore,

$$k = \frac{H_s}{V_s} \quad \left(\frac{\text{cal}}{\text{cm}^2\text{-sec-volt}}\right)$$

It is noted that the photodiode voltage output is linearly related to the light input only within certain limits. For the above equations to be valid, the irradiance must not exceed these limits.

A measure of the emittance of the Strobonar unit can be obtained from a measurement of the illuminance at one point--provided the light source is assumed to be a point source radiating uniformly into a

fixed solid angle.

Under this assumption:

$$L' \left(\frac{\text{lumen-sec}}{\text{cm}^2} \right) = \frac{A_D}{A_O} \quad \frac{c_D}{929} \quad \int_o^T V_D(t)\ dt \qquad (2)$$

where

L' = total luminous emittance of the source during time T

$c_D = \frac{E_s}{V_s} = \frac{3.6 \times 10^3 \text{ ft candles}}{\text{volt}}$ at distance D (100 cm for these measurements)

A_D = area of beam at 100 cm = 1.77×10^4 cm^2

A_O = surface area of light source = 18.2 cm^2

T = duration of light pulse

$V_D(t)$ = time varying photodiode voltage at distance D.

Since all of the measurements were made with the same photodiode placed at the same distance from sources of equal area,

$$L' \left(\frac{\text{lumen-sec}}{\text{cm}^2} \right) = C_D \int_o^T V_D(t)\ dt \qquad (3)$$

where

$$C_D = 3.77 \times 10^3 \left(\frac{\text{lumen}}{\text{cm}^2\text{-volt}} \right)$$

The average luminous emittance, $\overline{L}$ is given gy

$$\overline{L} = \frac{L'}{T} = \frac{C_D}{T} \int_0^T V_D(t)\ dt, \qquad (4)$$

and the maximum luminous emittance is given by

$$L_{max} = C_D\ V_{max}(t), \qquad (5)$$

where $V_{max}(t)$ is the peak voltage recorded.

Similarly, the total radiant emittance (W') of the Strobonar light pulse in physical units may be obtained from the expression:

$$W'\left(\frac{cal}{cm^2}\right) = \frac{A_D}{A_o} \times k_D \int_0^T V_D(t)\ dt \qquad (6)$$

where

$$k_D = 2.41 \times 10^{-2}\ cal/cm^2\text{-sec-volt}$$

Again we can write

$$W' = K_D \int_0^T V_D(t)\ dt \qquad (7)$$

where, for this case,

$$K_D = 23.45\ cal/cm^2\text{-sec-volt}$$

The average radiant emittance is given by

$$\overline{W} = \frac{W'}{T} = \frac{K_D}{T} \int_0^T V_D(t)\ dt, \qquad (8)$$

and the maximum radiant emittance is given by

$$W_{max} = K_D V_{max}(t) \qquad (9)$$

The duration of the pulse, T, was arbitrarily selected to include approximately 95% of the total energy content of the flash. In all cases T was 1.4×10^{-3} seconds.

3. PROCEDURE

To calibrate the SD-100 photodiode in physical and photometric units, a G.E. tungsten iodine bulb operating at 6.6 amps A.C. was used. The lamp was placed in a standard lamp holder at one end of an optical bench in such a manner that there was no reflecting surfaces near the bulb. For all measurements, the detectors were placed 100 cm away from the source.

The photometric calibration was accomplished using the average of the values measured by Weston 603 and Weston 756 light meters. The light meters were then replaced by the SD-100 in the circuit shown in figure 1 and its voltage response measured using an oscilloscope. Since it was necessary to shield the SD-100 with neutral density filters to prevent swamping the diode with the light from the Strobonar units the calibration was accomplished using a density 2 filter.

The physical calibration was done using an Eppley fourteen junction thermopile, also placed 100 cm from the G.E. bulb. This measurement, in conjunction with the voltage measured in the above paragraph, permitted calibration of the photodiode in the physical units.

Following calibration of the photodiode, a Honeywell Strobonar unit was placed 100 cm from the SD-100 photodiode and oscilloscope photographs (figure 2) made of the photodiode output when the flash unit was pulsed.

The pulse photographs were integrated graphically for use in the appropriate equations and the maximum height of each pulse was measured to obtain the maximum emittance.

The spectral distribution of the 600 strobe unit was measured using Optics Technology bandpass interference filters. With the light source set up about 275 cm from the SD-100 detector, oscilloscope photographs were made of the SD-100 output with different filter combinations. These filter combinations were chosen to give successive band passes approximately 50 millimicrons wide in the region from 400 to 700 millimicrons. These measurements were corrected for the transmittance of the filter

combination and the spectral sensitivity of the SD-100 diode to give the spectral distribution shown in figure 3.

The area of the light beam was measured by taking pictures of the area covered by the light beam (on a screen) as a function of distance from the Strobonar unit. The diameter of the beam was measured from these pictures and extrapolated to the diameter at 100 cm.

4. RESULTS AND DISCUSSION

The average value or irradiance for the two light meters used was 75.7 ft-candles. The photodiode output with the neutral density filters in place was 21 mv. giving a photometric sensitivity of 3.6×10^{-3} ft-candles/volt.

Using this sensitivity it was found that the total luminous emittance for the Honeywell 600 was 74.4 $\frac{\text{lumen-sec}}{\text{cm}^2}$ on battery operation and 72.7 $\frac{\text{lumen-sec}}{\text{cm}^2}$ on A.C. operation. The total luminous emittance for the Honeywell 65c was found to be 63.3 $\frac{\text{lumen-sec}}{\text{cm}^2}$ on A.C. operation.

The output voltage of the Emmley thermopile was measured as 440 microvolts which yielded an irradiance of 0.506×10^{-3} $\text{cal/cm}^2\text{-sec}$. This gave a physical sensitivity for the SD-100 with

density 2 filter of 24.1×10^{-3} cal/cm^2-sec-volt.

Using the physical sensitivity calibration, the total radiant emittance of the flash units was calculated to be 0.463 cal/cm^2 for the Model 600 on battery operation, 0.453 cal/cm^2 for A.C. operation, and 0.394 cal/cm^2 for the Model 65c for A.C. operation. For convenience, Table 1 lists all of the values calculated for the two Strobonar units.

It is seen from the oscilloscope photographs in figure 2 that both flash units have approximately the same light output and the same pulse shape.

The results of the spectral measurements on the Model 600 are shown in figure 3. Although no spectral measurements were made on the Model 65c it seems reasonable to assume that the spectrum for this model would be similar to that of Model 600.

TABLE I

Strobonar	$\int_0^T V_D(t)\,dt$ volt-sec	V_{max} volts	L' $\frac{\text{lumen-sec}}{\text{cm}^2}$	W' $\frac{\text{cal}}{\text{cm}^2}$	$\bar{L}$ $\frac{\text{lumen}}{\text{cm}^2}$	L_{max} $\frac{\text{lumen}}{\text{cm}^2}$	$\bar{W}$ $\frac{\text{cal}}{\text{cm}^2\text{-sec}}$	W_{max} $\frac{\text{cal}}{\text{cm}^2\text{-sec}}$
600 Battery Operations	19.74×10^{-3}	39	74.4	0.463	5.31×10^4	1.47×10^5	331	916
600 A. C. Operations	19.3×10^{-3}	36	72.7	0.453	5.19×10^4	1.36×10^5	324	845
65c A. C. Operations	16.8×10^{-3}	34	63.3	0.394	4.52×10^4	1.28×10^5	282	798

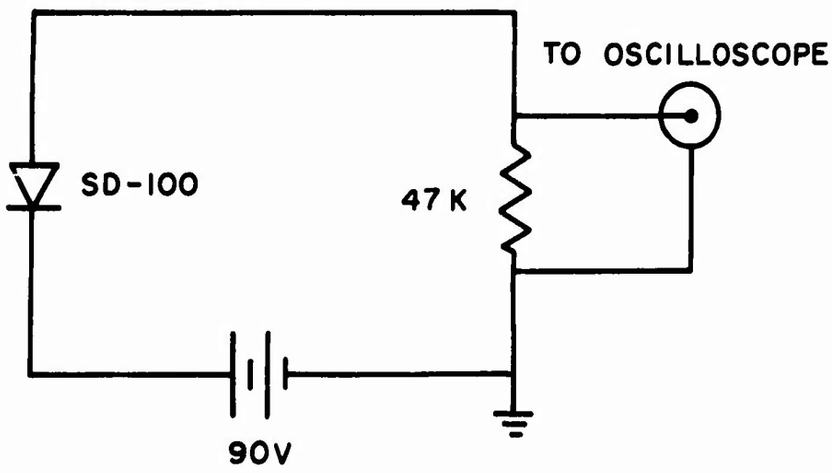

FIGURE 1. SD-100 circuit diagram.

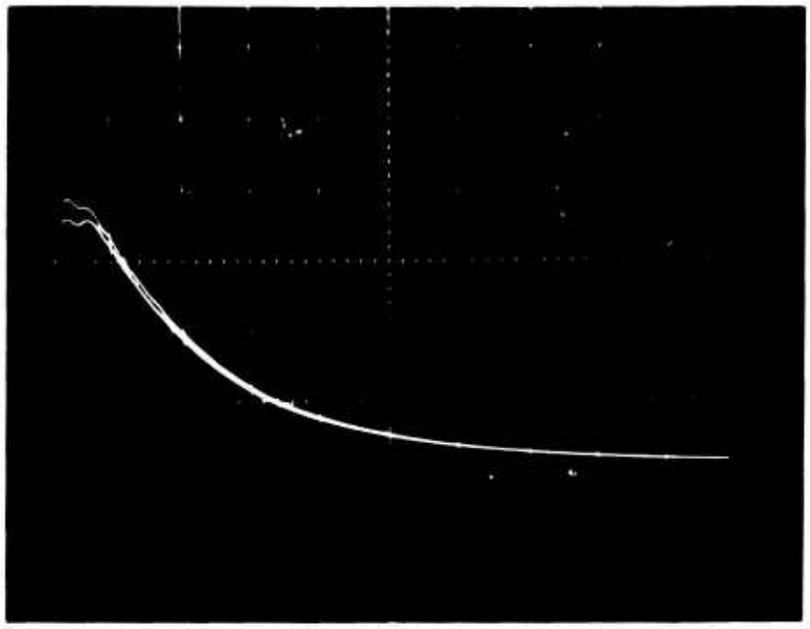

Honeywell Strobonar 600
Top Trace is Battery Operation, Bottom Trace is AC Operation

FIGURE 2A. SD-100 output for light pulse from Honeywell Strobonar Model 600 (DC and AC operation).

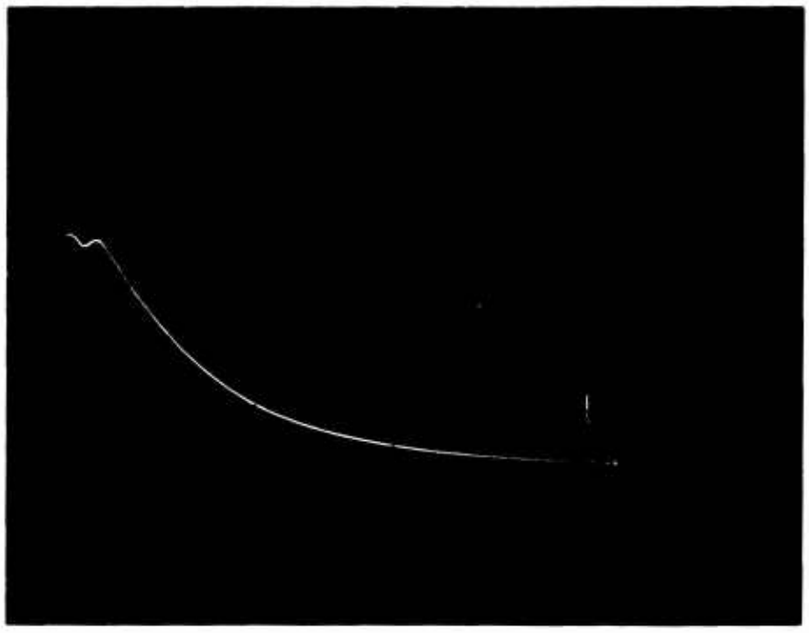

Honeywell Strobonar 65 C
AC Operation

FIGURE 2B. SD-100 output for light pulse from Honeywell Strobonar Model 65C (AC operation).

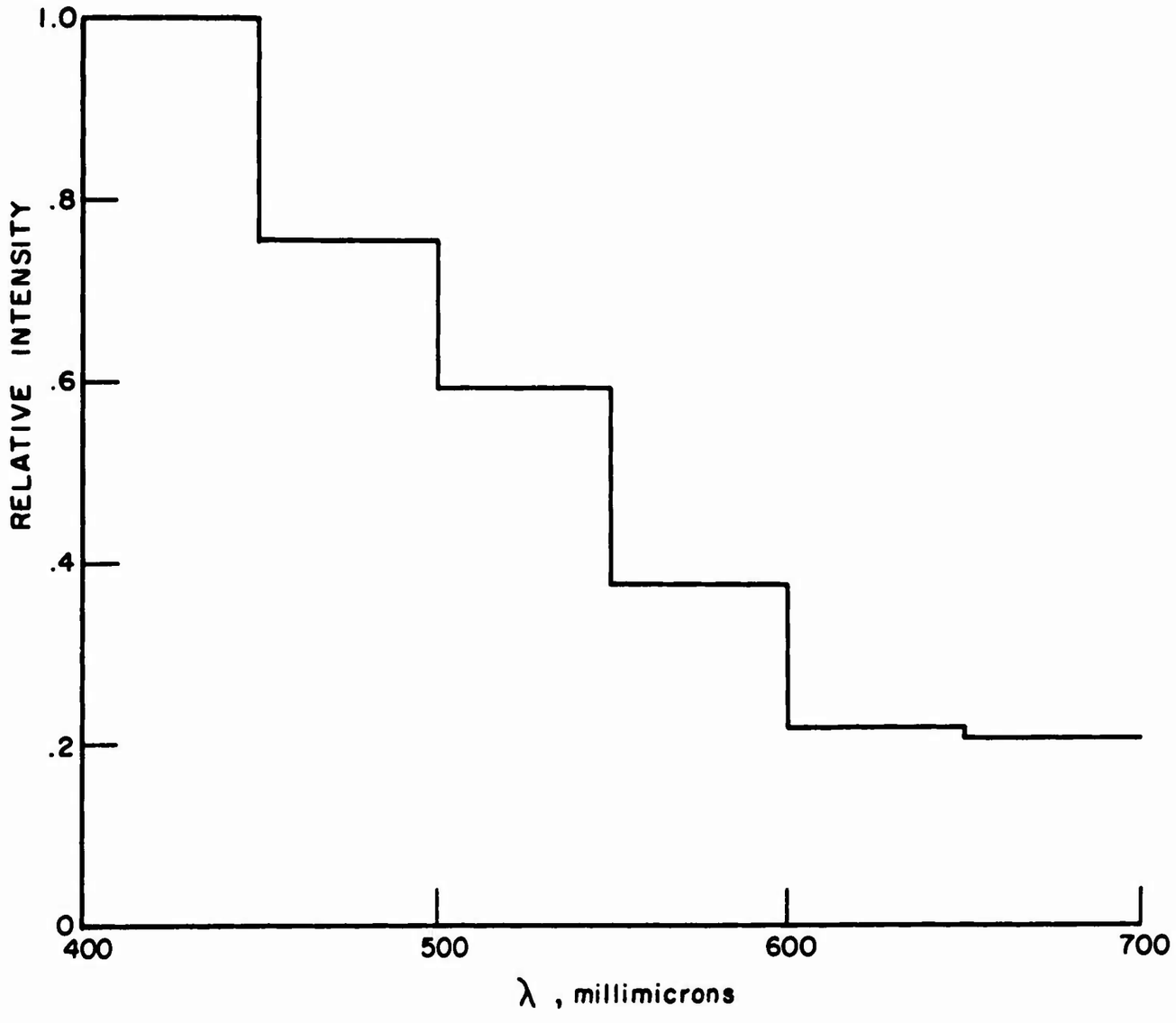

FIGURE 3. Spectrum for Honeywell Strobonar Model 600.